Mechanical Behavior of the Human Lumbar Intervertebral Disc with Polymeric Hydrogel Nucleus Implant: An Experimental and Finite Element Study

A Thesis

Submitted to the Faculty

of

Drexel University

by

Abhijeet Bhaskar Joshi

in partial fulfillment of the

requirements for the degree

of

Doctor of Philosophy

February 2004

Dedications

This work is dedicated to my Parents, Shubhada and Bhaskar, whom I owe everything in my life. Their life and the principles they believed in throughout the life has always been an endless source of inspiration for me. They willingly sacrificed many comforts in their life for us (me and my sisters) and for our whole family. I can only hope for to make that up to them, someday.

I would also like to dedicate this work to Piyu, who shared my dreams and encouraged me to pursue them. Her warm presence in my life and the boundless love given to me provided the much needed emotional support to complete this work.

I'm short of words to express my feelings towards my Mom, my Dad and Piyu, for their patience, their trust on me and the unconditional love given to me throughout the extremely difficult and challenging times in my life. Without three of them, my PhD would have been 'dream impossible'.

Acknowledgements

I would like to take this opportunity to express my deepest gratitude towards my advisor, Dr. Michele Marcolongo, for the trust shown on my abilities and her constant encouragement throughout my studies. I was extremely fortunate to have her as an advisor and without her undying support at all times, it would have been extremely difficult to accomplish this work.

I'd also like to express my sincere feelings towards Dr. Andrew Karduna and Dr. Edward Vresilovic for their unbound patience and innumerable things I learnt from them. Their input and guidance made invaluable contribution to this dissertation. Many people guided me throughout this study and I'd especially like to mention Dr. Anthony Lowman, Dr. Antonios Zavaliangos and Dr. Alex Radin for sharing their vast knowledge with me.

I'd like to thank my colleagues in the Materials Science and Engineering Department for many fruitful technical discussions, especially Dr. Jovan Jovicic, Dr. Abhishek Bhattacharya, Jing Zhang and Vishwanath Sarkar. I'd also like to thank all graduate students in the department, notably Emily Ho, Jonathan Thomas, Lalitkumar Bansal and Nikola Trivic, all of whom made every possible effort to make my stay in Drexel, a pleasant experience. I'd also like to acknowledge the indirect help from many researchers and peers through the literature, which paved the foundation for this work. I sincerely thank National Science Foundation (NSF) for funding of this research project.

I gratefully acknowledge the emotional support from my whole family, friends and all the wonderful things they did for me. I'm also grateful to two special friends, Manasi Deshpande and Dr. Pradnya Kulkarni, for their support and their trust on me with something which is very precious to them.

Table of Contents

List of Tables

List of Figures

Abstract

Mechanical Behavior of the Human Lumbar Intervertebral Disc with Polymeric Hydrogel Nucleus Implant: An Experimental and Finite Element Study

Abhijeet Bhaskar Joshi

Michele Marcolongo, PhD, PE

The origin of the lower back pain is often the degenerated lumbar intervertebral disc (IVD). We are proposing replacement of the degenerated nucleus by a PVA/PVP polymeric hydrogel implant. We hypothesize that a polymeric hydrogel nucleus implant can restore the normal biomechanics of the denucleated IVD by mimicking the natural load transfer phenomenon as in case of the intact IVD.

Lumbar IVDs (n=15) were harvested from human cadavers. In the first part, specimens were tested in four different conditions for compression: Intact, bone in plug, denucleated and Implanted. Hydrogel nucleus implants were chosen to have line-to-line fit in the created nuclear cavity. In the second part, nucleus implant material (modulus) and geometric (height and diameter) parameters were varied and specimens (n=9) were tested.

Nucleus implants with line-to-line fit significantly restored (88%) the compressive stiffness of the denucleated IVD. The synergistic effect between the implant and the intact annulus resulted in the nonlinear increase in implanted IVD stiffness, where Poisson effect of the hydrogel played major role. Nucleus implant parameters were observed to have a significant effect on the compressive stiffness. All implants with modulus in the tested range restored the compressive stiffness. The undersize implants resulted in incomplete restoration while oversize implants resulted in complete restoration compared to the BI condition.

Finite element models (FEM) were developed to simulate the actual test conditions and validated against the experimental results for all conditions. The annulus (defined as hyperelastic, isotropic) mainly determined the nonlinear response of the IVD. Validated FEMs predicted 120-3000 kPa as a feasible range for nucleus implant modulus. FEMs also predicted that overdiameter implant would be more effective than overheight implant in terms of stiffness restoration. Underdiameter implants, initially allowed inward deformation of the annulus and hence were less effective compared to underheight implants.

This research successfully proved the feasibility of PVA/PVP polymeric hydrogel as a replacement for degenerated nucleus. This approach may reduce the abnormal stresses on the annulus and thus, prevent/postpone the degeneration of the annulus. A validated FEM can be used as a design tool for optimization of hydrogel nucleus implants design and related feasibility studies.

1. Introduction

Lower back pain is one of the most important socioeconomic diseases and one of the most important health care issues today. Over five million Americans suffer from lower back pain, making it the leading cause of lost work days next only to upper respiratory tract illness[1-5]. On an average, 50-90% of the adult population suffers from lower back pain[6] and lifetime prevalence of lower back pain is 65-80%[7]. Lower back pain symptoms falls into three general categories based on the duration of the pain experienced. It is estimated that 28% experience disabling lower back pain sometime during their lives, 14% experience episodes lasting at least 2 weeks while 8% of the entire working population will be disabled in any given year[7]. The total cost of the lower back disabilities is in the range of $50 billion per year in the United States[8] and £12 billion per year in the United Kingdom alone[9]. The causes of lower back pain often remain unclear and may vary from patient to patient. It is estimated that 75% of such cases are associated with lumbar degenerative intervertebral disc disease[1].

The (lumbar) intervertebral disc is situated in between adjacent vertebrae. The disc is basically a composite structure made up of three different tissues; the central core is called the nucleus pulposus which is surrounded by the multilayered fibers of annulus fibrosus and the cartilaginous end plates. The nucleus is predominantly water in a matrix of proteoglycan, collagen and other matrix proteins[10]. The water content of the nucleus is very high at birth (90% or so) and then decreases at older age to 70% or even less[11,12]. The annulus surrounds the nucleus with successive layers oriented in alternating direction. The annulus is under tension when the nucleus absorbs water and swells[13].

The cartilaginous end plates have multiple perforations that allow exchange of water and nutrients into the disc[14].

In case of the normal healthy disc, any load acting on the disc is transferred to the annulus by means of swelling pressure (intradiscal pressure) generated by the nucleus. The water binding capability of the nucleus is a function of the chemical composition of the nucleus[14]. However, with aging and/or degeneration, the types of proteoglycans change[15] and the proteoglycan/collagen ratio decreases, which results in the lower water binding capability of the nucleus[16]. The load transfer mechanism in case of such dehydrated disc is significantly altered. The nucleus can not generate enough intradiscal pressure (because of low water content) and thus is unable to perform its normal function of load transfer to the annulus. As the nucleus dehydrates and shrinks, the loads on the nucleus decrease while those on the annulus increase[17]. It was observed that radial tears, cracks, and fissures occur first within the annulus[18]. If these do not heal in time, the nucleus may migrate from the disc center to the disc periphery through the annulus up to the nerve root. The contact of the migrated nucleus with the sinu-vertebral nerve root causes radicular back pain[14].

Many conservative treatment options exist for lower back pain. These generally aim for reducing the pain arising out of nerve root impingement and inflammatory response because of the migrated nucleus. Popular surgical treatments include Discectomy and/or Spinal Fusion and are sought when conservative treatments fail. Although these surgical treatments successfully relieve pain, they fail to restore the normal biomechanical function of the spine[19,20]. The nucleus is still dehydrated and the annulus fibers are still likely operating in compression. Furthermore, these procedures

may generate additional stresses (and hence accelerated degeneration) within the operated disc[20-23] (in case of discectomy) or on the adjacent discs and loss of mobility[24-26] (in case of spinal fusion).

The long-term objective of this research agenda is to treat a degenerated lumbar intervertebral disc by mimicking the physiological intradiscal pressure, whereby the annular degenerative process (including the associated pain) would be postponed or prevented and the normal biomechanical function of the spine would be restored. The goal of the present study is to evaluate the concept of nucleus replacement with a polymeric hydrogel implant in terms of restoration of normal biomechanics of the spine, in compression. We propose the use of poly (vinyl) alcohol (PVA) and poly (vinyl) pyrrolidone (PVP) copolymer blend as a substitute for a degenerated nucleus pulposus. These materials have generally shown behavior consistent with biocompatibility[27-29] although comprehensive studies have not been published yet. The Poisson effect of a hydrogel is proposed to exert intradiscal stress on the annulus fibers, similar to the physiological intradiscal pressure observed in case of the normal healthy disc. This would mimic the natural load transfer phenomenon and may restore the normal biomechanical behavior of the lumbar spine. Because of their shape memory characteristics, nucleus implant hydrogels offer an attractive potential solution for lower back pain treatment, with minimum invasive surgical procedures.

2. Background

2.1 Human Spine

The human spine is a mechanical structure that performs three fundamental biomechanical functions simultaneously[30]. First, it transfers the weights (and resultant bending moments) of the head, trunk and any weights being lifted to the pelvis. Second, it allows sufficient physiological motion between the head, trunk and pelvis. Third and most important, it protects the delicate spinal cord from the potential damaging forces (and moments) resulting from the physiological motions and trauma[30]. Figure 2.1 shows the schematic of the human spine, which is divided into three main regions. The upper region, with seven vertebrae, is called the 'Cervical Spine'; the middle region, with twelve vertebrae, is called the 'Thoracic Spine' and the lowermost, with five vertebrae, is called the 'Lumbar Spine'. At the distal end of the spine, there is a basin shaped structure called the 'pelvis' that supports the spinal column and is made of the 'sacrum' and the 'coccyx' with fused vertebrae. Human spine is not an exactly straight structure, but has specific curvature, as seen from Figure 2.1. The spine in the cervical and in the lumbar region is slightly convex anteriorly while in the thoracic and sacral region, it is slightly convex posteriorly. The specific shape allows the increased flexibility while maintaining the overall spinal stability. It also facilitates increased shock absorbing capacity along with adequate stiffness[30].

Each vertebra is made up of several parts. Figure 2.2 shows schematic of the vertebrae in a vertebral column. The body of the vertebra is the primary weight bearing area. It also provides the resting place to the intervertebral disc, which separates the

adjacent vertebrae and acts as a cushion between them. There is a large hole in the center part (spinal canal) which is covered by 'Lamina'. The spinal cord runs through this spinal canal. There is a protruded process in the central posterior region, called 'Spinous Process', which can be felt by running our hand down the back. There are pairs of 'Transverse Processes' which are orthogonal to the spinous process and provide attachment for the back muscles. There are also four facet joints associated with each vertebra. Four facet joints in two pairs (superior and inferior) interlock with adjacent vertebrae and provide the stability to the spine. An intervertebral disc is situated in between adjacent vertebrae. The discs are labeled with respect to the vertebrae levels, between which they are located. Thus, the T12/L1 disc is located between the 12th thoracic and 1st lumbar vertebrae while the L3/L4 disc is located between the 3rd and 4th lumbar vertebrae. Lower back pain is associated with the degenerative lumbar intervertebral disc disease and the discussion henceforth always refers to the lumbar spine, unless otherwise specified.

2.2 Intervertebral Disc

2.2.1 Structure

The intervertebral disc is the largest avascular tissue in the human body[30]. It constitutes about one third height of the entire spinal column. The disc is primarily made of three different tissues; the central jelly-like portion is 'Nucleus Pulposus' (NP), which is surrounded by the outer laminated structure of the 'Annulus Fibrosus' (AF). The thin cartilaginous endplates with multiple perforations are in between the disc and a vertebra. Figure 2.3 shows the schematic of the lumbar intervertebral disc (IVD).

The nucleus pulposus comprises about half of the healthy intervertebral disc and is essentially water in a matrix of proteoglycan, collagen and other matrix proteins[10]. The water content of the nucleus is very high at birth (90% or so) and then decreases at older age to 70% or even less[11,12]. The high water content of the nucleus is mainly due to the presence of hydrophilic proteins called Proteoglycans (PGs)[31]. PGs are the most abundant macromolecules present in the nucleus, accounting as much as 65% of the dry weight at young age, which may decrease to as low as 30% [11,12,32,33]. PGs consist of sulfated glycosaminoglycans side chains covalently bonded to core proteins. These molecules have the ability to attract and retain water due to ionic carbonyl and sulphate groups on the glycosaminoglycans chains[16,34,35]. These large molecules with their negatively charged sulfate groups are not free to diffuse out of the nucleus. They are highly hygroscopic as some of the PGs are linked to hyaluronic acid, a longer chain of very hydrophylic nonsulfated glycosaminoglycan[36-38]. Collagen comprises about 20% of the dry weight, while a variety of noncollagenous proteins and elastin account for the rest of its dry weight. The external load acting on the disc determines the equilibrium water content of the disc. As the load increases, the pressure inside the nucleus also increases and the water is squeezed out into the vertebrae through perforated endplates. When the load on the disc decreases, the pressure within the nucleus also decreases and the water returns. Such a mechanism essentially creates an effective pump, providing a circulation path for the inflow of water, nutrients and outflow of metabolic waste[14].

The annulus fibrosus gradually differentiates from the periphery of the nucleus to form outer boundary. The annulus is tough, outer fibro-cartilaginous layer of the disc. Water accounts for 60-70% of the total annulus mass[34]. The annulus is often compared to

the laminated automobile tire. The collagen fibers of the annulus are laid down in 15 to 20 multiple plies. The annulus fibers insert into the superior and inferior vertebral bodies[38]. The fibers in the alternate layers are oriented in the opposite direction, with an angle of ± 30º with respect to the radial direction. Figure 2.4 shows a schematic of the structure of the annulus fibrosus. Depending on location within the disc, the fibers are connected to vertebral endplates or directly to the vertebra. Because of this specific structure, the annulus essentially binds the adjacent vertebrae together and play major role in resisting of torsion[36,39]. It is the compressibility of the annulus, which accommodates the bending and twisting of the intervertebral disc. The outer annulus is primarily made of type I collagen while type II collagen is predominant near the nucleus. Other types of collagen, such as type V, VI and IX are also present in the annulus alongwith minor amount of type III collagen[32,34].

The cartilaginous endplates essentially separate the disc from the vertebral bodies. The endplates are recognizable as discrete entities at an early stage in the development of the axial skeleton and remain as cartilaginous endplates during the subsequent ossification of the vertebrae[40]. The cartilaginous component of the endplates consists of a gel of hydrated PG molecules that is reinforced by a network of collagen fibrils[41]. The cartilage in these endplates resembles the chemical structure of the adjacent portion of the disc[34]. Hyaline cartilage is the major component of the end plate, which is approximately 1 mm thick. The collagen content is highest, but the PGs and water content are lower as compared to the adjacent nuclear and annulus regions. In addition to serving as a semipermeable membrane that facilitates the diffusion of the solutes from vertebra to the disc, the end plate also prevents the nucleus pulposus from bulging into the adjacent

vertebral body[42] while absorbing the hydrostatic pressure resulting from mechanical loading of the spine[43].

2.2.2 Intervertebral Disc Mechanics

Elastic Characteristics

An intervertebral disc is situated in between adjacent vertebrae and acts as a cushion between them. A functional spinal unit (FSU) is the basic building block of spinal biomechanics and exhibits the generic characteristics of the spine. A FSU basically consists of an intervertebral disc in between adjacent vertebrae, along with facet joints and posterior elements (Figure 2.5). In general, the results obtained for a single FSU are a good reflection of the overall behavior of the spine[44].

A FSU has six degrees of freedom; 3 translational and 3 rotational, as shown in the Figure 2.6. Thus, any one of the motion components may be accompanied by five coupled motions. The basic loading modes acting on the spine while performing daily activities are axial compression, flexion/extension, lateral bending and torsion. The spine is always under compression, even in the supine position. It is important to distinguish between the loads acting on the disc and stresses produced within the disc.

In case of normal healthy disc, any vertical load acting on the disc is distributed horizontally by means of special load transfer mechanism. The compressive load is transferred from one vertebral end-plate to the next by means of nucleus pulposus and annulus fibrosus. The applied load on the disc creates hydrostatic pressure (Intradiscal Pressure) inside the nucleus. This pressure acts on the inner annulus fibrosus layers and pushes the surrounding annulus in all directions. The annulus fibers resist applied loads when they are in a stretched condition, which may occur either due to application of the

hydrostatic pressure exerted by the nucleus or upon application of tensile forces. Thus, after the application of a load, the central portions of the two adjacent end-plates are pushed away from each other[45,46] and the annular ring is pushed radially outward[47-49]. The compression load produces complex stresses within the annular ring. Figure 2.7 shows a non–degenerated disc under compression and the resulting stress distribution in the annulus, as proposed by White et al[30]. In the outer annulus layers, stresses are small. The annular fiber stresses are tensile while the axial, circumferential and radial stresses are compressive. In the inner annulus layers, a similar trend of stresses is observed, except that the stress magnitudes are much larger.

Compression testing has been the most commonly used method for the study of mechanical behavior of the disc, because the disc is a major compression-carrying component. Many experiments have been performed to determine the compressive mechanics of the intervertebral disc[48,50-52]. Typically, the load-displacement curve is of sigmoid type (Figure 2.8) with concavity towards the load axis (Y-axis) initially, followed by a straight line and then, convexity towards the load axis in the final phase. The specific nature of this curve indicates very little resistance at low loads. As the load is increased, the disc becomes stiffer. In that sense, the intervertebral disc provides flexibility at low loads and stability at high loads. Interestingly, it was observed that compression load alone is not responsible for herniation of the nucleus pulposus[51,53,54].

Generally speaking, the disc is rarely subjected to pure tensile loads. However, the annulus is subjected to tensile stresses because of the load transfer from nucleus intradiscal pressure. Also, in the case of flexion, the posterior region of the disc is under tension while in extension, the anterior part of the disc is under tension. In lateral

bending, the tensile stresses are produced on the convex side of the bend and at about 45º to the disc plane in case of the axial rotation[30]. The experiments done on the annulus section[55,56] confirmed the hypothesis that intervertebral disc is an anisotropic structure[30].

Bending and torsional loads are important to study because experimental findings suggest that pure compression loads do not damage the disc[50]. Bending of 6-8º in the sagittal, frontal and other vertical planes did not result in failure of the lumbar disc. But, after removal of the posterior elements and with 15º of bending (anterior flexion) failure of the disc was observed[48]. It was found that the disc bulged anteriorly during flexion, posteriorly during extension, and toward the concavity of the spinal curve during lateral bending. It was also observed that the bulging of the annulus is always on the concave side of the curve and that denucleation seemed to increase bulging[57]. The hypothesis that torsional loading may be responsible for disc injury was first proposed by Farfan[50,58]. When the lumbar spine specimens were subjected to torsional loads around a fixed axis, sharp, cracking sounds were heard emanating from the specimen at a deformation angle of 20º or so. It was hypothesized that those cracking sounds came from the injuries to the annulus. The angle of failure was less for the degenerated discs (14.5º) compared to normal discs (16º). Logically, it was also found that large disc exhibited higher torsional strength and round discs were stronger than oval discs[58].

In another experiment, a very high value of 260 N/mm for the shear stiffness (in anteroposterior and lateral direction) was reported, indicating that it is rare for an annulus to fail clinically because of pure shear loading[59]. Thus, it is logical to conclude that failure of the intervertebral disc probably occurs because of some combination of bending, torsion and tension loads[30].

Viscoelastic Characteristics

The intervertebral disc, like many other biological tissues, exhibits viscoelastic behavior. That means the mechanical behavior of the disc is sensitive to the rate of loading and time history. Viscoelastic behavior is typically composed of two components: viscosity and elasticity. Creep and relaxation testing are generally used for quantification of viscoelastic behavior. Creep tests involve application of a constant load (the resulting displacement is measured as a function of time) while relaxation tests involve application of a constant deformation (the resulting decrease in load is measured as a function of time).

In one experiment, three different loads were applied during creep testing, for 70 minutes, on lumbar spinal segments[54]. The higher loads produced greater deformation and faster rates of creep. It was also found that the creep behavior is closely related to the level of disc degeneration[60]. The normal discs creep slowly and reach their final deformation value after considerable time, as compared with the degenerated discs[30].

Typically, all viscoelastic structures exhibit hysteresis. Intervertebral discs also show this phenomenon in which there is loss of energy after repetitive loading-unloading cycles. Hysteresis in the intervertebral discs is observed to vary with the applied load, age and disc level[53]. It is directly proportional to the applied load level. Very few fatigue tests have been done on the lumbar intervertebral discs[30]. In one study, a small constant axial load and a repetitive forward bending motion of 5º was applied on the intervertebral disc. The disc showed signs of failure only after 200 bending cycles and failed completely after 1000 cycles[48,61].

The effect of preload on the lumbar spinal segment has been studied at length by Panjabi et al[61]. It was found that the spine became more flexible in the presence of preload, with the physiological forces directed laterally or anteriorly. However, the preloaded spine was less flexible when subjected to axial tension or axial torsion. No appreciable changes were noticed in case of axial compression, posteriorly directed force or extension moment due to preload.

2.3 Degenerative Disc Disease

As the human life progresses, significant changes occur in the lumbar disc components. Intervertebral Disc Degeneration (IVDD) can be defined as the loss of normal disc architecture accompanied by progressive fibrosis. At birth, the water content of the annulus fibrosus is about 80% and that of the nucleus pulposus is about 90%. This water content decreases eventually up to as low as 70% or less, in case of nucleus[62]. With age, nuclei transform from gelatinous substance (90% water) into more solid-like structure. A further decrease in the number of healthy nuclear cells also takes place. In the annulus fibrosus, macroscopic changes are not readily discernible unless nuclear changes are advanced. However, microscopic changes such as, fragmentation of fibers, mucinous degeneration of fibers leading to cyst formation and focal aggregation of the collagen to form round aggregates of amorphous material, are observed in early stage of degeneration[63]. Reduction in the disc height, to a limited extent, occurs during adult life as the water content of the nucleus reduces. This disc narrowing is also associated with the bulging of the annulus towards the circumference of the disc[64]. Loss of disc height is clinically important because it eventually leads to nerve root opening[14,65,66]. The salient features of IVDD are the loss of gelatinous nucleus pulposus, gradual disappearance of

the originally well defined border between the nucleus and annulus, coarsening of the annulus lamellae, progressive fibrosis and later fissuring of the annulus fibrosus with the deposition of the aging pigment[67-70].

With age and degeneration, total PG content decreases while the keratin sulfate / chondroitin ratio increases. It is suggested that degradation occurs in the hyaluronic acid binding region and that proteoglycan synthesis is slower in IVDD[71]. It was also proposed that the decrease in PGs content results from cell death due to lower pH[66]. Because of this, the nucleus is unable to retain enough water for generation of intradiscal pressure as in the case of the normal discs. The load transfer mechanism is clearly altered in the case of a dry nucleus. Because of this, the end plates are subjected to reduced pressure at the center and the more pressure around the periphery. The stress distribution in the annulus is also altered significantly. Figure 2.9 shows the load transfer mechanism in case of a degenerated disc, as proposed by White et al[30]. Outer annulus layers of the degenerated disc experience circumferential stresses which are near zero or tensile. In the inner layers, the fiber stress is compressive. The circumferential stress is very small, annular stress is tensile and peripheral stress nearly vanishes[72]. Essentially, the nucleus does not perform its function of load transfer and the load transfer occurs through an end plate – annulus – end plate route. The annulus is subjected to abnormal stresses (mostly compressive), although it is naturally structured to support tensile stresses. Because of this altered load mechanism, the annulus is more prone to injuries and cracks/fissures first develop into the annulus.

With continued degeneration, the central nucleus may migrate through the crack developed in the annulus towards the periphery. The migration of the nucleus material is

referred to as ‘disc herniation’. The migrated material may impinge on the nerve root. The contact of the migrated nucleus with the nerve root irradiates debilitating back pain. Also, the herniated material elicits an inflammatory response because of the avascular nature of the nucleus[14]. The reduction in the disc volume leads to instability, resulting in the growth of bone, endplates and ligaments to compensate for this volume loss (Spinal Stenosis).

It is difficult to distinguish between the effects of aging from that of degeneration on the biomechanical behavior of the lumbar disc. The biomechanical behavior of the disc is dependent upon its state of degeneration which in turn depends upon the age. It was found that disc degeneration first appears in males in the second decade and in females a decade later. It was also observed that by age 50, almost all lumbar intervertebral discs (97%) are degenerated[73], though not all are symptotatic.

2.4 Treatment Options

2.4.1 Conservative Treatments

The most common conservative treatment is bed rest. This helps in the reduction of the intradiscal pressure. However, this treatment is only effective for very early stage disease patients and does not provide much benefit when the pain/disease stage is severe. It may lead to muscle atrophy and deconditioning. There are many drugs including muscle relaxants, sedatives and analgesics to alleviate lower back pain. Other treatments such as ultrasound, chiropractic therapy, electrotherapy, magnetic fields are also in use. However, the effects by these treatments are temporary and furthermore, these do not treat the root cause of the lower back pain. When these treatments fail, the patient is generally referred for surgery.

2.4.2 Surgical Treatments

Discectomy and Spinal Fusion are the most popular surgical treatments for lower back pain. Discectomy is employed when disc herniation occurs and the migrated nucleus is impinging on the nerve root, causing back pain. This method is followed when the annulus degeneration is not severe. In this surgery, the impinging portion of the disc i.e. the nucleus pulposus and part of the annulus is excised in order to relieve the pressure on the nerve root. This eliminates the back pain in 90-95% of the cases[19]. However, the aim of this procedure is to reduce the back pain and not to restore the normal intervertebral disc biomechanics[20]. The nucleus pulposus is still in the dehydrated state and the annulus (or, part of it) is still likely under abnormal compressive stresses. Furthermore, after discectomy, the operated disc may experience additional stress leading to the path of degeneration for coming years.

Spinal fusion, on the other hand, is for patients having chronic back pain and whose annulus is severely damaged. This procedure involves inducing bone growth across the adjacent vertebrae (functional spinal unit). This reduces back pain and eliminates disc loading at the cost of mobility of the patient. Again, the aim of this approach is to reduce back pain and not to restore the normal intervertebral disc biomechanics. Regardless of the extent to which it is performed, the results of spinal fusion vary extensively. Also, the lack of motion within segments can lead to further degeneration of the adjacent discs[25], creating more instability and pain. This in turn, may lead to repeat surgeries until the entire lumbar spine is fused. In one long-term study of fusion, it was found that 44% of the patients were currently still experiencing low back

pain, 50% had back pain within the previous year, 53% were on medications, 5% had late sequeli secondary to surgery, and 15% had repeat lumbar surgery[74].

This suggests the need for new, effective alternatives to treat and cure the lower back pain.

2.5 Emerging Approaches for Lower Back Pain Treatment

The motivation behind exploration of new and better solutions for the treatment of lower back pain is the failure of current treatments (conservative and surgical) in terms of the restoration of the disc height and normal disc biomechanics. This is further aggravated by the complications that may occur after the surgical treatments, such as discectomy and/or spinal fusion.

Total disc replacement, where an entire diseased disc is removed and replaced by a synthetic implant is an emerging approach as an alternate to current surgical procedures for the treatment of the lower back pain. The other potential approach is nucleus pulposus replacement, where only the nucleus portion of the disc is replaced either by a synthetic implant or recreated using tissue engineering technique.

2.5.1 Total Disc Replacement

This approach target for later stages of disc degeneration (Galante Grade IV)[55], where the annulus is severely degenerated and is beyond repair. The diseased disc is entirely removed and replaced by a synthetic material. A similar approach for total knee and hip replacement is highly successful. Disc replacement may serve to eliminate the back pain and restore the physiological motion. This total disc prosthesis would be better option to spinal fusion and/or discectomy as it allows the physiological motion between the adjacent vertebrae. Another advantage would be that the effectiveness of the surgery

will not be dependent on the integrity of the annulus or degeneration state[8]. Total disc prostheses are susceptible to the inherent problems in the composite materials such as weak interfacial bonding and wear. To simulate the natural structure and function of the functional spinal unit, total disc prostheses should also have adequate fixation to the vertebral end plate and vertebrae.

The principal advantage of using an all-metal total disc prosthesis is the inherent high fatigue strength of theses materials. It was suggested that a material should withstand fatigue test loading up to 100 million constant amplitude cycles[3,75]. This is equivalent to a 40 year life span. This goal of the implant fatigue design is rational, because the degenerative disc disease progresses in the third decade or so.

Knowles[76] filed a patent for a device, which would serve as a wedge between the spinous processes posteriorly. However, it does not restore any natural flexibility to the disc[14]. Hedman et al[3]. designed an all-metal disc which is composed of two Ti-6Al-4V (Ti alloy with 6wt% Al and 4wt% V) springs placed between the hot isostatically pressed or forged CoCrMo endplates with CoCr beads sintered to the endplates to ensure bony ingrowth fixation. The device was fatigue tested up to 100 million cycles *in vitro*. It was, however, shown that this device generated wear particles from both the spring/endplate interface and hinge/pin interface[77]. An artificial disc composed of upper and a lower cup-shaped plate was designed by Patil[78]. The plates were anchored to the bone by a series of spikes, emanating from the plates. No detailed experimental results have been published on this device. It was speculated that[79] the spring system designs (such as by Hedman[3] and Patil[78]) grossly oversimplify the spinal motion and are subject to possible tissue interpenetration. A prosthetic device shaped as a ball and socket, was

proposed by Salib et al[80]. Although, six degrees of freedom were allowed, device motion while loaded in compression was expected to cause increased friction and generation of wear debris[14]. Artificial disc prostheses made up of polymers and elastomers were also proposed. Stubstad et al[81]. utilized all synthetic materials for prosthetic disc. The nucleus was made of silicone, while the annulus was made of weaved Dacron® fibers. This device supported the tissue ingrowth and fixation in the weave. Another disc was proposed by Downey[82] with the central core made up of soft polymeric foam and the end plates made up of more rigid silicone. One can found reports of many similar designs using polymeric materials in the literature[14]. Lee et al[83]. and Parsons et al[84]. proposed a novel approach by taking into consideration the compression-torsional stiffness in the design of an artificial disc. The disc was studied extensively in vitro, in vivo, and with finite element models[85]. However, a lack of fixation between the implant and the vertebral bodies prevented theses devices from being tested clinically[8].

The SB Charite III disc by German orthopaedic surgeons in conjunction with Link® has undergone the longest clinical trials among all the artificial discs proposed. It consists of an ultra-high molecular weight polyethylene (UHMWPE) sliding core positioned between two CoCrMo endplates. The clinical results of the disc showed that 92% of the group had preoperative back pain and 40-50% reported a reduction in leg pain. This device does not attempt to simulate the intact disc mechanics. It was claimed that[86] Charite III disc design is unconstrained with a center of rotation that is too anterior and projects that the polyethylene core would undergo cold flow in about four years. Lee et al[79]. suggested that dislocation of the implant *in vivo* is due to the unconstrained nature of the sliding polyethylene core. Over 2000 SB Charite discs have been implanted in

patients since 1984[8]. European clinical trials over 2-5 years showed satisfactory results in 63% of the patients[87].

In the United States, Steffee[88] developed an artificial disc, Acroflex®, in collaboration with Acromed Corporation. This prosthesis consists of a hexane based and carbon black filled polyethylene rubber core. This rubber core was vulcanized to two titanium plates, which was subsequently modified to avoid release of a carcinogenic chemical. This was the first intervertebral disc prosthesis approved by the FDA to undergo clinical trials.

Many research groups have proposed somewhat similar artificial disc design for replacement of the diseased disc. A few important designs proposed over the time are those by Fuhrmann et al.[89], Pisharodi[90], Main et al.[91] and Marnay[92]. Figure 2.10 shows some of the prostheses designs developed earlier.

2.5.2 Nucleus Pulposus Replacement

2.5.2.1 Synthetic Materials as a Substitute for the Nucleus Pulposus

The nucleus pulposus is a major component of the intervertebral disc and is actively involved in the disc function and load transfer mechanism. It is also involved with the pathologic changes of the disc. Researchers began to consider the nucleus replacement because of the benefits associated with it compared to the total disc replacement.

The advantages of the nucleus replacement, either by a synthetic material or by tissue engineering approach, are significant. The rest of the disc components i.e. the annulus fibrosus and the end plates, remain intact. Preserving of the natural tissue structure also preserves their natural function. This facilitates simpler implant design and

faster manufacturing process. The complexity and complications involved in the design and implantation of the total disc replacement are avoided. This approach would also be less invasive as compared to total disc replacement. The major problem of implant fixation to the vertebrae/end plate does not arise in the nucleus replacement. The time required for surgical procedure would be much smaller compared to the total disc replacement and may approach to the time required for a discectomy[8]. Nucleus replacement, as in case of total disc replacement, aims for restoration of the normal disc mechanics and functions, in contrast with the current surgical procedures of the discectomy and the spinal fusion, as described previously.

Bao and Yuan[93] have detailed the requirements for design of nucleus prosthesis. Nucleus implant, in addition to meeting the basic requirements such as biocompatibility and fatigue strength, should restore the normal load distribution. It should have sufficient stability in the space and should also avoid excessive wear on the end plate-implant interface. For that matter, the nucleus implant with low friction surface and good conformity with the nuclear cavity would be desirable. An ideal nucleus implant should also restore the natural body fluid pumping action. From a surgical point of view, the implant should be easy to implant in the patient and the implantation procedure should be compatible with various discectomy techniques with minimum invasive surgery.

Although Nachemson, in early 1960s used silicone as a nucleus replacement[94], the first human implanted nucleus prosthesis was developed by Fernstrom in 1966[95]. This device was made of solid stainless steel ball, which was designed to serve as a spacer allowing movement between the adjacent vertebrae. This did not restore the normal load distribution and was discarded because of the basic problems such as implant migration

within the cavity and subsidence. It was realized that the solid metals are too stiff as nucleus implants. The elastic nucleus prostheses made of elastomers were proposed, either into '*in situ* formed' nucleus prostheses or 'preformed state'.

The '*in situ* formed' nucleus prostheses are based on the concept of injecting the curable polymer into the created disc space and allow *in situ* curing of the polymer to form a prosthesis. Since the polymer is not in the final desired shape, it can be injected with a minimal surgical invasive procedure through small annular incision, before it is allowed to cure. The benefits of this approach would be better filling of the nuclear cavity, better load distribution and stability[93]. However, some points of concern would be the resulting load distribution, fatigue strength and curing time. As the polymerization would complete in the body, it should be achieved with minimum if any non-toxic leachables.

The 'preformed' nucleus implants, on the other hand, offer more consistent properties and better control on the design/manufacturing of the implants. Preformed implants are more suitable for characterization purposes and can be manipulated relatively easily to achieve the desired material properties. The potential problems with this approach would be the filling of the nuclear cavity and invasive surgical procedures. There is also a new design concept, which focuses on the nucleus implant shape/size. The implant size can be very small during the implantation and the original (desired) size can be regained after the implantation. Use of collapsible balloons is feasible for this approach, wherein, the collapsible balloon can be inserted in the cavity and then inflated using an incompressible fluid[93]. Implantation of hydrogel nucleus prosthesis in a dehydrated shape (before implantation), which would rehydrate in the disc, is also a

feasible approach[93]. Although, nucleus replacement is beneficial compared to the current surgical procedures, it will be of no use in the cases where the annulus degeneration is severe and the disc is in the later stages of degeneration.

Eysel et al.[96] studied the behavior of a prosthetic lumbar nucleus in flexion/extension, right/left side bending and right/left torsion, using a prosthesis disc nucleus (PDN) developed by Ray[38]. Three different conditions were tested as intact, after nucleotomy and after implantation of two PDN devices. They recorded an increase in the segmental mobility in all directions after nucleotomy, between 38-100%. Implantation of two PDN implants restored the segmental mobility as compared to the intact segment. Creep response of these implants was also studied[97]. It was recorded that the PDN device restored the viscoelastic behavior of the intact spine. The PDN device was also studied in the baboon lumbar spine[98]. However, the results in that experiment were not satisfactory. A progressive loss in disc height, end plate degeneration, implant subsidence and increasing sclerosis at adjacent vertebrae were observed. In summary, the nuclear cavity was not filled properly and migration of the implant in vivo could be one of the potential problems. The size of these implants, which are placed side-by-side in medial-lateral position, requires annular window to be bigger than that required in case of discectomy[8]. Plus, their specific shape may not mimic the natural load transfer mechanism, where the hydrated nucleus generates intradiscal pressure and applies tensile stresses to the annulus.

In another study, fatigue durability of the disc nucleus system in a calf spine model was studied[99]. An *in situ* polymerizable protein hydrogel device (BioDisc) was used as a nucleus implant. It is introduced as a liquid into the disc space, which cross-links to form a durable hydrogel, which would maintain the disc height and stability

while preserving motion. The specimen was loaded to 10 million cycles to assess the mechanical durability of the implant.

Biomechanics of the multisegmental lumbar spine with a prosthetic nucleus was studied by Dooris et al.[100] The nucleus implant was *in situ* curable polymer. A catheter and balloon system was used for the implantation purposes. A liquid polymer was injected using this system under controlled pressure, by inflating the balloon. The implant is advantageous in the sense that it requires the minimum invasive procedure and potential to be performed arthroscopically. However, localized heating of the tissue could be a potential problem, as polymerization is an exothermic process.

Hou et al.[101] used silicone rubber for nucleus replacement *in vitro* and in monkeys. The results from the monkey model were satisfactory as no adverse reaction was observed from the surrounding tissue. A concept of fluid filled bladders was also proposed[102] in order to mimic the fluidic nature of the natural nucleus pulposus. However, in such a design, rupture of the bladder wall could often pose serious problems.

A poly (vinyl alcohol) (PVA) nucleus prosthesis was proposed by Bao et al.[14,103] The nucleus prosthesis aimed for restoration of the normal function of the intervertebral disc by means of mimicking both the mechanical and physiological properties of the disc. The PVA hydrogel material can absorb large quantities of water, more similar to the natural nucleus. It can act similarly to the nucleus pumping action, where the implant can absorb and release water, based on the applied load. A baboon test model of the PVA nucleus implant showed no adverse local or systemic tissue reaction[8]. However, this PVA implant may not be stable in the human body considering the fact that PVA is a semi-crystalline polymer, which is hydrophilic in nature. The implant can undergo

dissolution in the body, which involves unfolding of the polymer crystal chains that can join the amorphous part of the polymer chain, then disentangle and dissolve eventually. This may lead to decreased mechanical properties as a result of larger mesh size[104,105]. Another design was proposed by Bao et al.[106] which consist of an aperture sealing device. This aperture sealing device is proposed to be used with the implantable PVA nucleus replacement.

It has been shown that sheep lumbar intervertebral discs can be used as a model for the human discs[107]. Recently, Meakin et al.[108] replaced the nucleus pulpous of the sheep intervertebral disc by polymeric material. The effect of denucleation and effect of nucleus replacement by a polymeric material on the bulging of the annulus was observed. Video recording of sheep discs, sectioned in the sagittal plane was performed. When the nucleus was removed from the specimen, inward bulging of the annulus was observed. Three polymeric implants with different shapes and different material moduli were used as a nucleus replacement. It was observed that the outer annulus bulged outwards during the compression, for both intact and denucleated condition. However, in the denucleated condition, the inner annulus bulged inwards. This inward bulging of the annulus was reversed by inserting the polymeric implants into the denucleated specimen. Based on the experimental observations and finite element modeling, it was concluded that a solid implant with a Young's modulus in the range of 0.2 – 40 MPa can prevent the inward bulging of the annulus, observed in case of the denucleated condition. They also concluded that a nucleus should ideally have a Young's modulus of 3 MPa with total fill of the nuclear cavity. However, their prediction generates couple of concerns. The specimens used were sheep specimens and the results of the sheep specimens may not be

valid for the human lumbar intervertebral discs. It was difficult to determine the fill of the nuclear cavity with the implantation approach followed in that experiment. Also, the ideal value of the implant modulus predicted using the finite element model (E=3 MPa), is based on the selected properties of the annulus fibrosus, as an isotropic, elastic material for simplicity. Actually, the annulus is an anisotropic structure and can exhibit large strains, in contrast to the definition used by Meakin et al.[108] Although, this experiment provided some novel insights into the sheep disc mechanics, care should be taken in drawing the conclusions for the human lumbar discs from their data.

2.5.2.2 Regeneration of Nucleus Pulposus using a Tissue Engineering Approach

Use of tissue engineering for the regeneration of the degenerated nucleus pulposus of the lumbar intervertebral disc is still in infancy. Very few groups have tried to use this approach for the replacement of the nucleus, with a moderate success.

Stone[109] has attempted to regenerate the intervertebral disc using a scaffold of biocompatible, bioresorbable glycosaminoglycan fibers. This was designed so as to allow cell growth in the scaffold. Another tissue engineering approach for the nucleus replacement was proposed by Gan et al.[110,111] They implanted nucleus pulposus cells on PLGA (polylactide-co-glycolide) and bioactive glass substrates. The results were encouraging in terms of cell adhesion and proliferation of cells on both scaffolds. The bioactive glass with calcium phosphate rich layer was found to induce cellular activity better than that of PLGA. However, it was not clear whether the matrix was of healthy nucleus pulposus cells. Also, considering the avascular nature of the disc/nucleus pulposus, there are concerns with the feasibility of this approach into the practice.

Because of the avascular nature of the nucleus, it would be very hard to perform basic functions in the tissue engineering viz. cell migration, cell adhesion and cell growth.

This approach is reasonable in an era of tissue engineering solutions. However, cell and molecular biologists are still struggling to determine the nature of the nucleus pulposus cells, and so setting and meeting the requirements of regenerating the tissue, although promising, has many challenges to overcome before its adaptation into the clinical practice.

2.6 Nucleus Implant Biomechanics

Very little work is done that reveals the details of the resulting disc mechanics after the nucleus replacement, either by a synthetic material or by a tissue engineering approach. Although, there are reports of the mechanical behavior of the nucleus implanted lumbar disc[75,85,87,96-101,108,112-115], there is not much understanding about how the nucleus implant would work, the design requirements of an 'ideal' implant and how it will mimic the natural mechanical behavior of the intervertebral disc for restoration of the normal biomechanics.

As described in the previous section, Bao et al.[93] have mentioned the requirements of an ideal nucleus implant. Ideally, the nucleus implant parameters will also play major role in the resulting mechanical behavior of the nucleus implanted intervertebral disc. Especially, the implant material properties (e.g. Young's modulus and Poisson's Ratio), implant geometrical parameters (such as height and diameter) in reference with the created nuclear cavity and shape of the nucleus implant (cylindrical, spherical, spiral, pillow-shaped or cone shaped) would determine the nature and extent of restoration of the mechanical behavior of the implanted intervertebral disc.

Ideally, a nucleus implant should mimic the natural load transfer mechanism observed in a healthy disc. It should generate the stress on the inner annulus layers, which is equivalent to the natural intradiscal pressure generated by a hydrated nucleus pulposus. This would facilitate the restoration of the stiffness/mechanics of the implanted disc by means of applying tension to the annulus fibers, exactly as in the case of normal intervertebral disc. At the same time, it should not put additional or abnormal stresses, especially on the cartilaginous end-plate and annulus layers. The implant should have good fatigue strength in order to serve for a reasonable time period of at least 15 years, which corresponds to 15 million loading cycles approximately.

2.7 Finite Element Modeling of the Lumbar Intervertebral Disc

Considering the complex structure of the IVD and the diverse stresses to which it is subjected under physiological loading conditions, it is clear that experimental techniques alone are not sufficient to fully characterize the overall mechanical behavior of the motion segment. This was corroborated by the technical complexities which precluded the measurement of the stress state, deformation and disc bulge at different locations throughout the motion segment. This provided the motivation for the development of numerical methods, such as finite element analysis, to expand the experimental data in order to characterize the IVD parameters, which may be difficult to measure experimentally.

Many researchers have simulated the intervertebral disc mechanics using the finite element method. Belytschko et al.[116] were the first to use the finite element method for understanding of the intervertebral disc mechanics. The disc-body unit was assumed to be an axisymmetric object and annulus as a linear orthotropic material. This model

was further expanded to accommodate the nonlinear (orthotropic) properties for the annulus keeping all other parameters unchanged[117]. Values of the required properties of the annulus were found by matching the predicted Load-Displacement behavior with the corresponding experimental Load-Displacement behavior. A different approach was followed by Lin et al.[118], in which the annulus was defined as a linear orthotropic material. The required parameters of the annulus were determined by using an optimization scheme. Spilker[119] followed a different path for understanding of the disc mechanics. He reported the results of a parametric study based on a simple model of the disc, where the annulus was defined as a linear isotropic material. These models all fail to capture the orthotropic, non-linear behavior of the annulus fibrosus, clearly a challenging objective.

The first attempt to make a realistic finite element model of the lumbar intervertebral disc, considering the composite nature of the annulus fibrosus was made by Shirazi-Adl et al.[72] For the first time, this model accounted for both material and geometric nonlinearities alongwith the representation of the annulus as a composite of collagenous fibers embedded in a matrix of ground substance. The nucleus was modeled as an incompressible, inviscid fluid. The model was based on the lumbar L_2-L_3 functional spinal unit. This model was compared to the experimental observations of Load-Displacement behavior, disc bulge, end-plate bulge and intradiscal pressure. The stress distribution and strains in the cortical/cancellous bones, end-plates, annulus fibers and annulus ground substance were reported under compressive load. It was found that with a fully incompressible nucleus, the most vulnerable elements under the compressive loads are the cancellous bone and the end-plate adjacent to the nucleus. Interestingly, for

a fully denucleated spinal unit (simulating a degenerated condition) under compressive load, it was predicted that annulus bulk material was also susceptible to failure. The model predicted that the annulus fibers however, would remain intact under compressive load. Although this model was a milestone in the finite element modeling of the lumbar intervertebral disc, their modeling approach raises couple of concerns. Every test specimen is a different in terms of its mechanical behavior because of the biological variation with age, sex, disc level, work habits and loading history it had endured. This model takes into account two extreme conditions of intervertebral disc, for nucleus pulposus definition, either as an incompressible fluid or totally devoid of a nucleus. This may be sufficient for modeling purposes. However, in reality the nucleus is neither an incompressible fluid, nor it is totally removed for most of the patients. The nucleus pulposus structure is actually gum-like and is somewhere in between the solid-fluid with almost incompressible properties and it exhibits significant viscoelastic behavior (a function of rate of loading)[10,33,120]. Similarly, the annulus of every disc is different and thus precludes the common definition of the annulus with certain number of lamellar layers and fibers in a matrix substance. The type of collagen in the annulus also changes with age, thus altering its mechanical properties.

The same model[72] was expanded to assess the effect of axial torque in combination with compression[121] and sagittal plane moments[122]. It was found that axial torque, by itself, can not cause the failure of the disc fibers, but can enhance the vulnerability of those fibers located at the postero-lateral and posterior locations. In flexion, relatively large intradiscal pressures were predicted while in extension, negative pressures (i.e. suction) of low magnitude were predicted. It was concluded that[122] the

large flexion moments in combination with other loads is a most likely cause of disc prolapse, generally found at postero-lateral location of the annulus. The model was also expanded to simulate the changes in the fluid content of the human lumbar discs[123]. Change in the nucleus volume directly affected the resulting intradiscal pressure. Loss of fluid content increased the contact forces on the facet joints and surprisingly, diminished the tensile forces in the annulus fiber layers. In general, it was observed that the fluid gain increased the segmental stiffness while the overall stiffness was reduced with loss of fluid. This model supported the hypothesis that a loss of nucleus fluid would alter the normal mechanical function of the nucleus and would expose the annulus layers to lateral instability and disintegration. Such abnormal stress state of the annulus would lead to further degeneration of the disc.

There were significant efforts by other researchers also, to understand the intervertebral disc mechanics using numerical approach by taking into consideration the experimental results and physiological conditions of other spine components. Crisco and Panjabi[124] compared the lateral stabilizing potential of the lumbar spine muscles as a function of the architecture in a finite element model. The neuro-musculoskeletal system was modeled as an elastic system. It was concluded that the critical load of the spine can be increased by increasing its stiffness. Stabilizing effects of muscles on the overall mechanics of a ligamentous lumbar spine were observed by Goel et al.[125] It was observed that muscles provide the stability to the ligamentous segment. The model predictions supported the hypothesis that osteoarthritis of the facet joints may follow the disc degeneration. In another study, an isolated vertebral body was modeled to assess the effect of material properties and loading conditions on the end-plate and cortical shell

stress distribution[126]. The osteoporotic condition was modeled by reduction of vertebrae moduli and/or removal of cortical shell. To simulate the disc degeneration process, the annular tears, nuclear clefts and end-plate fractures were simulated by Natarajan et al.[127] The model was simulated for three different loading conditions of axial compression, extension and flexion. It predicted that failure always started in the end-plate and not in the annulus, indicating the end-plate as the weakest structure in the spinal motion segment. It was hypothesized that the intradiscal pressure generation within the nucleus produces the bulging of the end plates, which in turn produces the high bending stresses in the end-plates. It was shown that the compressive load to initiate the failure of the annulus was about twice as high as that required to initiate the fracture in the end-plate. Interlaminar shear stresses and laminae separation of a ligamentous spinal segment was studied by Goel et al.[128] The model reinforced the clinical observations that the tears originate in the postero-lateral region of the disc. It was hypothesized that the large interlaminar shear stresses, caused by asymmetry in the disc structure, along with the chemical/structural changes in the disc with age, may be an important cause of further degeneration through laminae separation. The effect of disc height variation on the mechanical behavior of the disc was analyzed[129]. It was found that the variations in the disc height had a significant influence on the axial displacement, postero-lateral disc bulge and tensile stress in the peripheral annulus fibers. However, the intradiscal pressure and stress distribution in the longitudinal direction at the endplate-vertebra interface was minimally affected by intervertebral disc height variation. From the surgical point of view, the influence of annulotomy technique selection on the disc competence and stability was studied by Natarajan et al.[130] The analysis showed that

both the ‘box’ and ‘slit’ type annular incisions produced similar changes in the biomechanical behavior of the herniated disc. It was predicted that there is no preference between these two types of annular incisions (box and slit) as far as the post-surgical stability of the disc is concerned. Pitzen et al.[131] did an interesting study to determine the load sharing within the healthy and osteoporotic human lumbar spine in compression. They found that for an intact healthy condition, 91% of the load was transferred through the vertebral bodies and the disc. Facet joints accounted for only 8% of the total load acting. However, in case of osteoporotic motion segment, 86% of the load was transferred through the anterior part and 14% was transferred through the facets.

A viscoelastic model to study the changes in load sharing during the fast and slow loading rate was analyzed by Wang et al.[132] They showed that during the complex flexion loading, the motion segment experienced the smaller deformation at faster loading rate, which produced smaller loads on facet joints and ligaments. But, the annulus stresses and intradiscal pressure increased during the faster loading rate. It was hypothesized that the higher stresses during the fast movement may constrain the tissue and thus safeguards the facet joints by reducing the total angular rotation of the motion segment.

It is known since long time that the biphasic nature (solid and fluid phase) of the disc components plays major role in the loading mechanism of the hydrated intervertebral disc. In the late 1980s, there has been an increasing interest in the modeling of the disc as a saturated porous media by using poroelastic approach. This is a special form of viscoelastic model in which one phase (the fluid) can move with respect to the other phase (the solid). An important feature of the poroelastic models is that at equilibrium,

the pressure becomes zero for the fluid phase, which thus cannot contribute to load bearing. Simon et al.[133] were the first to define the poroelastic model for the intervertebral disc in linear form. The annulus was modeled as an isotropic material. Laible incorporated the swelling pressure into a poroelastic model and analyzed the effect of swelling pressure on load bearing capacity, overall stiffening of the disc and changes in the internal strains of the disc[134]. This concept was further expanded by Argoubi and Shirazi-Adl[135] to accommodate posterior elements (facet joints), geometrical and material nonlinearities and variable permeability of the disc components. The effect of facet joints, coupled flexion-rotation, nonlinear strain-dependent permeability and boundary pore pressure on the creep pressure was analyzed in this study. In a similar study, Martinez et al.[136] showed that the matrix permeability plays a major role in determining the transient response of the tissue. It was also shown that the disrupted regions of the annulus fibrosus play a minimal role in load bearing, thus producing increased principle stresses in the nucleus region. Time dependent responses of the intervertebral joints to static and vibrational loading were studied by Cheung et al.[137] A poroelastic model was established to analyze the responses of the fluid flow and stress distribution. It was observed that the loads carried by the annulus and the facet joints increased with time under static loading. The loading frequency significantly altered the fluid flow and deformation of the intervertebral disc. It was concluded that the vibrational loading may be able to enhance disc fluid exchange via the fluid pumping mechanism.

There are very few models of the artificial disc prosthesis in the literature. Langrana et al.[85] developed a model for a synthetic disc, which included the geometric information and variation of materials characteristics of nucleus, annulus, fibers and

ground substance. The model prediction was compared to the experimental results. According to the authors, this model can be used for the design of the synthetic disc prosthesis can be used as well as for the understanding of the pathophysiology of certain painful disc diseases. In another study[138], mechanical behavior of the tissue engineered intervertebral disc was simulated under complex loads. The validated model predicted that a well designed tissue engineering scaffold should preferably have a modulus in the range of 5 to 10 MPa and a compressive strength exceeding 1.7 MPa, for restoration of disc height and normal stress distribution.

The only nucleus replacement finite element model available in the literature is by Meakin et al.[108] It followed simplified approach of modeling the annulus as an isotropic solid and nucleus a fluid with a high bulk modulus. A parametric study of the implant modulus variation was done to predict the feasible range of implant modulus. Based on the annular bulging in the intact, denucleated and implanted state, the model predicted 3 MPa as an ideal implant modulus to prevent inward bulging of the annulus fibrosus with total filling of the nuclear cavity.

2.8 PVA/PVP Hydrogels

PVA has been studied extensively for potential biomedical applications. The swelling, chemical and mechanical properties of PVA were formulated by Peppas[139-141]. PVA hydrogels are easy to manufacture and can be produced from a solution. During the process, the solution is subjected to freeze-thaw cycles, which increases the crystallization, changes the dissolution properties, mesh size and diffusion properties of the hydrogel[142]. The mechanical characteristics of the hydrogels can be improved by γ - irradiation[143]. PVA can release therapeutic drugs from its polymer network[105]. It has

also been investigated as a potential keratoproshteses[144] and its potential for a bioartificial pancreas design[145]. Stammen et al.[146] have proposed using a freeze-thawed PVA hydrogel in a number of applications including artificial cartilage and spinal disc replacement. They characterized the mechanical properties of the crosslinked PVA hydrogels. An increase in the tangent compressive modulus was observed between 1-18 MPa up to 60% strain. It was also found that shear tangent modulus is in the range of 0.1-0.4 MPa depending upon the strain magnitude.

PVP is a hydrogel that also has been investigated for number of biomedical applications. It was used as colloidal plasma substitute[147] and has also been used in soft lenses[28]. It was also investigated by Kao et al.[148] for applications such as single-layer hydrogel wound dressings and tissue adhesives. The biocompatibility of the PVP/ β - Chitosan hydrogel membrane was also evaluated recently[29]. The membranes were found to be biocompatible. They also found that the additions of PVP gave the hydrogel polymer network increased strength due to the viscoelastic properties of the polymer.

Characterization of PVA/PVP copolymer blend has shown that a higher PVP molecular weight within the blend will lead to more interactions between the PVA and PVP. It also leads to higher blend crystallinity[149]. Actually, interactions between PVA and PVP occur through interchain hydrogen bonding between the carbonyl group of PVP and the hydroxyl group of PVA. Figure 2.11 shows the schematic of the PVA/PVP network. These interactions can be studied by using standard characterization techniques, such as FTIR and NMR. Both are soluble materials and thus can be purified before blending. A significant benefit of the PVA/PVP blend is that the structure of the

proposed implants relies on physical cross-linking, rather than covalent chemical cross-linking to hold polymer chains together.

2.9 Summary

Lower back pain is generally associated with the degeneration of the lumbar intervertebral disc. With age, the water retaining capacity of the central portion of the disc i.e. nucleus pulposus reduces significantly due to compositional changes. As a result of this, the load transfer mechanism in case of the degenerated disc is clearly altered than the normal, healthy disc. The outer portion of the disc i.e. annulus fibrosus, is subjected to abnormal stresses (mostly compressive in nature) and thus becomes more prone to injuries as it is naturally designed to support the tensile loading. The nucleus material migrates from center to periphery through the cracks/fissures generated in the annulus. The contact of the migrated nucleus material with the nerve root results into the debilitating back pain.

Current surgical treatments such as Discectomy and Spinal Fusion, although fairly successful in relieving the lower back pain, fail to restore the normal biomechanical motion of the human spine. The post-surgical problems associated with these treatments and their low clinical success rate is an added cause of concern.

New approaches are emerging for the treatment and cure of the lower back pain as a better alternative to the current surgical procedures. These approaches (Total disc replacement and Nucleus replacement) aim to relieve the back pain and restore the normal biomechanical motion of the human spine. Total disc replacement aims for replacing the whole degenerated lumbar disc with an artificial structure similar to the

natural lumbar disc. Because of the complexity of the disc structure, this approach requires the sophisticated design of the artificial disc implant.

Nucleus replacement by an artificial material or by a tissue engineering technique is another potential approach for the treatment of lower back pain. Nucleus replacement aims for replacing only the degenerated nucleus, keeping the remaining disc structure intact. This approach is however, not feasible for the discs where the annulus is severely degenerated.

Finite element modeling of the lumbar intervertebral disc mechanics has been done extensively. However, there is not much information available in the literature about the nucleus implant mechanics and effect of nucleus replacement on the restoration of the disc mechanics. Especially, precise information about the design requirements of the nucleus implant and the effect of individual implant parameters on the resulting mechanics of the implanted disc is not available. This study aims to fill this gap in the literature and assess the effect of nucleus replacement by a physically cross-linked hydrogel implant on the resulting disc mechanics in axial compression, using both experimental methods and finite element modeling.

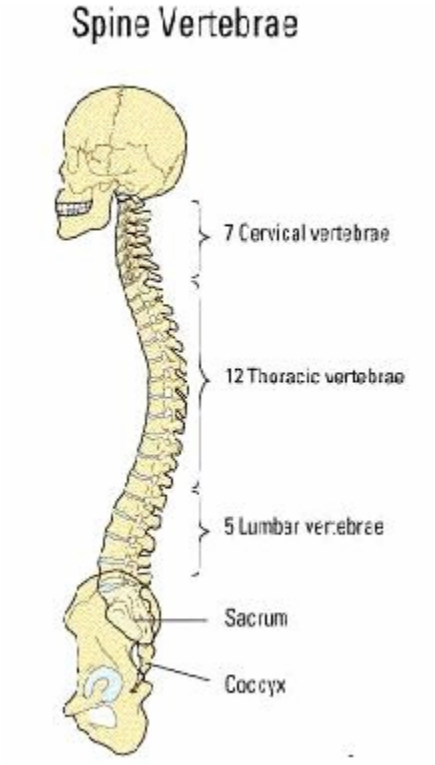

Figure 2.1. Schematic of the Human Spine (www.adam.com)

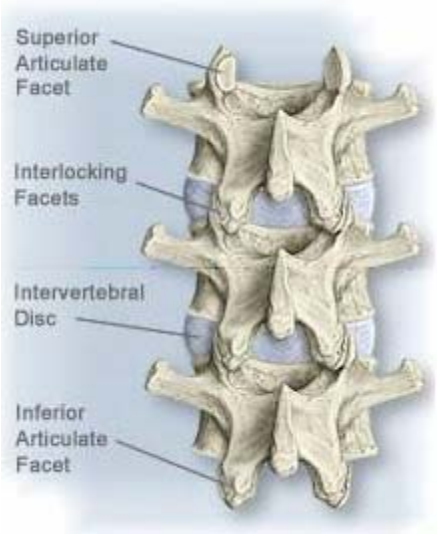

Figure 2.2. Schematic of the Human Spine Structure (www.adam.com)

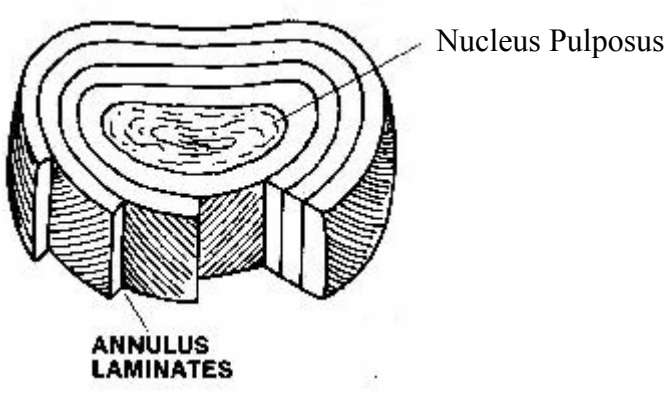

Figure 2.3. Schematic of the Lumbar Intervertebral Disc[30]

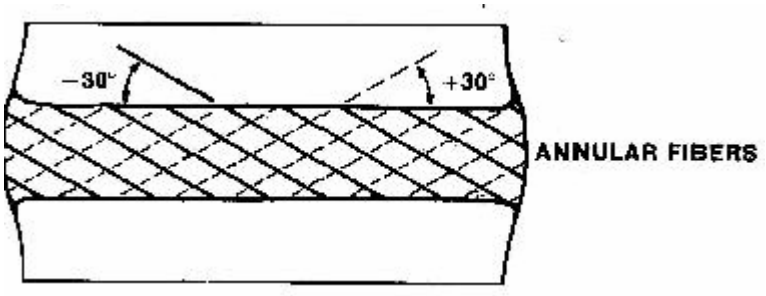

Figure 2.4. Schematic of the Annulus Fibrosus and Fiber Orientation[30]

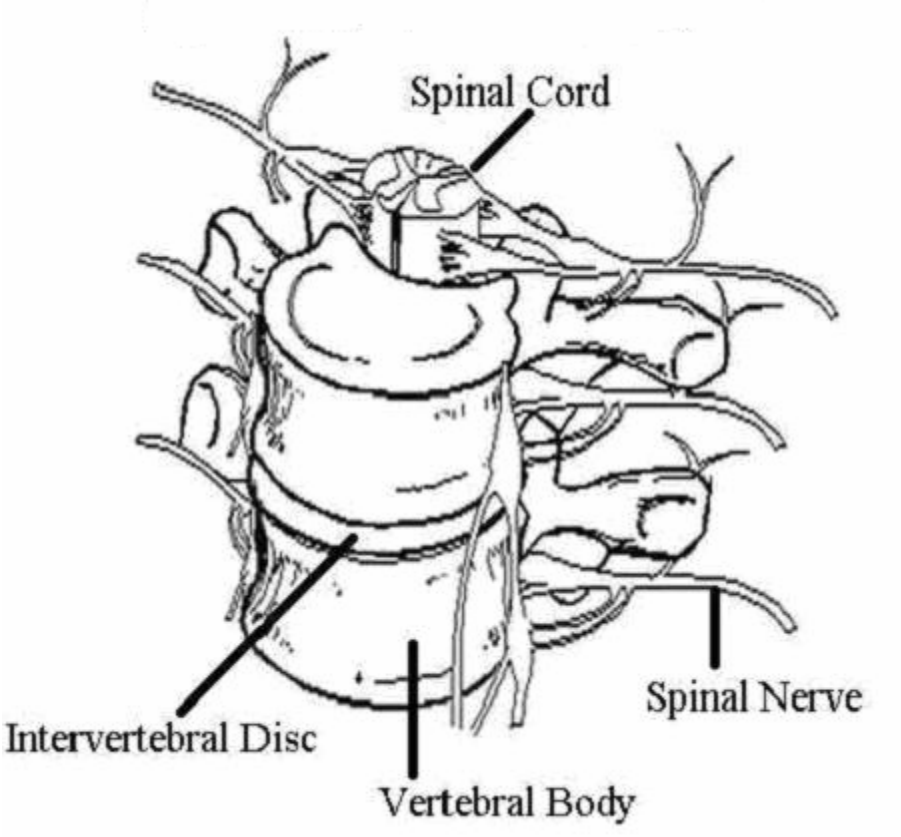

Figure 2.5. Schematic of the lumbar functional spinal unit

(http://cpmcnet.columbia.edu/dept/nsg/NSGCPMC/images/spinalmotion.jpg)

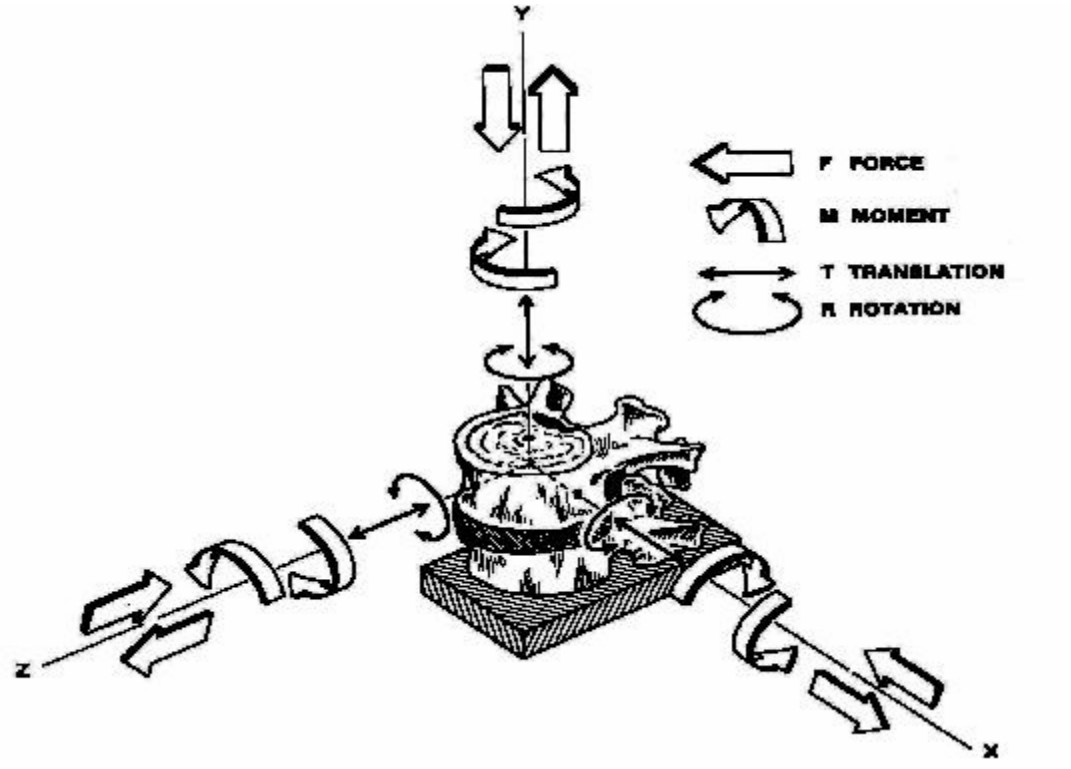

Figure 2.6. Three Dimensional coordinate system for the lumbar functional spinal unit[30]

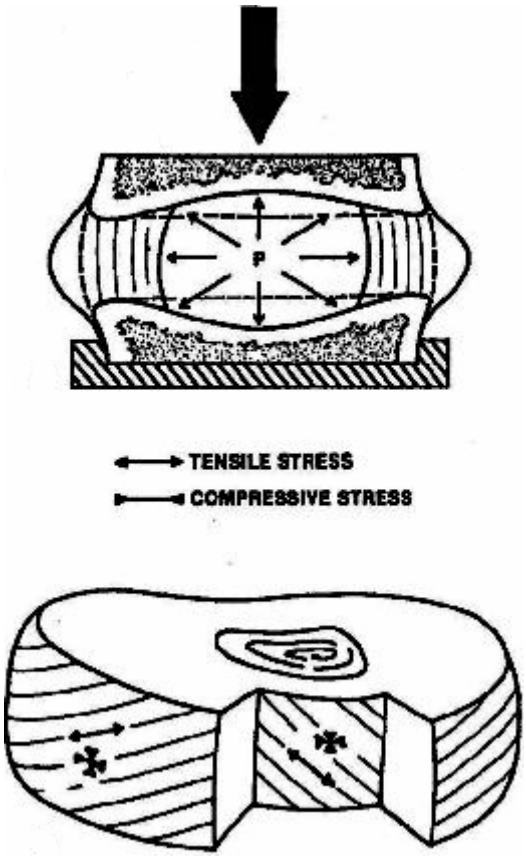

Figure 2.7. Non-degenerated lumbar disc under compression[30]

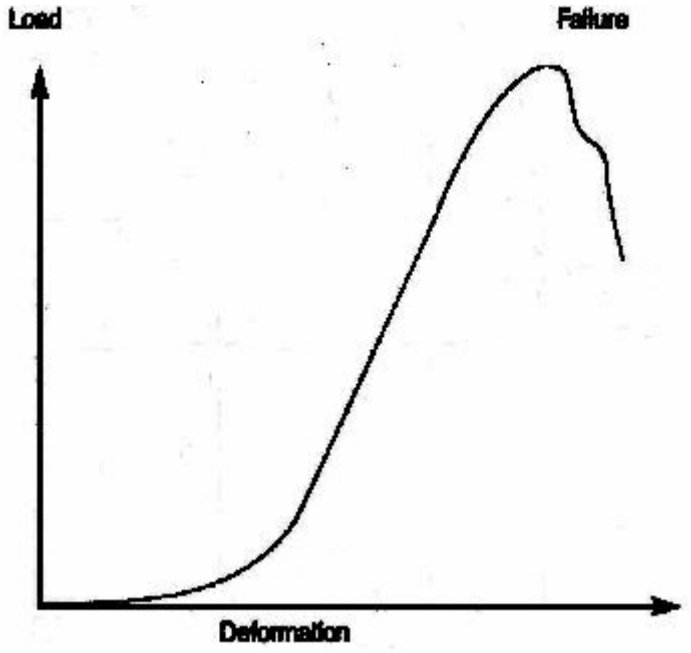

Figure 2.8. Typical Load-Displacement curve for the lumbar functional spinal unit[30]

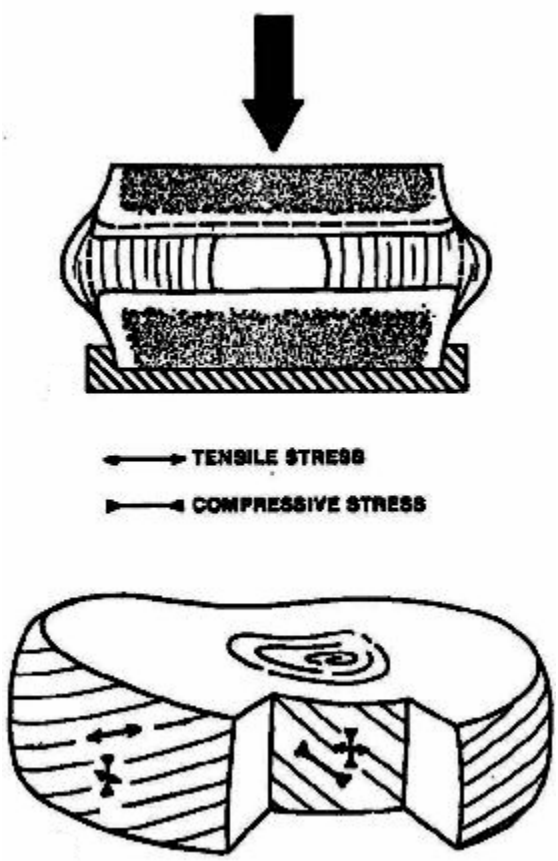

Figure 2.9. Degenerated lumbar disc under compression[30]

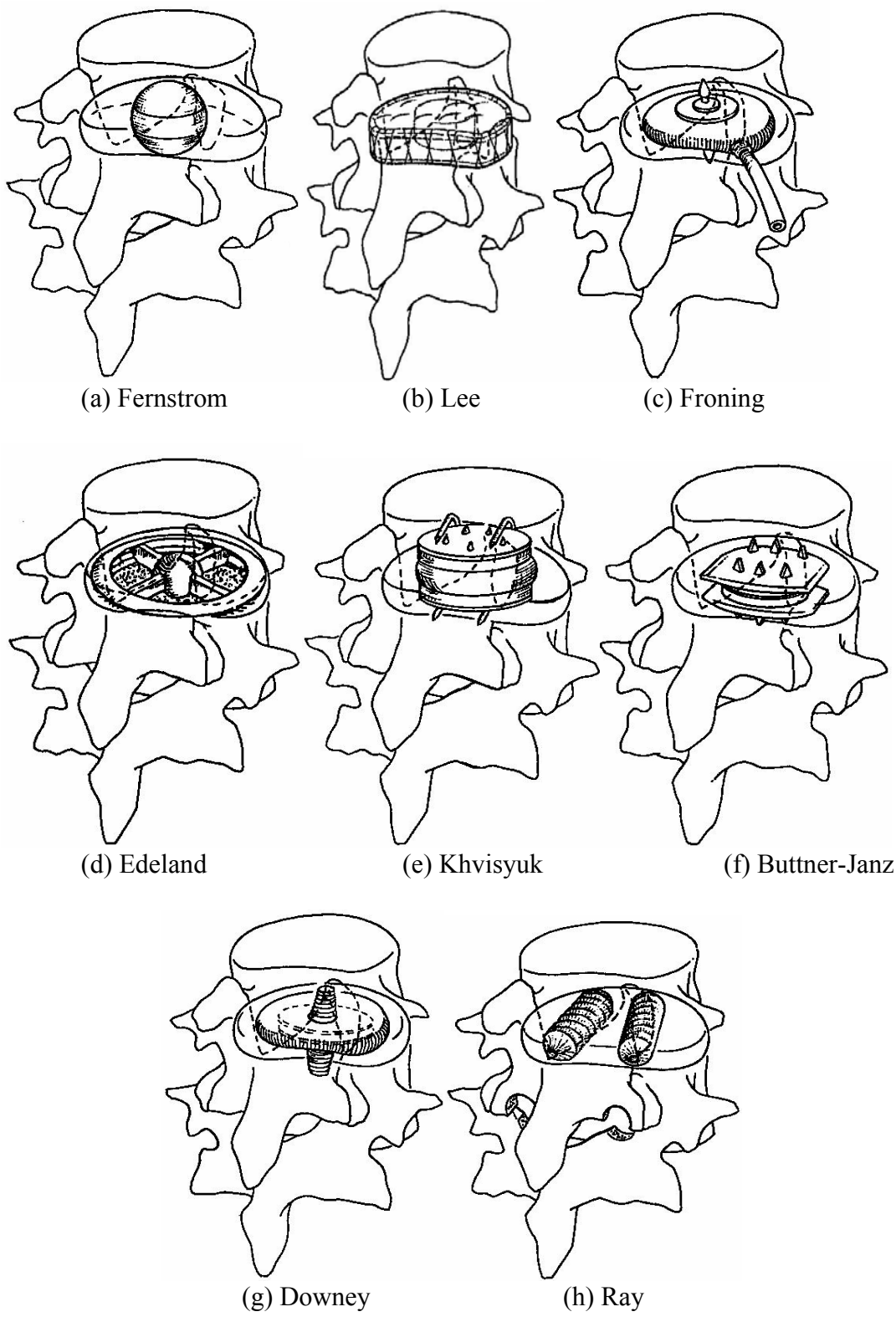

Figure 2.10. Artificial Disc Prostheses[38]

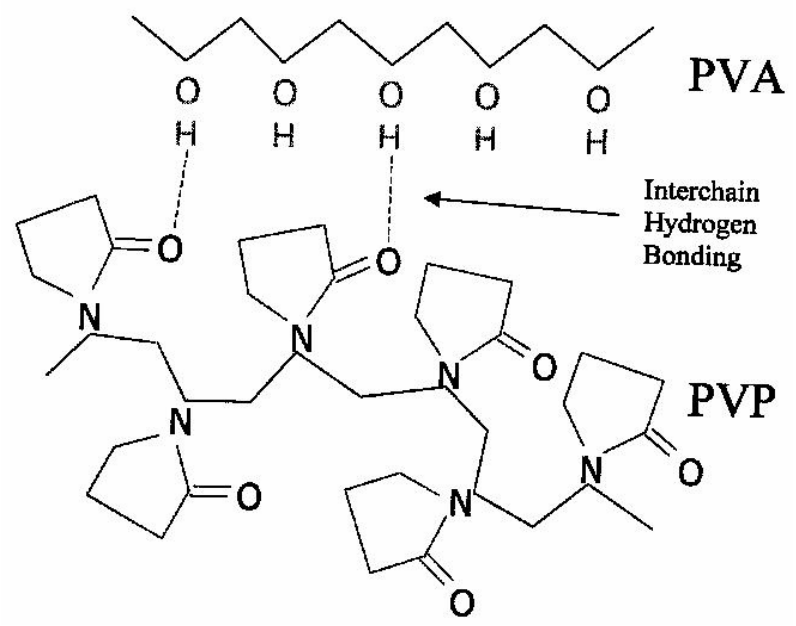

Figure 2.11. Interchain hydrogen bonding within a PVA/PVP blend

3. Objectives

We propose the use of PVA/PVP hydrogel as a replacement to the degenerated nucleus pulposus of the lumbar intervertebral disc. The focus of this study is to assess the hydrogel nucleus implant mechanics in detail, using both an experimental and finite element method for the human lumbar intervertebral disc in axial compression.

Our general premise is that the dehydration of the degenerated nucleus pulposus leads to a reduction in hydrostatic pressure on the internal surface of the annulus. This results in an abnormal stress state in the annulus tissue and consequently a breakdown of the annular tissue seen macroscopically as fissures and tears.

We hypothesize that a polymeric hydrogel nucleus implant can restore the biomechanics of the denucleated lumbar intervertebral disc in axial compression, by generating stresses (which are similar to the normal intradiscal pressure in a healthy disc) on the inner annulus layers. We also hypothesize that the nucleus implant material (modulus) and geometric (height and diameter) will have a significant effect on the stress distribution within the lumbar intervertebral disc and its overall mechanical behavior, in axial compression.

We propose the following specific aims:

a) **Specific Aim 1 (SA-1):** (Chapter 4)

- Development of the test protocol for the human lumbar intervertebral disc in axial compression.
- To assess the effect of partial denucleation on the compressive behavior of the lumbar intervertebral disc.

b) **Specific Aim 2 (SA-2)**: (Chapter 5)

- Development of an '*in vitro*' implantation method for a PVA/PVP hydrogel nucleus implant in the denucleated lumbar intervertebral disc.
- Determine the compressive stiffness of human lumbar intervertebral disc in three different experimental conditions of Intact, Denucleated and Implanted.

c) **Specific Aim 3 (SA-3):** (Chapter 6)

- Develop a parametric test protocol to assess the nucleus implant mechanics and significance of nucleus implant material and geometric parameters.
- Experimentally determine the effect of nucleus implant modulus variation and 'fit and fill' effect of the nuclear cavity by nucleus implant geometry variation, on the compressive mechanics of the lumbar intervertebral disc.

d) **Specific Aim 4 (SA-4)**: (Chapter 7)

- Development of an axisymmetric finite element model of the human lumbar disc and validation of that model against the corresponding experimental results.
- Development of a representative finite element model of the human lumbar disc to assess the effect of nucleus replacement on the resulting stress distribution and prediction of feasible implant moduli range.

e) **Specific Aim 5 (SA-5):** (Chapter 8)

- Examine the effect of nucleus implant material parameters on the compressive mechanics of the lumbar intervertebral disc, using a finite element method.

- Examine the ‘fit and fill’ effect of the nuclear cavity by nucleus implant height and nucleus implant diameter variation on the compressive mechanics of the lumbar intervertebral disc, using a finite element method.
- Expand the experimental results of the parametric study of the nucleus implant parameter variations (Chapter 6) to have better understanding of the nucleus implant mechanics and role of individual nucleus implant parameters in the compressive behavior of the implanted lumbar disc.

4. Contribution of the Nucleus Pulposus towards the Compressive Stiffness of the Human Lumbar Intervertebral Disc

Introduction

The intervertebral disc (IVD) is the largest avascular tissue in the body and constitutes about one third of spinal column height[30]. It plays a major role in the transmission and distribution of spinal loads. Three different types of tissues are observed in the IVD: central nucleus pulposus (NP), outer annulus fibrosus (AF) and cartilaginous end plates (EP). The central gel like NP is essentially water in a matrix of proteoglycan, collagen fibers and other proteins. The high anion charge content of the IVD creates an oncotic (osmotic) pressure, which pulls water into the IVD[150]. Swelling is contained by the relatively stiff vertebral EP and the AF creating a hydrostatic intradiscal pressure (IDP). The IDP creates tension in the AF fibers, which resists any further deformation. The balance of this oncotic pressure and the hydrostatic IDP plays a major role in the normal physiologic load transfer mechanism of the disc. Any vertical load acting on the disc is distributed horizontally by means of the IDP and AF fibers in tension[151,152].

Many investigators have studied the dependency of IVD mechanical behavior on alteration of the NP. These studies of NP alteration include examination of changes in composition with aging and degeneration[16,73,120,151,153,154], changes with pressurization[155], and changes with partial or total discectomy, removal of NP tissue. Most investigators report significant dependency in the *in vitro* IVD mechanical behavior on removal of NP tissue[21,22,49,51,54,72,117,156-158]. Compressive loading after removal of NP tissue increases

disc deformation, decreases disc height and increases radial bulging, when compared to the intact disc[49,158]. Increased disc deformation results in increased AF deformation and has lead to the hypothesis that AF internal stresses increase with NP tissue removal. Observation of inner AF layers bulging inward under conditions of compressive loading subsequent to partial removal of the NP suggests increased radial stress within the AF and supports the hypothesis[114,115,157]. Loss of disc height, increase in radial bulging and decrease in intervertebral disc pressure are dependent on the quantity of NP tissue removed[21,22,159]. However, observations on the IVD mechanical behavior as affected by NP tissue removal were made in each case with partial injury to the AF[21,22,49,51,54,72,117,156-158]. Annulotomy alone increases disc deformation compared to the intact disc under load and the mechanical behavior of the IVD has shown dependency on type, size and location of the annulotomy[22,160,161]. The mechanism for the mechanical change with annulotomy has been attributed to both depressurization and to the annular injury.

With discectomy, annulotomy and NP tissue removal, the relative contribution of the AF injury, the NP depressurization and the NP resection to the AF deformation has not been fully delineated. No information has been reported on the effect of removal of the NP on the compressive stiffness of the IVD without surgical injury to the AF. The objectives of the present study were: 1) to develop a method for assessing the contribution of the NP to the *in vitro* mechanics of the disc without injury to the AF caused by incision of the AF, a normally followed approach[22,49,157,158,160-164] and 2) to investigate the effect of denucleation on the compressive stiffness of the IVD.

Materials and Methods

Mechanical tests were performed on human lumbar IVDs in axial compression. An approach for removing the NP tissue was developed that avoids injury to the AF. Denucleation was obtained by drilling through the superior vertebra to the IVD level and excising the NP while maintaining an intact AF.

Specimen Preparation: FSUs were harvested from 8 cadavers (3 males and 5 females) with an average age of 65 years, within 72 hours of death. Fifteen lumbar FSUs from L1-S1 levels were selected for testing based on visual inspection eliminating those with obvious damage or degeneration. Intervertebral motion segments were prepared by removing the facet joints, posterior elements and other soft tissues. Parallel cuts in the transverse plane were made through the vertebrae above and below the disc to ensure alignment of the axial compression load. Thus, the specimen consisted of an intervertebral disc in between adjacent vertebrae. The fifteen specimens were frozen in sealed bags until the day of testing. On the day of testing, specimens were thawed for at least 2 hours at room temperature in sealed bags prior to compression testing.

Anatomical measurements of the specimen (disc height, superior and inferior vertebrae height, disc major and minor diameter) were performed using a digital caliper. To minimize the measurement error, the average of 3 different measurements at different locations was used.

In addition to the fifteen non-degenerated specimens noted above, one degenerated specimen was similarly prepared and tested for observation, but not included in statistical analysis.

Mechanical Testing Method: The intervertebral specimen was constrained in a custom-made test fixture with help of screws, which connected the inferior vertebrae to the test

fixture. A commercially available potting mixture (Cargroom®, U.S. Chemical and Plastics, OH) was used for potting of specimens in the custom made fixture. Only the inferior vertebra was potted. Care was taken to ensure both that the potted material was not touching the IVD and the upper cut surface of the intervertebral specimen was in the plane of the upper compression plate, which was attached to the load cell. The superior vertebra of the segment was compressed against this flat compression plate to ensure axial loading, while allowing adequate access for denucleation of the specimen as the compression plate and inferior vertebra were not attached physically. A solution of protease inhibitor was sprayed on the specimens throughout testing.

Compression Testing Protocol: An Instron (Canton, MA) mechanical testing hydraulic machine (Model 1331) was used for the testing. The initial baseline position of the upper compression plate and lower actuator was ensured and maintained using digital position indicators through each tested condition. The specimens were preconditioned for 50 cycles at 3% strain (based on the average IVD height). The load range corresponding to this preconditioning was 40N – 140N. Specimens were axially compressed to 15% of total average IVD height. The testing was performed with a triangular waveform at 0.5 Hz with a loading rate of 15% strain/sec for 5 loading cycles, for each tested condition. The data of the fifth loading cycle was taken for further analysis from each tested condition.

Test Sequence: A series of axial compressive tests were completed on each specimen, as shown in Figure 4.1. First, the intact specimen was tested using the compression testing protocol (Intact Condition - IC). Then, a Cloward core drill bit of 16 mm outer diameter and 15.5 mm inner diameter was used to drill perpendicular to the cut surface of the

superior vertebra through the bone to the IVD. This hollow core drill was centered in the medial/lateral axis of the vertebral body and positioned approximately 2mm posterior to the centerline in the anterior/posterior axis. A cylindrical bone plug (height equal to that of superior vertebra and diameter equal to 15.5mm) above the disc was removed. For the second test condition, the cylindrical bone plug was reinserted and the test protocol was repeated (Bone plug Inserted condition – BI). The bone plug was then removed from the upper vertebrae and the nucleus was incised in line with the core drill. The central portion of the nucleus in line with the core drill (equal to 16mm diameter, wet weight 2.5 to 3.0 gm) was removed using standard surgical instruments, keeping the residual NP and the AF intact. The testing protocol was then run on the denucleated specimen without replacing the bone plug (Denucleated condition - DN).

Data Collection and Analysis: The data for each tested condition in terms of force-displacement history were collected using a Labview® program with a sampling rate of 1000 Hz. Data for the fifth loading cycle were taken for analysis and instantaneous compressive stiffness values (N/mm) were calculated at representative strain levels of 5%, 10% and 15%, for each condition, for each specimen. The stiffness values were obtained by numerically differentiating the raw data, taking the slope of the line passing through the points corresponding to the representative strain levels. For each strain level (5%, 10% and 15%), a one-way, repeated measures ANOVA was performed for compressive stiffness with one subject factor (surgical condition: IC-BI-DN). Fisher's LSD post-hoc analysis was conducted to assess the effect of surgery (IC vs. BI) and effect of denucleation (BI vs. DN). The acceptable rate for a type-I error was chosen as 5% for all tests.

Results

Figure 4.2 shows a typical load-displacement curve for an intact lumbar intervertebral segment under axial compression. A non-linear force-displacement curve was observed. Figure 4.2 also shows load-displacement curves corresponding to test conditions of BI and DN, for a representative specimen with similar non-linearity. These nonlinear force-displacement curves were observed for all specimens under all conditions.

Figure 4.3 shows the intervertebral motion segment compressive instantaneous stiffness (N/mm) vs. the strain (%) for three testing conditions of IC, BI and DN. The 1-way ANOVA calculations comparing the IC, BI and DN stiffness at 5%, 10% and 15 % strain showed significant differences ($p < 0.001$ at all strain levels).

Drilling into the vertebrae significantly reduced the stiffness compared to the intact condition (for e.g. BI stiffness value 81% of IC @ 15% strain, $p < 0.001$ at all strain levels). A more dramatic reduction in the stiffness was observed for denucleated specimens (for e.g. DN stiffness value 41% of IC @ 15% strain, $p < 0.001$ at all strain levels) after removal of NP material.

Figure 4.4 compares the compressive stiffness values of all fifteen specimens for three testing conditions of IC, BI and DN at 15% strain. All specimens demonstrated a drop in stiffness with the simulated surgery (BI) and a further drop when denucleated (DN). It also shows the data for the degenerated specimen, for which stiffness values for three conditions were not different, thus generating almost flat line.

Discussion

Compressive stiffness values for intact human motion segments reported in the literature vary widely in a range of 700 - 3200 N/mm[30,44]. This large variation in the reported stiffness is the result of specimen differences with respect to age, degeneration stage, disc level, sex and testing protocol. Nonetheless, the compressive stiffness values for intact motion segments reported here, at 10% and 15% strain (1046 N/mm and 1924 N/mm respectively) are in the reported range for motion segment stiffness thus validating our testing protocol.

Interestingly, we observed a loss of intact motion segment stiffness at all strain levels with core drilling of the upper vertebral EP (BI condition) with an observed range of 2-38% and a mean decrease of 19%. Three possible mechanisms for the reduction in stiffness observed in the BI condition are offered: 1) NP volume loss 2) EP structural change and 3) NP depressurization.

Previous observations, as well as, observation of our denucleated condition suggest that removal of NP tissue reduced segment stiffness and decreased IVD height[22,49,157,158,160-164]. A relatively linear relation between reduction in disc height and volume of tissue removed (0.8 mm/1.0 g) was noted by Brinkman and Grootenboer[159]. One could argue that NP tissue could be forced into the saw kerf in the upper vertebrae when the bone plug was replaced and the segment tested. This was not observed at the time of bone plug removal after the test completion, at least supporting the lack of plastic deformation of nucleus material into the kerf. However, elastic deformation remains a possibility. Simple geometric considerations suggest that the kerf volume is no more

than 7% of the excised total volume for a disc with 10mm height. Figure 4.5 shows a schematic of IDP change and NP tissue migration for different test conditions.

Frei et al.[165] have recently reported the effect of partial nucleotomy on EP strains under compressive loading. The maximum principle and shear strains were observed to be greatest in the central EP with shear strain approximately 1.5 times the principle strain at maximum loading of the intact disc. They also found that discectomy reduced the central strain approximately 20%, but the ratio of shear to principle strain remained essentially unchanged. Drilling through the central EP would significantly alter the shear strain in the central EP under axial load. However, the high modulus of trabecular and cortical bone compared to that of NP and AF, suggests that the bone would act as a relatively rigid body in terms of deformation in comparison to the soft tissues of the disc, and therefore, it is hard to explain the loss of stiffness of the BI condition due to the EP damage alone.

Although the loss of stiffness in the BI condition may have contributions from all three proposed mechanisms, the most likely candidate for the loss of stiffness is depressurization. Recently, Adams et al.[166] observed a 25% reduction in IDP with fracture while producing minimal EP damage, which compares to our saw kerf. As water is incompressible, very small changes in volume have the potential to change the hydrostatic pressure in a confined space. However, the majority of the water is held in the NP matrix under the balance of oncotic and hydrostatic forces. There may be a small amount of loosely bound water that is capable of flow under very low pressure gradients. It is hypothesized that this small volume fraction is depressurized with the saw kerf leading to the observed reduction in stiffness in the BI condition. This hypothesis is not

tested, but is supported in considering the converse. In non-degenerated disc, saline injection into the NP immediately and dramatically increases IDP and stiffness[49,155]. After removal of the NP tissue (DN condition) additional deformation of the IVD is noted in further reduction of disc height at a given load. This is seen in the typical load-displacement curves of Figure 4.2 and is consistent with the reports of disc displacement in response to trans-annular discectomy[22,49,55,158,159]. As previously noted, annulotomy alone decreased disc height, but removal of NP tissue further increased the deformation[22,49,158,160,161]. This behavior is similar to what was found in our study, although annulotomy is not performed leading to speculation that the annulotomy in addition to injuring the AF, depressurizes the disc in a manner similar to EP drilling and that NP tissue itself contributes to preventing disc deformation.

Removal of the central NP inline with the core drilling showed on an average 60% reduction in the motion segment stiffness over the intact condition at 15% strain in axial compression and 50% reduction over the BI condition at this strain level. The NP tissue presents several potential mechanisms for contributing to the stiffness of the IDP: 1) Hydrostatic pressurization of the EP and AF 2) Direct loading of the EP and 3) Poisson effect - loading of the AF. The unconfined modulus of the NP is low compared to that of the AF suggesting that direct loading of the EP (parallel spring) does not make a significant contribution to the IVD stiffness[10]. The NP has very high water content in young age, which diminishes with age and degeneration[10-12]. The degenerated disc specimen in the Figure 4.4 provides additional insight into the role of NP in the overall disc mechanics. The compressive stiffness values for three conditions of IC, BI and DN were almost same for this specimen generating a flat line, unlike the other tested

specimens, which showed a substantial reduction in stiffness with each intervention. This disc was in a severely degenerated condition and on resection the NP was observed to be dry in comparison to those of the other tested specimens. This suggests that in the dehydrated NP state, where no (or minimum) IDP generation is possible, the NP is unable to perform its normal role in the load transfer mechanism. In other words, the intact motion segment acted as if it was in the denucleated state offering minimal increase in resistance to the deformation over the denucleated state. The normally observed stiffness reduction for BI condition also was not observed in this specimen, probably because it was already depressurized prior to testing. It appears that the NP can exhibit an effective hydrostatic pressurization and Poisson effect to load the AF and EP, which is dependent on bulk modulus and (the bulk modulus dependency on) water content. It is therefore hypothesized that the NP loads the EP and AF through such a mechanism.

In our experiments, only the nucleus material in line with the drill cavity was resected, thus leaving some residual nucleus material in the disc, which was outside the circumference of the drilled hole. After the mechanical testing for the DN condition, this residual tissue encroached into that circumference but did not fill it. This observation of inward bulging of the residual NP and inner AF after discectomy is consistent with observations made by Seroussi et al.[157] and more recently by Meakin et al.[114,115] Again this suggests that partial removal of the NP alters the internal stresses within the AF.

Brinkmann and Grootenboer[159] observed that the residual NP rearranged itself to fill the void created by the removal of NP tissue in discs that had less than Galante grade IV[55] degeneration. They argue that it is this spatial rearrangement of NP tissue that justifies use of the term intradiscal pressure after discectomy. However in our case, this

was not observed after the loading protocol where the central NP void was maintained. In both experiments similar amounts of NP tissue were removed (approx. 3 g). However, their technique with use of a rongeur through an annular incision, allowed removal of only small pieces of nucleus material in several steps as compared to the single step bulk removal of the nucleus material in our method. This basic difference in technique for removing the nucleus material may have caused these contradictory observations of rearrangement of NP tissue in the cavity.

Our observation of a reduction in motion segment stiffness with drilling and removal of NP tissue differs with the observations of Shea et al.[22] They report that the motion segments in which they had performed either standard or percutaneous discectomy did not appreciably change motion segment stiffness at 800N loading. Observation of Figure 4.2 and Figure 4.4 suggests significant change in the motion segment stiffness after drilling through the end plate (BI) and after denucleation (DN). The majority of our data was obtained at loads lower than 800 N (for DN condition) making direct comparison to their data difficult. This leaves a question as to whether this difference is real or a perturbation of the testing methodologies. Hypothetically, it may suggest that the NP has a greater effect on stiffness at lower loads; however no additional speculation seems reasonable without further observation.

The relatively early hypothesis of Markolf and Morris[54], that the compressive viscoelastic and elastic behaviors of the IVD are determined by the AF and that the deformation under compressive loading is dependent on the NP, may still hold. The DN condition approximates the AF only condition and further testing at greater loads for comparison to the intact condition is warranted. Nonetheless, loss of NP tissue results in

lower IVD stiffness and probable alteration in the internal AF stresses, particularly in the low load/deformation range (toe region) consistent with normal daily activity. Moreover, Panjabi et al.[158] showed nearly twenty years ago that compression deformation was smallest in response to discectomy considering the six degrees of mechanical freedom. This belies the importance of the NP tissue in IVD function and suggests further investigation into the biomechanical behavior of this model under other loading conditions.

Total disc replacement and NP replacement are emerging as two possible treatments for restoration of the IVD function. Nucleus replacement (NR) with a synthetic material[94,112,167] or with tissue engineered structure[110], targets earlier stages of disc degeneration with the goal of eliminating pain while restoring the height of the disc and the normal biomechanics of the IVD. This later approach may help to preserve the AF. The experimental model presented may serve as an excellent *in vitro* test bed for assessing mechanical efficacy of NRs. Typical *in vivo* insertion of an NR requires injury to the AF. *In vitro* injury to the AF is difficult to effectively repair; hence a trans-annular approach for NR implantation alters the mechanical behavior of the motion segment in addition to the NR treatment and may sometimes predict the higher nucleus implant material properties than required ideally. Removing the vertebral bone plug and replacing it after introduction of the NR may create fewer artifacts in mechanical testing. This approach is similar to that of Karduna et al.[168] where they cut open the bone, rather than cut open the capsule, while studying the kinematics of the shoulder. Though this is more invasive to the bone, it creates less damage to the soft tissue.

Conclusions

An *in vitro* model for investigating the contribution of the NP tissue to the mechanics of the intervertebral motion segment was presented which avoids consideration of mechanical artifact introduced by annulotomy. Removal of the nucleus tissue resulted in the 60% stiffness decrease of the intact motion segment at 15% strain. Results from this study of compressive loading are in line with prior observations but avoid dependencies on annulotomy type, size, and location. Decreased stiffness associated with entrance into the nucleus pulposus seen with trans-annular approaches are mimicked for the most part by the trans-endplate approach presented here, which suggests a depressurization phenomenon. This trans-endplate approach may provide an experimentally useful model for evaluation of material or tissue engineering based nuclear replacements.

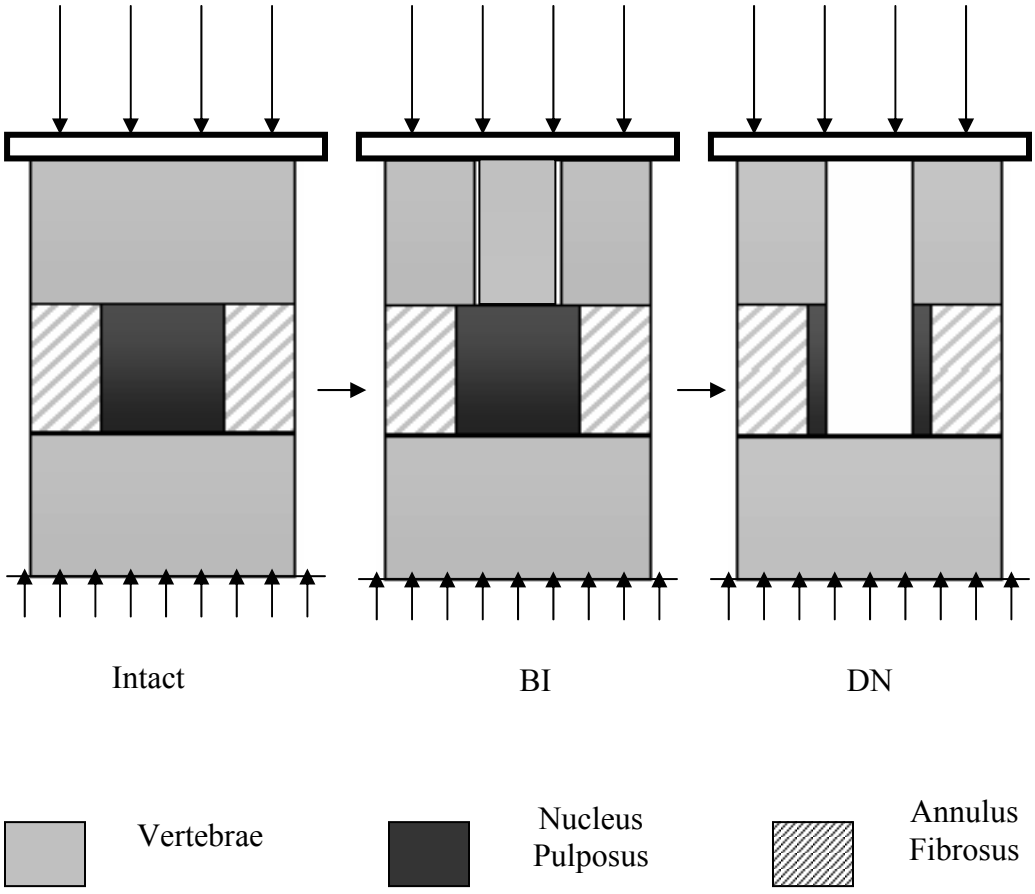

Figure 4.1. Schematic of testing protocol and implantation method of a lumbar FSU, showing the intact, Bone in plug (BI) and Denucleated (DN) condition

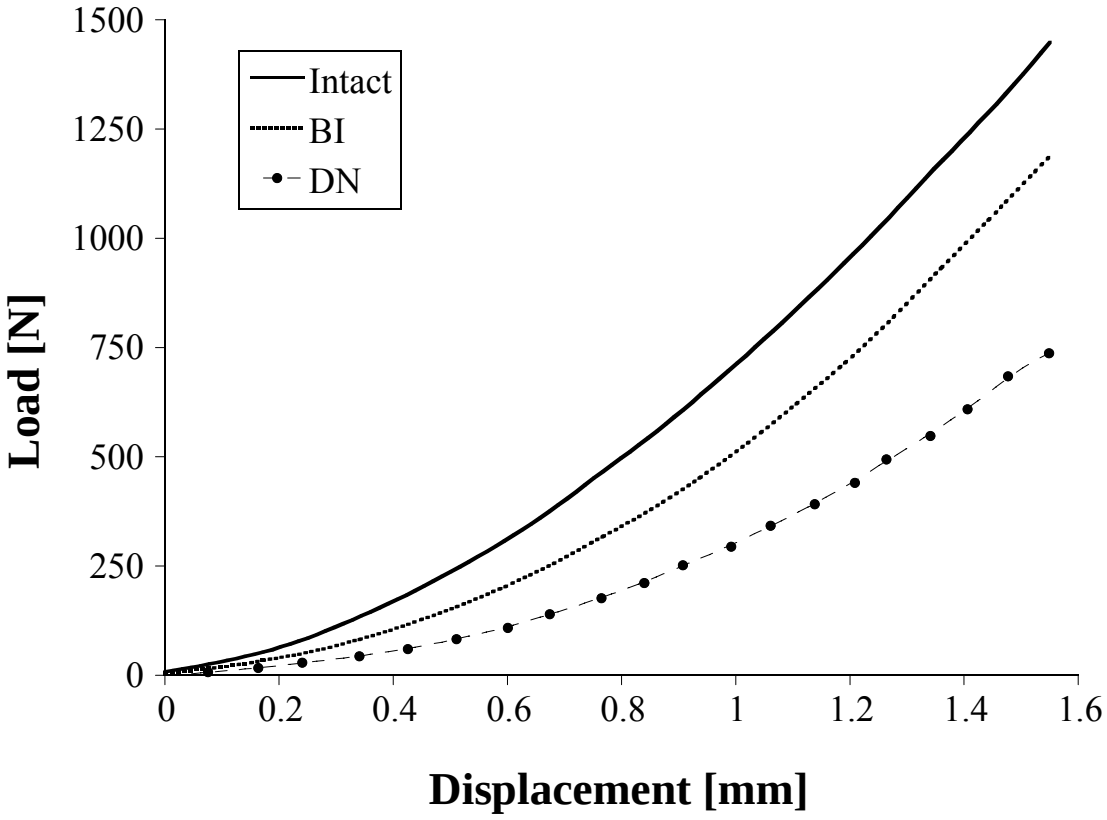

Figure 4.2. Load-Displacement curve of a typical specimen for different test conditions of Intact, Bone in plug (BI) and Denucleated (DN) shows the non-linear behavior for each condition

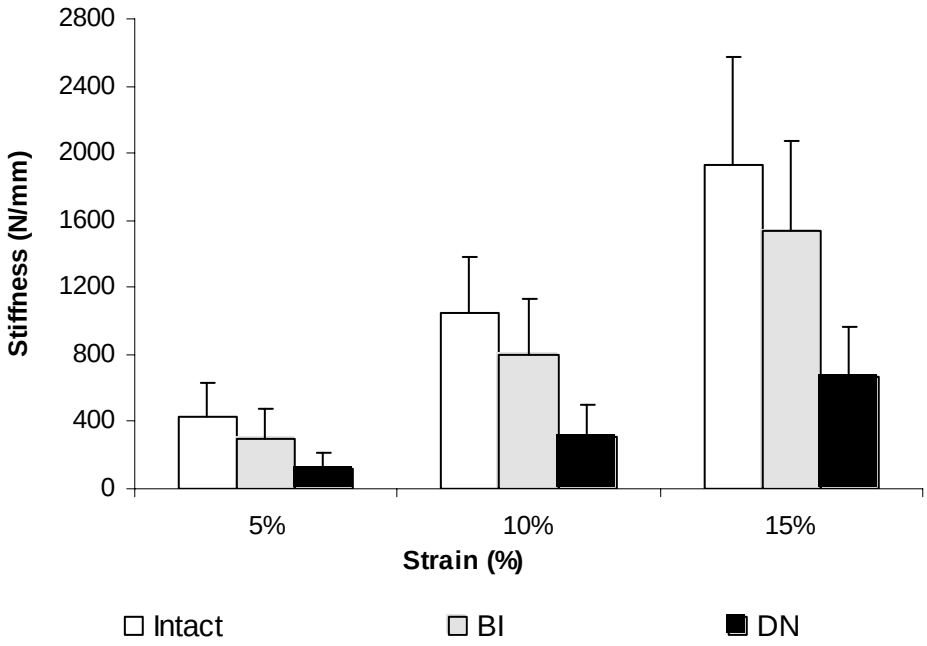

Figure 4.3. FSU compressive instantaneous stiffness (N/mm) vs. compressive strain (%) for different test conditions of Intact, Bone in plug (BI) and Denucleated (DN)

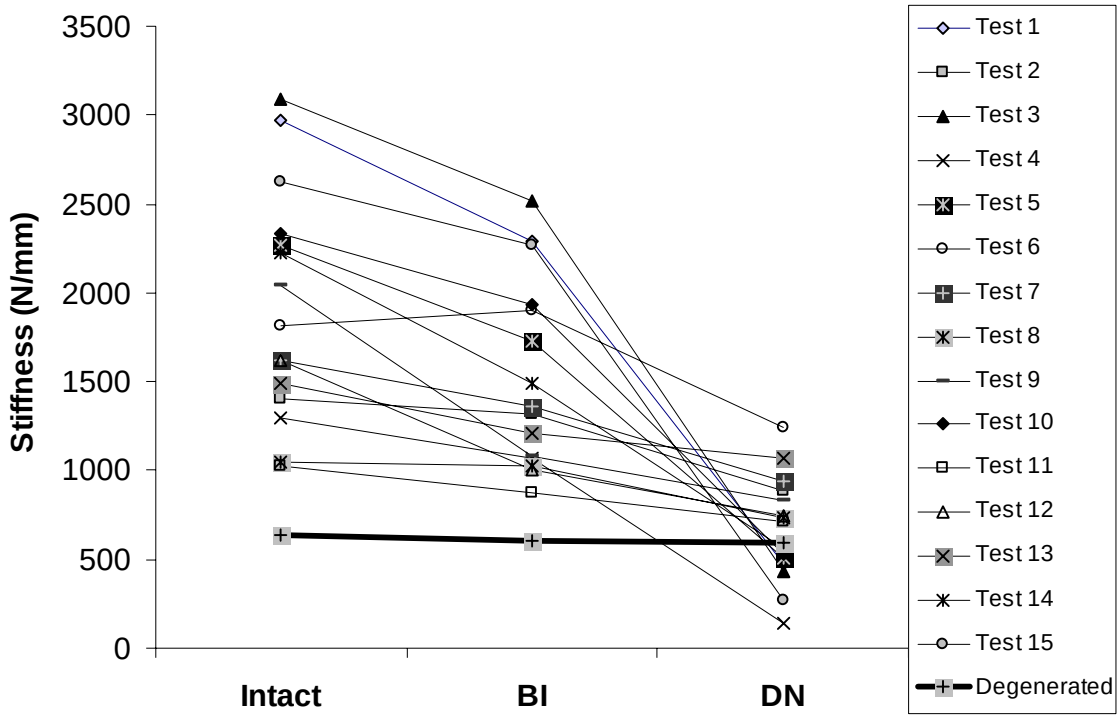

Figure 4.4. Plot of Stiffness (N/mm) at 15% strain of the FSU for each of the three test conditions: Intact, Bone in plug (BI) and denucleated (DN)

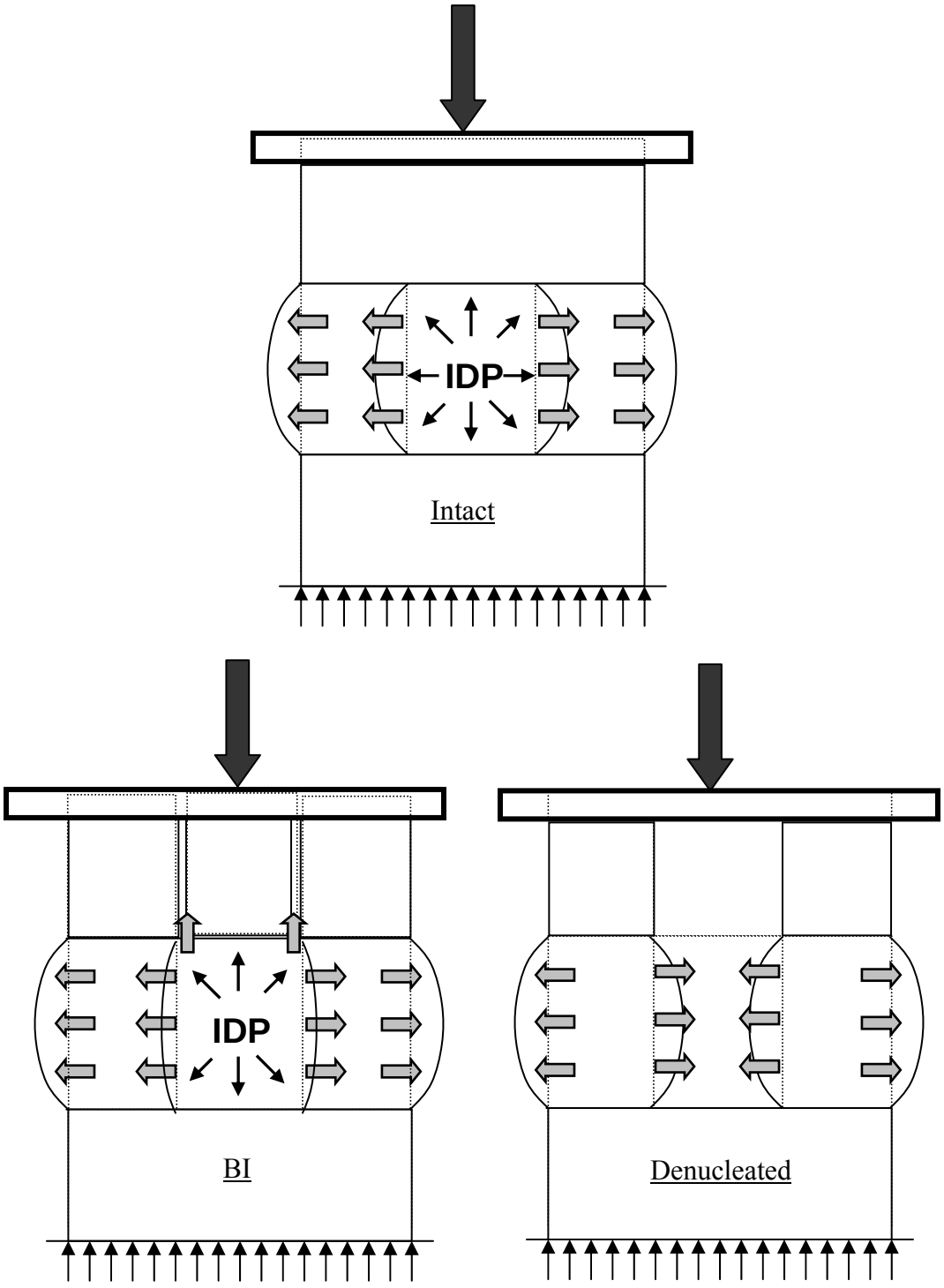

Figure 4.5. Schematic of Intradiscal Pressure (IDP) change and nucleus tissue displacement (gray arrows) for different test conditions

5. The Effect of a Hydrogel Nucleus Replacement on the Compressive Stiffness of the Human Lumbar Functional Spinal Unit

Introduction

Over five million Americans suffer from chronic lower back pain making it the leading cause of lost workdays in the United States. While the causes of lower back pain vary and remain unclear to date, it is believed that at least 75% of the cases are associated with lumbar degenerative disc disease[1].

Under physiological loading, the hydrated nucleus pulposus (NP) exerts a hydrostatic pressure (Intradiscal Pressure) on the internal annulus fibrosus (AF) layers, creating tension in the AF fibers[151,152]. In case of a degenerated/damaged intervertebral disc (IVD), the dehydration of the NP reduces the intradiscal pressure (IDP) in the IVD resulting in greater deformation under load, where the AF is then likely loaded in compression[14,17,169]. It is our working premise that the loss of disc mechanical integrity with NP dehydration results in a cascade of loss of normal mechanical function, tissue injury and tissue response.

Current treatment options such as discectomy and spinal fusion are fairly successful in alleviating the pain[14,20]. Discectomy is employed when the disc is herniated and the annulus degeneration is not severe[19]. Spinal fusion on the other hand, treats later stages of disc disease by inducing bone growth across the functional spinal unit[14,26]. These procedures may promote further degeneration of either the initially affected disc, in case of discectomy[21,23] or adjacent IVDs in case of spinal fusion[25,26]. The ultimate solution to treat for disc degeneration would be the restoration of anatomy and biomechanics to that of the healthy disc[170].

Two main approaches are emerging for restoration of the IVD function: total disc replacement[14,78,80,171] and nucleus replacement[14,94,112]. Currently, total disc replacement targets the later stages of disc degeneration to eliminate the pain. Nucleus replacement with a synthetic material[94,112,167] or with a tissue engineered structure[110], targets earlier stages of disc degeneration.

We propose the use of polymeric hydrogels for replacement of the nucleus pulposus. Prior work in our laboratory has focused on the development of a chemically stable hydrogel polymer system[172,173]. Hydrogels are polymeric three dimensional crosslinked structures that are able to absorb large amounts of water and swell to equilibrium[141]. Hydrogels offer many advantages including biocompatibility[29,174], shape memory properties[172], and fatigue[175]. The objective of this study was to assess the effect of nucleus replacement by a hydrogel implant on the compressive stiffness of the lumbar functional spinal unit (FSU). It is hypothesized that replacing the NP with a hydrogel, the Poisson's effect of a polymeric hydrogel under compression will mimic the effect of natural intradiscal pressure of a normal NP on the AF and that this reproduced pressure, will enable stiffness restoration of a denucleated IVD to that of an intact IVD.

Materials and Methods

Nucleus Implant Preparation. A polymer blend containing 95-weight% poly (vinyl alcohol) (PVA) (molecular weight, 138,400 – 146,500 g/mol) and 5-weight% poly (vinyl pyrrolidone) (PVP) (molecular weight, 10,000 g/mol) was prepared. 10% polymer solutions (by weight) of PVA and PVP were prepared by dissolving a mixture of the two polymers in deionized water at 90°C overnight. The solution was homogenized for 30 minutes using sonication and cast into Plexiglas® molds (16 mm diameter with various

heights). The filled molds were gelled by six repeated cycles of freezing for 21 hours at –19°C and thawing for 3 hours at 25°C.

Nucleus Implant Compression Testing. Unconfined compression tests on cylindrically shaped hydrogels were performed on an Instron (model 4442; Canton, MA, USA) mechanical test machine at a loading rate of 100% strain/min. The samples were compressed up to 60% strain. The compression test data was recorded in the form of load – displacement curves.

Human Cadaver Mechanical Testing. Lumbar FSUs were tested in axial compression to assess the ability of the hydrogel to replace the NP and thus restore the biomechanics of the intact disc. Because the biomechanics of the intact disc is dependent on the NP-AF interaction, assessment of the hydrogel nucleus implant replacement on the disc mechanics can best be achieved if the AF is maintained intact. Keeping this in mind, a novel approach was developed for FSU denucleation. Denucleation was obtained by drilling through the superior vertebra to the IVD level and excising the NP. Thus, we avoid injury to the AF, which remained intact throughout the experiment[176].

Specimen Preparation: FSUs were harvested from 8 cadavers (3 males and 5 females) with an average age of 65 years, within 72 hours of death. Fifteen lumbar FSUs from L1-S1 levels were selected based on visual inspection eliminating those with obvious damage/degeneration. Intervertebral segments were prepared by removing muscle and posterior elements including facet joints and pedicles. Parallel cuts were made perpendicular to the longitudinal axis of the FSU through the vertebrae above and below the disc to ensure alignment of the axial compression load. Thus, the specimen consisted of an intervertebral disc in between adjacent vertebrae. The fifteen specimens were

frozen at –19°C in sealed bags until the day of testing. On the day of testing, specimens were thawed for at least 2 hours at room temperature in a sealed bag prior to testing. Anatomical measurements of the specimen (disc height, superior and inferior vertebrae height, disc major and minor diameter) were performed using standard digital measuring instruments.

Mechanical Testing Method: The test specimen was constrained in a custom made test fixture with help of screws, which connected the inferior vertebrae to the test fixture. A commercially available potting mixture (Cargroom; U.S. Chemical and Plastics, OH, USA) was used for potting of specimens in the fixture. Only the inferior vertebra was potted with care to ensure that the potted material was not touching the IVD. The cut flat and parallel surfaces of the vertebrae ensured the axial loading. The superior vertebra was compressed against the flat compression plate attached to the load cell. This allowed adequate access for denucleation of the specimen and insertion of the hydrogel implant, as the compression plate and proximal vertebra were not attached physically[176]. Specimens were kept moist throughout the experiment by spraying a protease inhibitor.

Compression Testing Protocol: An Instron (model 1331; Canton, MA, USA) mechanical testing machine was used. The initial baseline position of the upper compression plate and lower actuator was ensured and maintained through each tested condition. The specimens were preconditioned for 50 cycles at 3% strain (based on the average IVD height). The load range corresponding to this preconditioning was 40N – 140N. Specimens were axially compressed to 15% of total average IVD height. The testing was performed with a triangular waveform at 0.5 Hz with a loading rate of 15% strain/sec for 5 loading cycles, for each tested condition.

FSU Implantation and Test Protocol: A series of axial compressive tests were completed on each specimen, as shown in Figure 5.1. First, the intact specimen was tested using the compression testing protocol (Intact condition). Then, a Cloward core drill bit of 16mm diameter was used to drill perpendicular to the cut surface of the superior vertebra through the bone to the IVD. This hollow core drill was centered in the medial/lateral dimension of the vertebral body and positioned approximately 2mm posterior to the centerline in the anterior/posterior dimension. A cylindrical bone plug (height equal to that of proximal vertebra and diameter equal to 15.5mm) above the disc was removed. For the second test condition, the BI condition[176], the cylindrical bone plug was reinserted and the test protocol was repeated. Then, the bone plug was removed from FSU and the central portion of the nucleus in line with the core drill (equal to 16mm diameter) was removed using standard surgical instruments, keeping the residual NP and the AF intact (Figure 5.2). The testing protocol was then run on the denucleated specimen without the bone plug (DN–1, denucleated condition). A cylindrical hydrogel implant with a diameter equal to 16mm and height equal to that of measured average disc height was implanted into the cavity formed by removal of the nucleus material. This formed a line-to-line fit of the nuclear defect. The bone plug was again placed in its original position over the hydrogel implant and the testing protocol was repeated (Implanted condition). Finally, the implanted hydrogel and bone plug were removed and the specimen was tested again (DN–2, denucleated condition) to determine if there was any damage to the specimen during testing.

Data Analysis: The load-displacement history data for each tested condition was collected using a Labview® program (sampling rate=1000 Hz). Data for the fifth loading

cycle were taken for analysis and instantaneous compressive stiffness values (N/mm) were calculated at representative strain levels of 5%, 10% and 15%, for each condition, for each specimen. The stiffness values were obtained by numerically differentiating the raw data, taking the slope of the line passing through points corresponding to the representative strain levels. For each strain level (5%, 10% and 15%), a one-way, repeated measures ANOVA was performed for compressive stiffness with one subject factor (surgical condition: Intact-BI-DN-1-Implanted-DN-2). Fisher's LSD post-hoc analysis was conducted to assess the effect of surgery (Intact vs. BI), effect of denucleation (BI vs. DN-1), restoration ability of the hydrogel (BI vs. Implanted) and crosscheck (DN-1 and DN-2). The acceptable rate for a type-I error was chosen as 5% for all tests.

Results

Figure 5.3 shows five different load-displacement curves corresponding to different conditions of intact, BI, DN-1, implanted and DN-2, for a representative specimen. This nonlinear nature of load-displacement curve was observed for all specimens under all conditions. Figure 5.4 shows the plot of FSU compressive instantaneous stiffness (N/mm) vs. the strain (%) for all five testing conditions. The one-way ANOVA calculations comparing stiffness of these five conditions at 5%, 10% and 15 % strain showed significant differences ($p < 0.001$). In all the specimens (at 5%, 10%, 15% strain), the stiffness for the denucleated conditions (DN-1 vs. DN-2) was not significantly different (p=0.92, 0.60, and 0.23, respectively), indicating a return to the original denucleated condition after implant removal.

Drilling into the vertebrae (BI) reduced the stiffness compared to the intact condition and was significantly different (e.g. stiffness value 80% of Intact at 15% strain, $p < 0.001$ at all strains levels). A more dramatic reduction in the stiffness was observed for denucleated specimens (e.g. stiffness value 44 % of BI at 15% strain, $p < 0.001$ at all strain levels). Insertion of the hydrogel implant restored the stiffness of the FSU to a value of 88 % of BI at 15% strain and was significantly different than DN-1 at all strain levels ($p<0.001$). This restoration of stiffness by the hydrogel implant was 92%, 88%, and 88%, of BI stiffness at respective strain levels. Stiffness of BI compared to Implanted was not significantly different, $p>0.05$ at all strain levels.

Table 1 shows the stiffness of the denucleated FSU, the hydrogel alone, and hydrogel implanted FSU at various strain levels. The effect of hydrogel implantation in the denucleated specimen is clearly shown in the resulting increased stiffness of the implanted specimen (Table 1). Moreover, the implanted specimen stiffness is far greater than the corresponding algebraic sum of the denucleated specimen stiffness and the hydrogel.

Discussion

This work examined the ability of a PVA/PVP hydrogel to restore the normal biomechanics of the lumbar FSU, in axial compression, keeping the AF intact. The hydrogel implant insertion method was intended to maintain an intact AF[176] to see if insertion of a hydrogel in the nucleus cavity restores the FSU compressive stiffness in an 'ideal' setting. The insertion method was clearly not intended to represent a clinical implantation technique, which would need a significant modification.

Earlier work has been performed for nucleus replacement with a synthetic material in cadaveric FSUs[96,97,100,113] and in animals[98,108]. No human cadaver studies have reported the effect of nucleus implant replacement on the pure compressive behavior of the FSU. However, Meakin et al.[108] used sheep discs to assess the effect of nucleus implant on bulging direction of the AF fibers, in pure compression. The idea of nucleus replacement by a synthetic material was demonstrated to be feasible in all of the above studies. However, in all of the cases, the nucleotomy was facilitated by making a small incision through AF. Our novel approach to nucleus implantation precluded AF damage, enabling full interaction of the nucleus implant and intact AF.

Calculated stiffness values for intact specimens agreed well with those previously reported for lumbar FSUs in the literature (772 N/mm – 3040 N/mm)[30,44]. The restoration of stiffness to the denucleated FSU after implantation with the PVA/PVP hydrogel is evident from Figure 5.4. The general premise that the IVD biomechanics and load transfer mechanism results from synergistic effect between the implanted hydrogel and the surrounding intact annulus is shown through this experimentation. Considering the data in Table 1, one can clearly see that the summation of the stiffness of the 'denucleated' FSU (e.g. 672 N/mm @ 15% strain) and that of 'hydrogel only' (e.g. 2 N/mm @ 15% strain) do not equal the stiffness of the 'implanted' FSU (e.g. 1351 N/mm @ 15% strain). We hypothesize that this non-linear increase in the stiffness observed after implantation of the polymeric hydrogel is due to the interaction between the polymeric implant and the intact annulus. The Poisson's effect of the hydrogel ($\upsilon \approx 0.49$) results in a significant radial displacement in compression. In case of an intact disc (Figure 5.5), load transfer occurs by pushing the annulus radially outwards, which is

facilitated by IDP, generated by the hydrated NP. In case of the denucleated disc (Figure 5.6), the inner AF fibers bulge inwards and are in compression. In case of a nucleus implanted disc (Figure 5.7), the radial displacement of the implant causes a stress at the implant/annulus interface. It is this stress that mimics the IDP of a normal nucleus and presumably creates tension in AF fibers. The tension in the AF fibers may then allow the AF to bear more loads, resulting in higher stiffness of the FSU, through this synergistic interaction. Based on the present study results, the resultant increase in stiffness of the implanted condition is not a function of volumetric replacement alone. It also indicates that nucleus implant mechanical properties have significance in the restoration FSU mechanics. In addition, the geometry of the implant (diameter, height and overall shape) may also play a role in the stress transfer between the implant and annulus. A large gap, for example, between the nucleus implant and the annulus may not create an intradiscal stress of the same magnitude as a line-to-line fit.

This method of nucleus replacement by a hydrogel may provide an enhanced long-term outcome as compared to the current treatment methods, discectomy and fusion. Theoretically, hydrogel implantation may preserve the natural AF tissue structure by delaying damage to the annulus, associated with alternate loading of the annulus resulting from discectomy. Unlike fusion, the load transfer of the implanted IVD would occur much like the intact disc, theoretically avoiding degeneration in adjacent IVD segments.

The implantation of a PVA/PVP hydrogel nucleus in the lumbar FSU showed promise in restoration of IVD biomechanics in terms of compressive stiffness. However, considering the complex loading on the spine, restoration of the spine biomechanics under combined loading with hydrogel implantation is also of prime importance. In

present study, almost complete restoration (~ 88%) of the stiffness in the implanted FSU was observed as compared to the 'BI' condition. Further optimization may be achieved through alteration in the nucleus implant modulus and 'fit and fill' of the nuclear cavity.

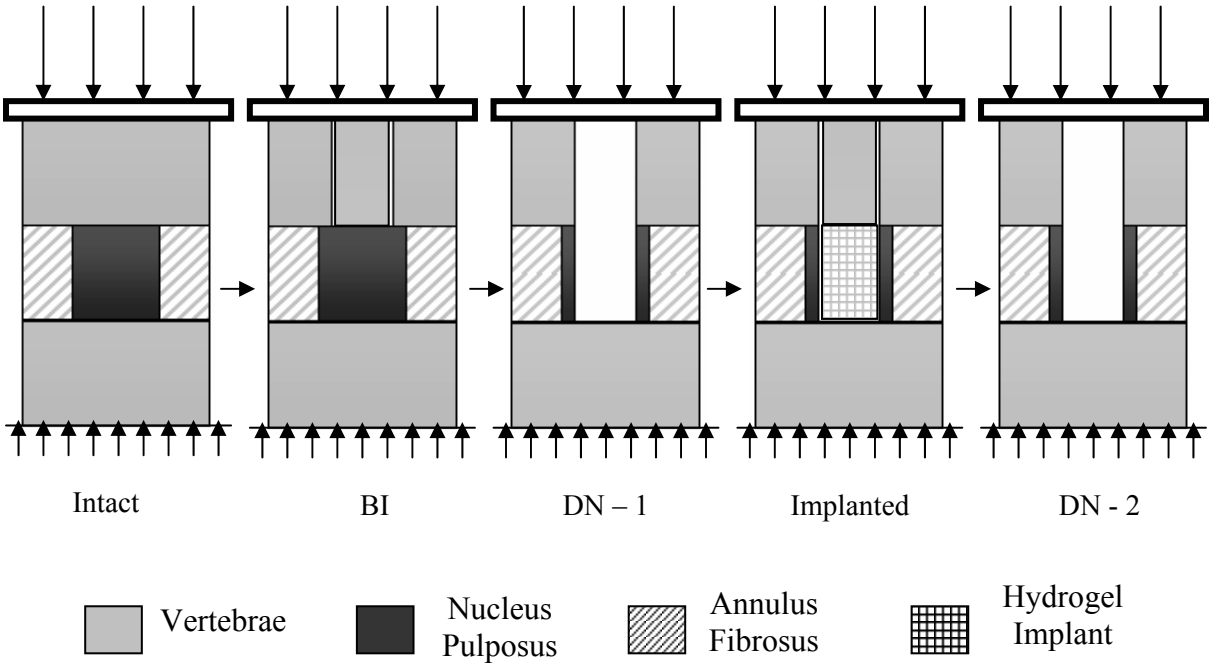

Figure 5.1. Schematic of Testing Protocol and Implantation Method of a Lumbar FSU

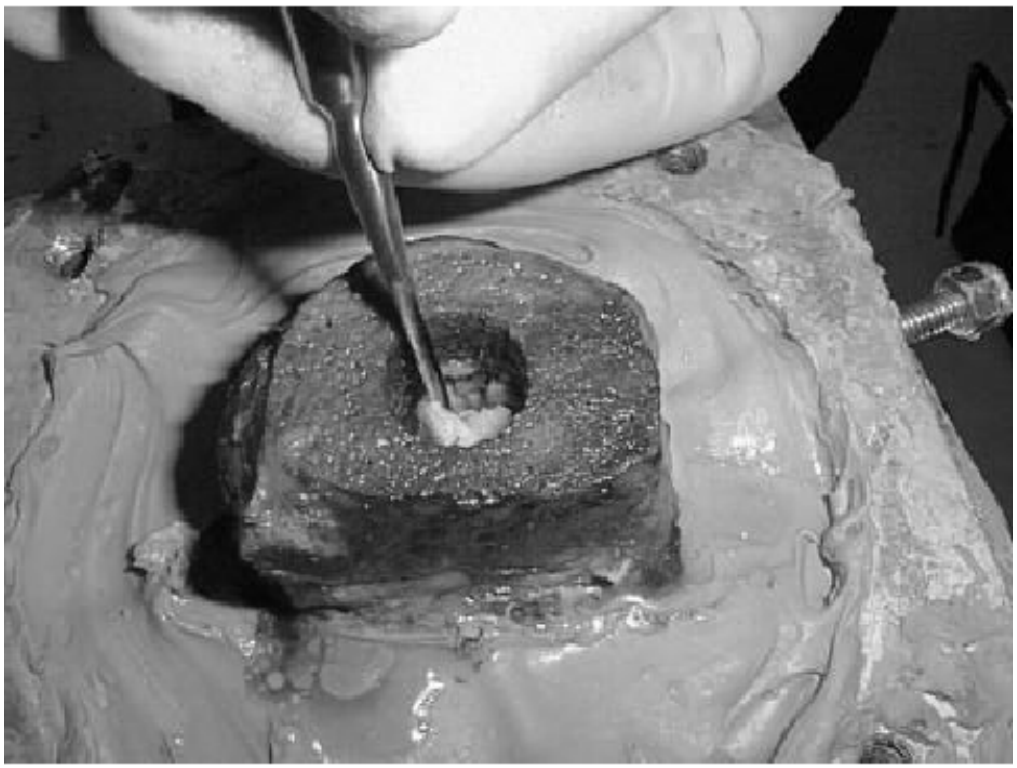

Figure 5.2. Denucleated Specimen

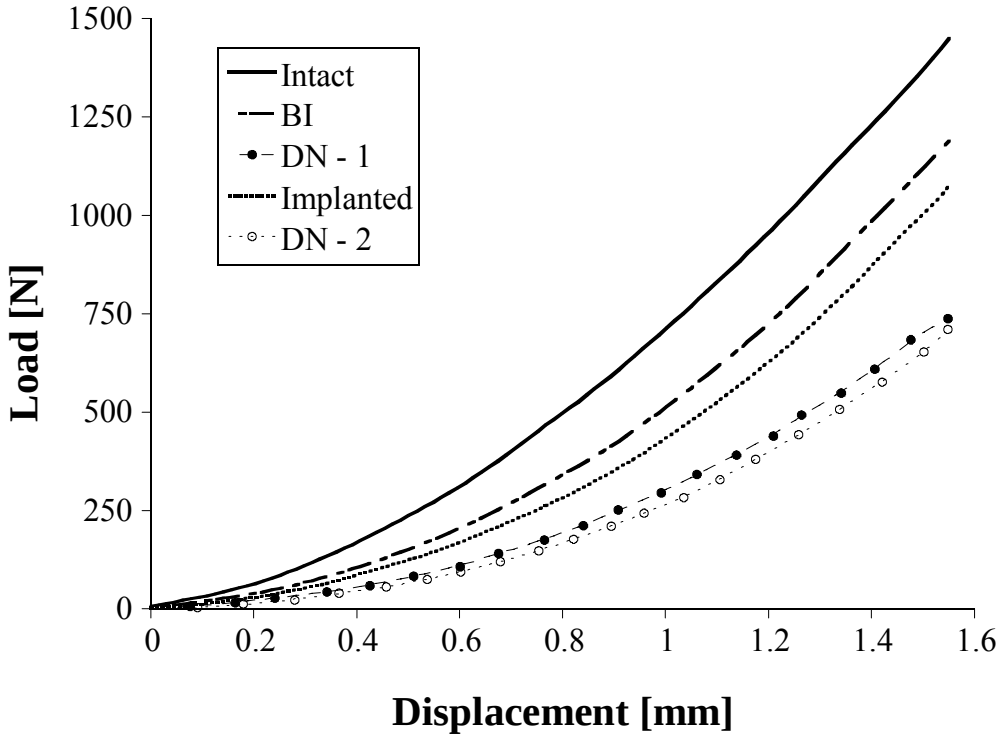

Figure 5.3. Load – displacement curves of one specimen for five different testing conditions

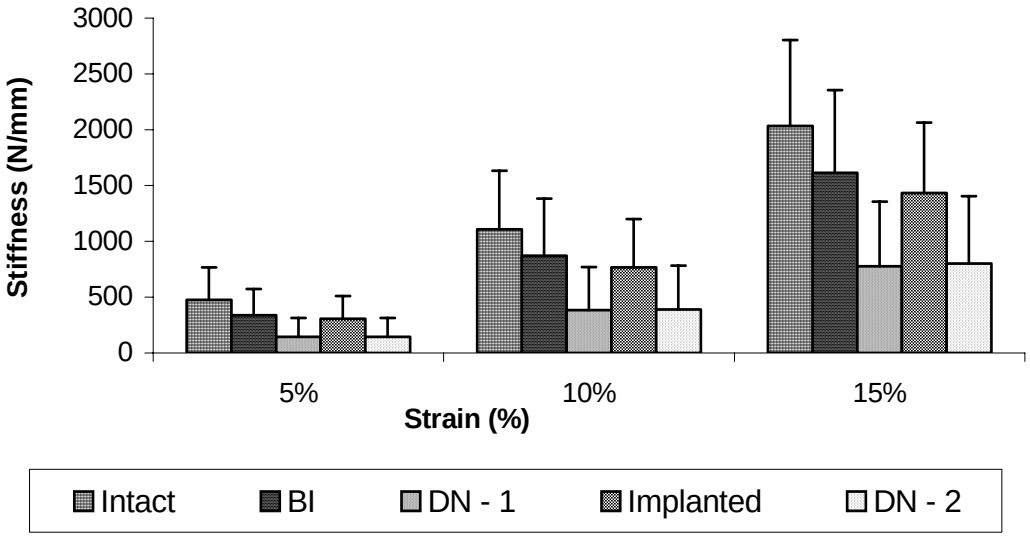

Figure 5.4. FSU Compressive Instantaneous Stiffness (N/mm) vs. Strain (%)

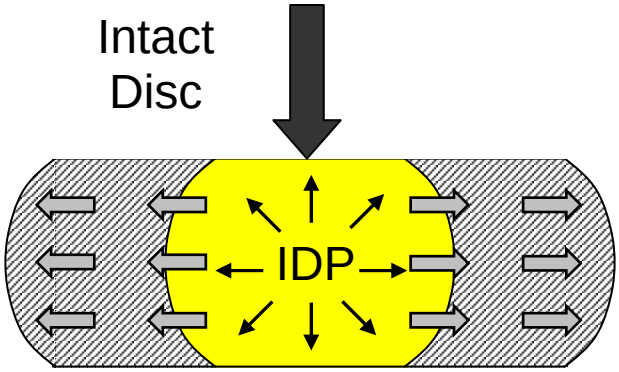

Figure 5.5. Load transfer in an intact disc by intradiscal pressure generation

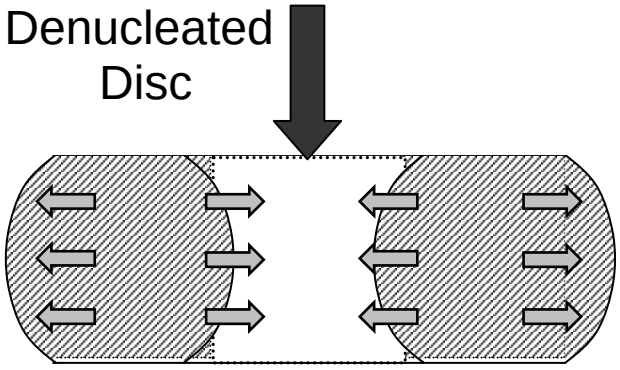

Figure 5.6. Inward bulging of annulus in the denucleated disc

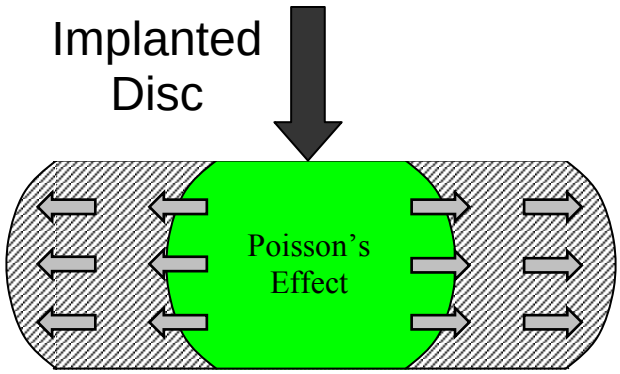

Figure 5.7. Poisson's effect of polymeric hydrogel nucleus implant

Table 5.1. Compressive stiffness comparison of the Denucleated disc, Hydrogel only and Implanted disc

Stiffness (N/mm)	**5% Strain**	**10% Strain**	**15% Strain**
Denucleated	116.0	311.0	672.0
Hydrogel Only	0.8	1.7	2.5
Implanted	277.0	702.0	1351.0

6. Nucleus Implant Parameters Significantly Change the Compressive Stiffness of the Human Lumbar Intervertebral Disc

Introduction

Low back pain is one of the most important socioeconomic diseases and one of the most expensive health care issues today. The causes of low back pain vary from patient to patient and remain unclear to date. In more than 75% of the cases, the origin of the lower back pain is a degenerated lumbar intervertebral disc (IVD)[1]. In the normal healthy disc, the hydrated NP exerts a hydrostatic pressure (intradiscal pressure) on the AF fibers. This intradiscal pressure (IDP) is mainly responsible for load distribution in the disc, by creating tension in the AF fibers near the interface with the NP[30]. However, this load transfer mechanism is altered in case of the diseased disc. The water content of the NP in the degenerated disc is significantly reduced with corresponding decrease in IDP[14,30,120]. This results in the AF experiencing compressive stresses, even though it is primarily designed to sustain tensile stresses[17,30,169]. An abnormal stress state of the AF in the degenerated disc over repeated loading, may provide the stimulus for the formation of cracks or fissures in the AF and thereby a path for the NP migration from the center of the AF toward periphery. The contact of migrated NP material with the nerve root may cause debilitating back or leg pain[14,30,120].

Non-fusion techniques such as total disc arthroplasty[78,80,171] and nucleus replacement[94,112] are the two main approaches emerging as a solution to this condition. The exploration of these concepts for low back pain solutions is mainly motivated by the limited success of the current treatments such as spinal fusion and discectomy. Both of these current procedures relieve pain, but are unable to restore the spinal biomechanics to

a normal state[14,19-21,23]. Moreover, these procedures may promote further degeneration of either the initially affected disc, in the case of discectomy[21,23] or adjacent IVDs in the case of spinal fusion[25,26]. The ultimate goal of the non-fusion solution for the treatment of low back pain would be to relieve the pain completely and to restore the motion and stress state to that of the normal physiological condition[170]. Currently, total disc arthroplasty targets the later stages of disc degeneration (Galante grade IV)[55]. Nucleus replacement with a synthetic material[94,112,167] or with a tissue engineered structure[110], targets earlier stages of disc degeneration (Galante grade I, II and III)[55] where the annulus is not fully compromised with the same goal of eliminating pain while restoring the height of the disc as well as the normal biomechanics of the IVD. This later approach may help to preserve the AF and be more amenable to minimally invasive surgical techniques.

Our laboratory has been investigating the use of polymeric hydrogels for replacement of the nucleus pulposus. Prior work has focused on the development of a chemically stable hydrogel polymer system[173,177,178]. Hydrogels are polymeric three dimensional crosslinked structures that are able to absorb large amounts of water and swell to equilibrium[141]. In our earlier studies, we assessed the effect of hydrogel nucleus replacement on the compressive stiffness of the lumbar intervertebral disc[176,179]. In that work, we demonstrated the feasibility of replacing the NP with the hydrogel implant. We have developed a novel trans-end plate approach for *in vitro* testing of the nucleus implant capability by avoiding any injury to the AF[176]. This was achieved by creating a bone plug from the superior vertebra using a standard core drill. The hydrogel implant restored 88% of the compressive stiffness of the denucleated IVD when implanted in the

created nuclear defect[179]. This restored stiffness was a result of synergistic effect between the hydrogel implant and the intact AF. It is assumed that the Poisson's effect for the hydrogel nucleus implant played a major role in the restoration of the compressive stiffness by tensioning the AF fibers under compressive stress, mimicking the normal IDP acting on the AF inner layers. The interaction is both a function of the mechanical properties and the geometric fit of the nucleus pulposus implant. Therefore, it is postulated that a complete restoration of the denucleated IVD stiffness can be achieved by altering the nucleus implant parameters such as modulus, height and diameter. The objective of the current study is to systematically assess the effect of variation in these nucleus implant parameters (material and geometric) on the compressive stiffness of the lumbar IVD. It is hypothesized that by altering these nucleus implant parameters, the synergistic interaction effect (which is responsible for the stiffness restoration) between the implant and the intact AF can be modulated, thereby achieving the complete restoration of the compressive spinal biomechanics.

Materials and Methods

Nucleus Implant Preparation. A polymer blend containing 95-weight% poly (vinyl alcohol) (PVA) (molecular weight, 138,400 – 146,500 g/mol) and 5-weight% poly (vinyl pyrrolidone) (PVP) (molecular weight, 10,000 g/mol) was prepared. 10% polymer solutions (by weight) of PVA and PVP were prepared by dissolving a mixture of the two polymers in deionized water at 90°C overnight. The solution was then homogenized for 30 minutes using sonication. The solution was then cast into the custom made molds of three different diameters (D_1= 15mm, D_2= 16mm and D_3= 17mm) to achieve variation in the hydrogel implant diameter. The filled molds were gelled by six repeated cycles of

freezing for 21 hours at -19°C and thawing for 3 hours at 25°C. Variation in the implant height was based on the measured average height (H_2) of an IVD of the test specimen and achieved by cutting the implants, as either undersize ($H_1=H_2$-1mm) or oversize ($H_3=H_2$+1 mm). Variation in the implant modulus (E_1=50 kPa @ 15% strain, E_2=150 kPa @ 15% strain) was achieved by varying the number of freeze-thaw cycles (2 cycles for lower modulus and 6 cycles for higher modulus) during the preparation[142]. A third higher modulus implant (E_3=1500 kPa @ 15% strain) was made from Silastic T2, a commercially available polymer mixture (Dow Corning, MI, USA). Thus, implants with three different moduli, three different heights and three different diameters were used for assessment of change in the compressive stiffness of the lumbar IVD.

Human Cadaver Mechanical Testing. We performed mechanical tests on lumbar IVDs in pure axial compression in order to assess the effect of nucleus implant (material and geometric) parameters on the IVD mechanical behavior with the goal of restoring the IVD compressive stiffness. Because the biomechanics of the intact disc is dependent on the interaction of the NP and AF, assessment of the hydrogel nucleus implant replacement on the disc mechanics can best be achieved if the AF is maintained intact. Keeping this in mind, we developed a novel approach to denucleate the specimen[176]. Denucleation was obtained by drilling through the superior vertebra to the IVD level and excising the NP. Thus, we avoid injury to the AF, which remained intact throughout the experiment.

Specimen Preparation: Functional spinal units (FSU) were harvested from 4 cadavers (1 male and 3 female) with an average age of 63 years, within 72 hours of death. Nine lumbar FSUs from L1-L5 levels were selected for testing based on visual inspection,

eliminating those with obvious damage or degeneration. Intervertebral segments were prepared by removing muscle and posterior elements including facet joints and pedicles. Parallel cuts were made perpendicular to the longitudinal axis of the intervertebral segment through the vertebrae above and below the disc to ensure alignment of the axial compression load. Thus, the specimen consisted of an intervertebral disc in between adjacent vertebrae. (This bone-disc-bone segment will be referred to as the IVD or the intervertebral segment throughout this paper.) The nine specimens were frozen at –18°C in sealed bags until the day of testing. On the day of testing, specimens were thawed for at least 2 hours at room temperature in a sealed bag prior to compression testing.

Anatomical measurements of the specimen (disc height, proximal and distal vertebrae height, disc major diameter and disc minor diameter) were performed using standard digital measuring instruments. In order to minimize the measurement error, measurement at 3 different locations was averaged. Based on the average IVD height (H_2) of a specimen, nucleus implants for height variation were prepared accordingly to obtain height variation, as either undersize or oversize.

Mechanical Testing Method: The IVD specimens were constrained in a custom made test fixture with help of screws, which connected the distal vertebrae to the test fixture. A commercially available potting mixture (Cargroom®, U.S. Chemical and Plastics, OH) was used for potting of specimens in the custom made fixture. Only the inferior vertebra was potted, with care to ensure that the potted material was not touching the IVD. The cut flat and parallel surfaces of the vertebrae ensured the axial loading. The superior vertebra was compressed against the flat compression plate attached to the load cell. This allowed adequate access for denucleation of the specimen and insertion of the hydrogel

implant, as the compression plate and superior vertebra were not attached physically. In order to keep the specimen moist, a solution of protease inhibitor was sprayed on the specimen, throughout the test protocol.

Compression Testing Protocol: An Instron (Canton, MA) mechanical testing hydraulic machine (Model 1331) was used for the testing. The initial baseline position of the upper compression plate (load cell) and lower actuator was ensured and maintained using digital position indicators through each tested condition. The specimens were preconditioned for 50 cycles at 3% strain (based on the average IVD height). The load range corresponding to this preconditioning was 40N – 140N. Specimens were then axially compressed to 15% strain based on the measured average disc height. The testing was performed with a triangular waveform at 0.5 Hz with a loading rate of 15% strain/sec for 5 loading cycles, for each tested condition. The data of the fifth loading cycle was taken for further analysis from each tested condition.

Implantation Sequence: For each specimen, implant modulus was varied ($E_1/E_2/E_3$) with a constant implant height (H_2) and diameter (D_2). Similarly, implant height was varied ($H_1/H_2/H_3$) with a constant implant modulus (E_2) and diameter (D_2). Finally, implant diameter was varied ($D_1/D_2/D_3$) with a constant implant modulus (E_2) and height (H_2). Figure 6.1 shows a schematic of the implantation sequence used in the mechanical testing. For each specimen, the order of the implants inserted was chosen randomly to minimize any effect of implant parameters on the test specimen. Overall seven different nucleus implants (same implant was used for medium modulus E_2, medium height H_2 and medium diameter D_2) were used to assess the effect of implant parameters for total of

nine (three moduli variation, three height variation and three diameter variation) different mechanical tests on a specimen.

IVD Implantation and Test Protocol: A series of axial compressive tests were completed on each specimen, as shown in Figure 6.2. First, the intact specimen was tested using the compression testing protocol (Intact Condition - IC). Then, a 16 mm diameter Cloward core drill bit was used to drill perpendicular to the cut surface of superior vertebra through the bone to the IVD level. A cylindrical bone plug (height equal to that of superior vertebra and diameter equal to 15.5mm) above the disc was removed. For the second test condition, the cylindrical bone plug was reinserted and the test protocol was repeated (Bone plug Inserted condition – BI). Then, the bone plug was removed from the upper vertebra and the nucleus was incised in line with the core drill. The central portion of the nucleus in line with the core drill (equal to 16mm diameter, wet weight 2.5-3.0 g) was removed using standard surgical instruments, keeping the residual NP and the AF intact. The testing protocol was then run on the denucleated specimen without the bone plug (first DeNucleated condition, DN–1). The nucleus implants were inserted in the nuclear defect, in a random fashion, as described previously. For all the nine implanted conditions, the bone plug was again placed in its original position over the nucleus implant and testing protocol was repeated (Implanted conditions – E_1,E_2,E_3,H_1,H_2,H_3,D_1,D_2,D_3). Finally, the implanted hydrogel and bone plug were removed and the specimen was tested again (second DeNucleated condition, DN–2) to determine if there was any damage to the specimen during testing.

Data Analysis: The data for each tested condition in terms of force and displacement history was collected using a custom written Labview® program at a sampling rate of

1000 Hz. Data for the fifth loading cycle was taken for analysis and instantaneous compressive stiffness values (N/mm) were calculated at representative strain levels of 5%, 10% and 15%, for each condition, for each specimen. The stiffness values were obtained by numerically differentiating the raw data, taking the slope of the line passing through points corresponding to the representative strain levels. A two-way, repeated measures ANOVA was performed for compressive stiffness with two subject factors; implant parameter variable (modulus, height or diameter) and strain level (5%, 10% and 15%). Fisher's LSD post-hoc analysis was conducted to assess the individual effects of modulus variation, effect of height variation, effect of diameter variation, restoration ability of the nucleus implant (BI vs. all nine implanted conditions) and crosscheck (DN-1 and DN-2). The acceptable rate for a type-I error was chosen as 5% for all tests.

In our earlier studies, we explained the significance of the BI condition in relation to the intact condition[176]. There was an observed decrease (approx. 20%) in the stiffness of the BI condition as compared to the intact condition. The physical condition of the implanted intervertebral segment more closely matched to the BI condition (as compared to the intact condition). In both cases, the BI and the implanted condition, the upper vertebra is drilled and then tested with the cylindrical bone plug in place. Hence, the implanted specimen results are compared to the BI condition results rather than to those of intact condition.

Results

Figure 6.3 shows the stiffness comparison of different testing conditions at representative strain levels of 5%, 10% and 15% for the effect of various implant parameters. The two-way, repeated measures ANOVA for IVD compressive stiffness

with two subject factors; implant parameter variable (modulus, height or diameter) and strain level (5%, 10% and 15%) showed significant interaction between the two factors ($p<0.05$). Significant differences in compressive stiffness were observed for variation in strain across all implant parameter variables ($p<<0.001$). Moreover, significant differences in stiffness were observed for variation in implant height ($p=0.003$) and implant diameter ($p=0.003$) across strain levels. However, no significant differences were seen for variation in implant modulus across strain levels ($p=0.14$).

Using the Fisher's LSD tests for comparison of the compressive stiffness of the denucleated conditions (DN-1 and DN-2) for all specimens at all strain levels (5%, 10%, 15%), no significant differences were observed ($p>0.60$). This suggests that the specimen returned to its original denucleated condition after implant removal without any damage. Hence, Figure 6.3 compares only one denucleated condition as DN (DN ≅ DN-1 ≅ DN-2).

Denucleating the IVD (DN) significantly reduced the compressive stiffness in comparison to the BI condition at all strain levels ($p<0.001$). The compressive stiffness of the IVD with the nucleus removed was 52% of the BI stiffness at 15% strain. The compressive stiffness of all implanted intervertebral segments was significantly greater than that of the denucleated IVD (DN-1) at each strain level ($p<0.001$). Moreover, with the exception of the H_1 and D_1 conditions at 10% and 15% strain, all implanted conditions were not significantly different than the corresponding BI condition ($p>0.05$). At 10% and 15% strain, the H_1 and D_1 condition IVD stiffness was significantly less than that of the BI condition ($p=0.01$). In Summary, for all implants (except the undersized H_1 and D_1 implants), the implanted IVD had a compressive stiffness that was

comparable to the BI condition and was significantly greater than the denucleated condition. Hence, implantation of the IVD restored the IVD compressive stiffness after denucleation to that of BI condition.

Fisher's LSD tests showed significant differences ($p \leq 0.03$) between the implanted conditions of the modulus variation (E_1 vs. E_2, E_1 vs. E_3, E_2 vs. E_3), height variation (H_1 vs. H_2, H_1 vs. H_3, H_2 vs. H_3), and diameter variation (D_1 vs. D_2, D_1 vs. D_3, D_2 vs. D_3) at all strain levels with three exceptions. These exceptions were E_2 vs. E_3 at 15% strain (p=0.31), H_2 vs. H_3 at 15% strain (p=0.08) and D_2 vs. D_3 at 5% strain (p=0.09). Table 2 shows the details of the statistical comparison of the different test conditions.

Discussion

This work examined the effect of nucleus implant parameters on the compressive behavior of the human lumbar IVD and utilized a novel nucleus implant insertion method previously developed in our lab to assess the implanted IVD mechanics[176]. Earlier work has been performed on nucleus replacement with a synthetic material in cadaveric IVDs[96,97,100,113] and in animals[98,108]. To our knowledge, no human cadaver studies have reported the effect of nucleus implant parameters on the compressive behavior of the IVD. However, Meakin et al. used sheep discs to assess the effect of nucleus implant modulus on bulging direction of the AF fibers, in pure compression[108]. They showed that inward annular bulging can be prevented by inserting the nucleus implant with suitable material properties. Using finite element modeling, they also demonstrated that the stress state in the annulus is dependent on the nucleus implant material properties. The concept of nucleus replacement by a synthetic material was proven feasible in terms of restoration of IVD biomechanics, in all of the above studies. The interaction between the NP

implant and the AF is central to the IVD mechanics; however, in all of these studies, the nucleotomy and implantation was facilitated by making an incision through the AF. The incisional damage to the AF may compromise it and therefore, alters the interaction between the NP implant and the AF. A trans-annular implantation may not be the ideal *in vitro* approach for assessing the effect of nucleus implant on IVD mechanics. Our trans-vertebral approach to *in vitro* nucleus implantation precluded AF damage, ideally enabling full interaction of the nucleus implant and intact AF.

Our assumption that the restoration of IVD compressive stiffness by a nucleus implant was due to the Poisson effect of the implant tensioning the AF fibers was supported by the results of this experiment. In our earlier experiments[179], a line-to-line nucleus implant fit was observed to produce the almost complete (88% of the BI condition) restoration of the denucleated IVD stiffness. Thus in that experiment, we showed that replacing the NP of the lumbar IVD by a hydrogel implant can significantly restore the compressive stiffness of the denucleated IVD . The observed increase in the compressive stiffness of the implanted IVD was the result of a synergistic interaction between the hydrogel implant and the intact AF mimicking the normal intradiscal pressure acting on the AF inner layers. We hypothesized that the interaction was a function of geometric fit and the mechanical properties of the nucleus pulposus implant. The results presented in Figure 6.3 support this hypothesis.

Moreover, it was assumed that an under-sized implant would have less interaction with the AF while an over-sized implant will have better interaction with the AF. The results presented in Fig 6.3 also support these hypotheses. Thus, nucleus implant parameters have a significant effect on the mechanical behavior of the IVD and complete

restoration of the IVD mechanical behavior can be achieved by creating more interaction by means of an oversize implant (between the AF and the implant). As noted above, the IVD compressive stiffness increases and decreases with both height and diameter of the implant. This can be visualized graphically in Figure 6.4, where the volumetric ratio (defined as the ratio of Implant Volume [V_i] to that of Drilled cavity Volume [V_c]) vs. the compressive stiffness (N/mm) at different strain levels is plotted. The IVD stiffness was sensitive to the volumetric ratio of the size of the implants investigated. An increase in total volume of the nucleus implant resulted in increased compressive stiffness. At 15% strain level, increase in implant height produced 15 N/mm change in the compressive stiffness per % increase while increase in implant diameter produced 21 N/mm change in the compressive stiffness per % increase. Figure 6.5 shows the schematic of the under-diameter and over-diameter implant in compression. For an under-diameter implant, there is a gap in between the implant and the AF, resulting in zero preload and "less" interaction between the implant and the AF as the disc is loaded. With the initial compressive loading of the disc, the under-diameter implant would allow an inward radial deformation of the AF fibers initially, before interaction may take place. But an over-diameter implant results in preload with increased interaction between the implant and the AF. The resulting stiffness of the implanted specimen is therefore, a function of both preload and interaction, which are dependent on the Poisson's ratio and the geometric parameters, height and diameter studied here.

The effect of implant geometry can be compared to the effect of implant material modulus. The implant modulus increase produced 0.04 N/mm change in the compressive stiffness per % increase, at 15% strain level. Therefore, small changes in the height and

diameter of the nucleus implant produced changes in the IVD compressive stiffness, which were much greater than those resulting from implant modulus changes, which varied over two orders of magnitude. This suggests that within the range of the nucleus implant parameters investigated, the resulting compressive stiffness of the implanted IVD had a greater dependency on implant geometry as compared to the implant modulus.

This study indicated that the resulting IVD compressive stiffness after nucleus implantation is a complex phenomenon. The resulting implanted IVD stiffness is a function of three major factors: the Poisson effect of polymeric implant, synergistic interaction between the nucleus implant and the AF (preload and constrained bulk modulus effect) and compressive strain levels. Further understanding of these interactions in compression as well as under other loading conditions, may result in more effective nucleus implant design and performance.

Conclusions

The significant effect of nucleus implant modulus and 'fit and fill' effect of the nuclear cavity was demonstrated in this study. It was observed that variations in geometric parameters of an implant are more effective in modifying the compressive stiffness of the implanted IVD than those of implant modulus over the ranges examined. It is possible to restore the normal compressive stiffness of the IVD with a nucleus implant replacement. This may have clinical implications in restoration of disc biomechanics of the degenerated IVD. Considering the complex loading on the spine[30], future studies of the additional loading conditions will help us further elucidate the role of the nucleus implant in the restoration of intervertebral disc mechanics.

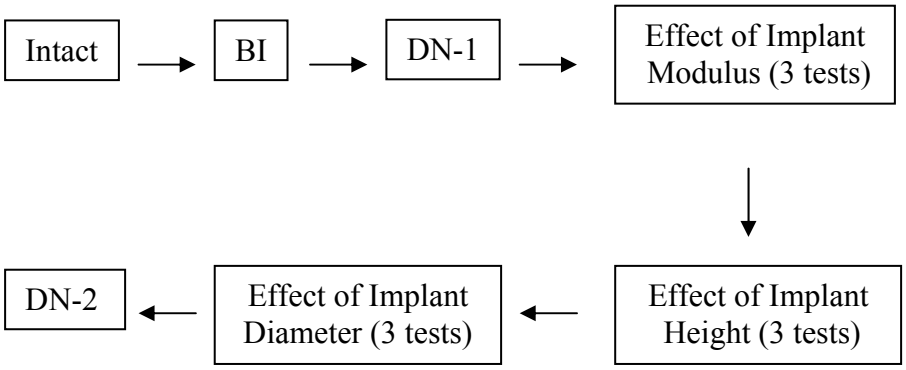

Figure 6.1. Schematic of testing protocol

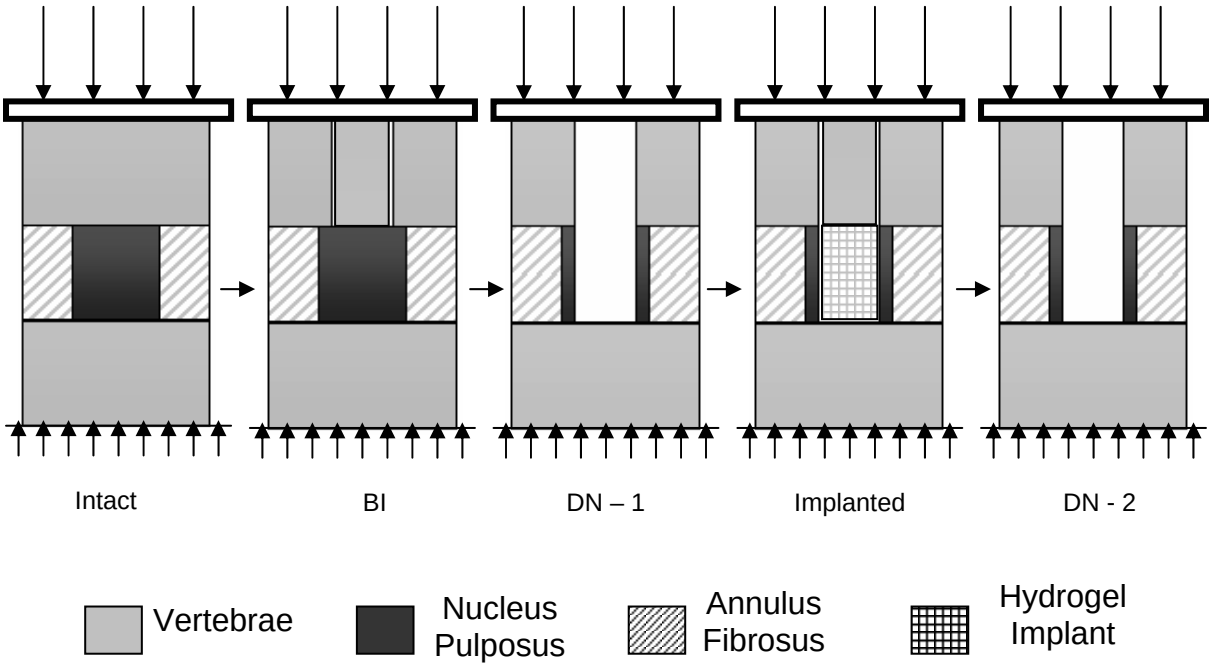

Figure 6.2. Schematic of implantation method of a lumbar IVD

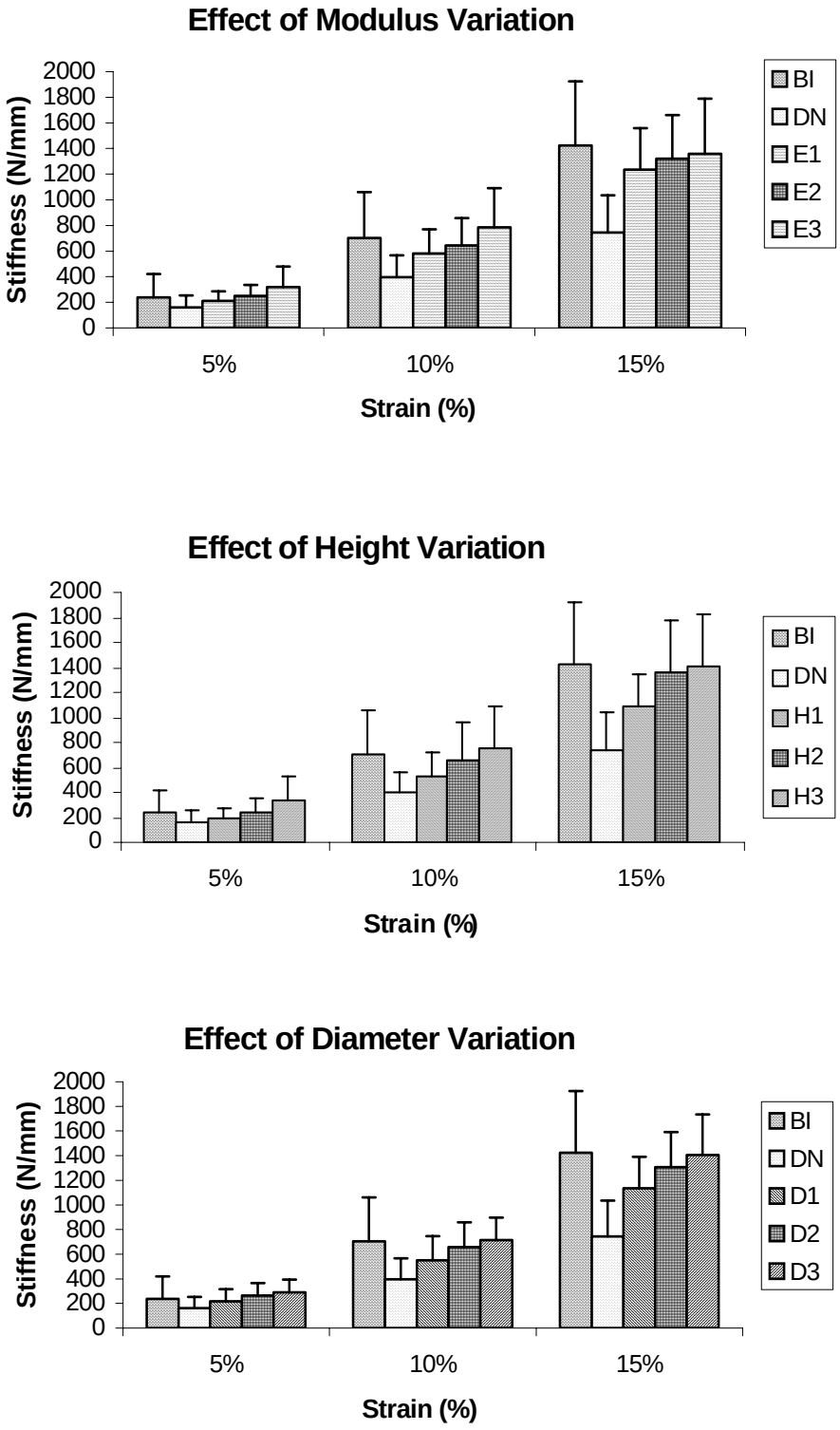

Figure 6.3. Effect of nucleus implant parameter variations on the compressive stiffness

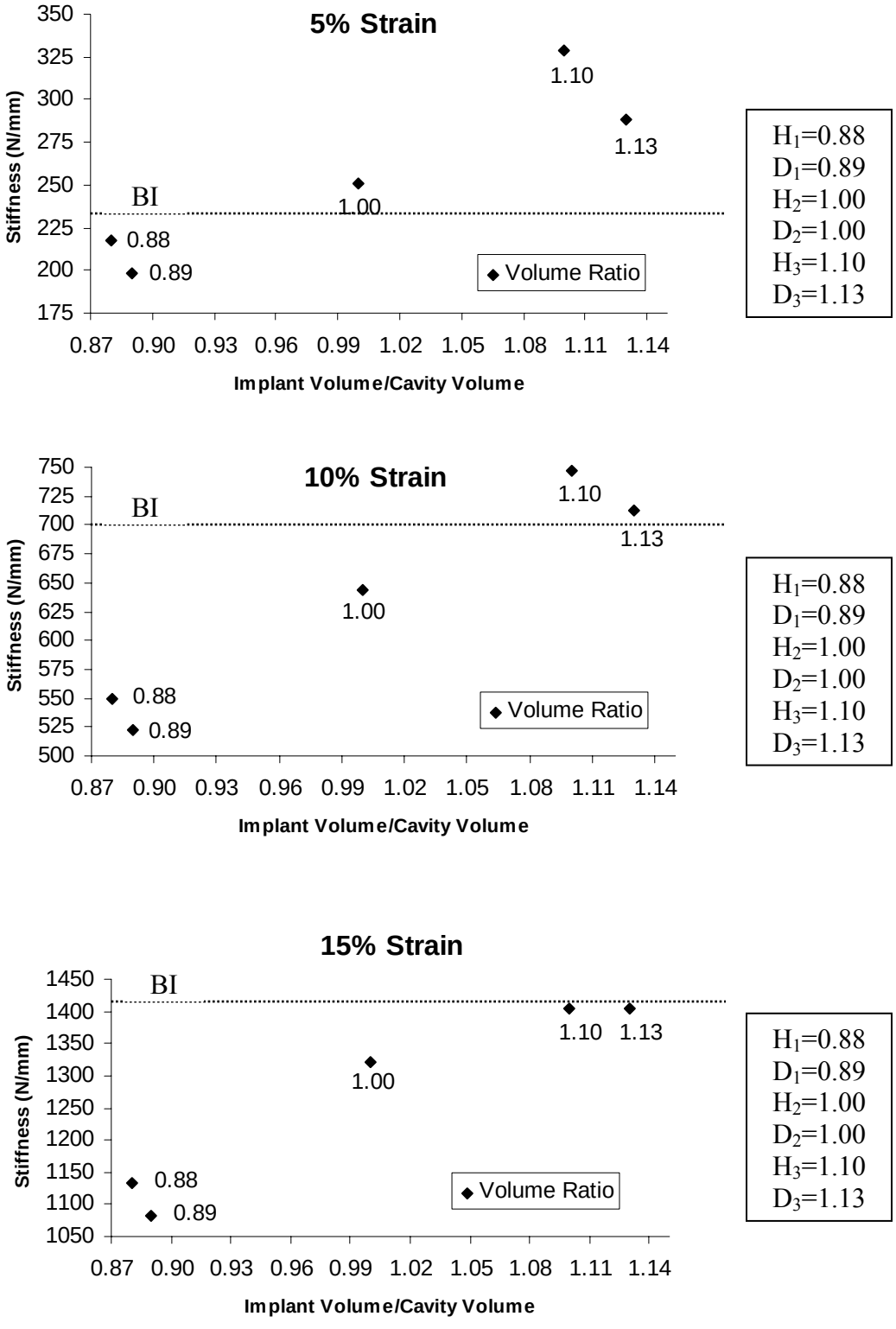

Figure 6.4. Stiffness vs. implant volume ratio of nucleus implant at different strain levels

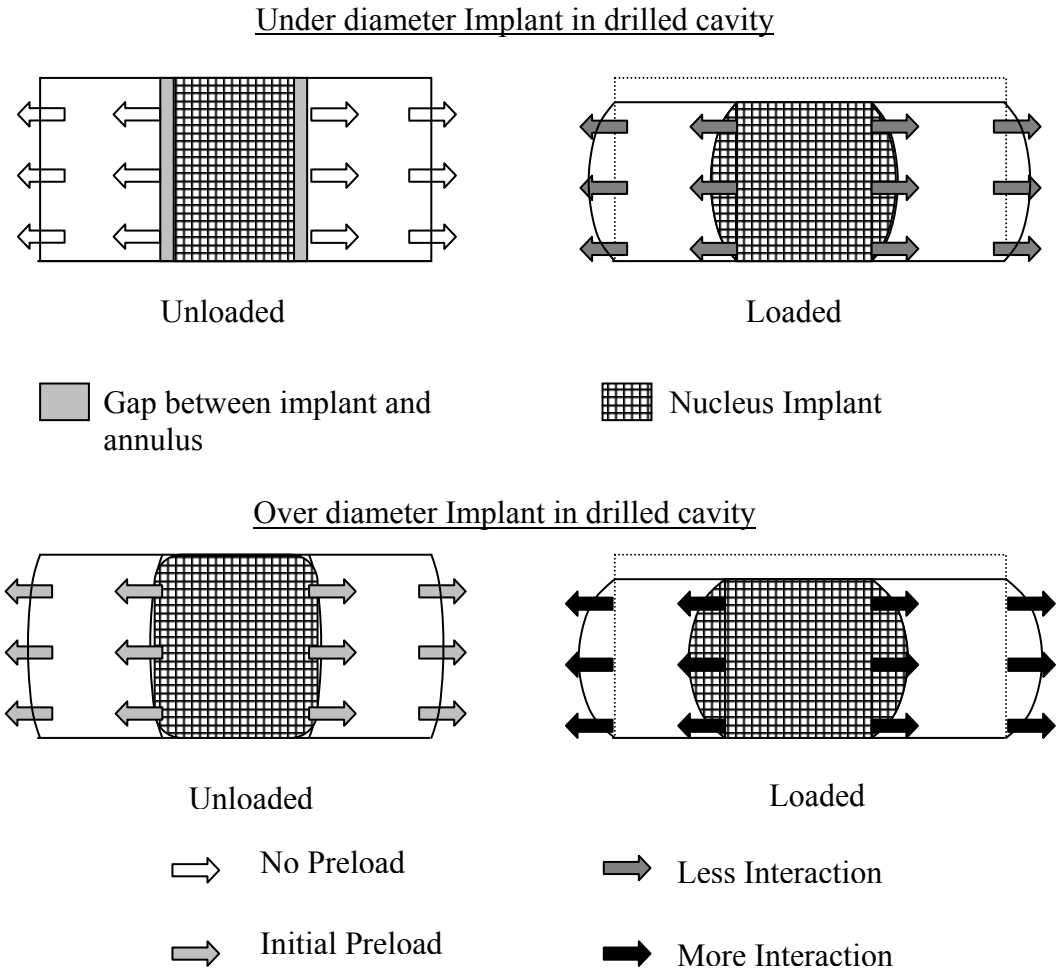

Figure 6.5. Schematic of under-diameter and over-diameter nucleus implant interaction

Table 6.1. Statistical comparison of different testing conditions

Test Condition	***'P'* value**		
	5% Strain	**10% Strain**	**15% Strain**
E_1 vs. E_2	≤ 0.02	≤ 0.02	≤ 0.02
E_1 vs. E_3	≤ 0.02	≤ 0.02	≤ 0.02
E_2 vs. E_3	≤ 0.02	≤ 0.02	***0.31**
H_1 vs. H_2	≤ 0.02	≤ 0.02	≤ 0.02
H_1 vs. H_3	≤ 0.01	≤ 0.01	≤ 0.01
H_2 vs. H_3	< 0.05	< 0.05	***0.08**
D_1 vs. D_2	≤ 0.01	≤ 0.01	≤ 0.01
D_1 vs. D_3	≤ 0.01	≤ 0.01	≤ 0.01
D_2 vs. D_3	***0.09**	≤ 0.03	≤ 0.03

* Statistically insignificant

7. The Effect of Nucleus Replacement on the Stress Distribution of the Lumbar Intervertebral Disc: A Finite Element Study

Introduction

The role of the lumbar intervertebral disc (IVD) in the lower back pain and related problems is well known. The impact of this socioeconomic disease on the society is significant. Although, the causes of lower back pain may vary from patient to patient, in more than 75% of the cases, the origin of the lower back pain is the degenerated lumbar intervertebral disc[1]. Motion segments of the human lumbar spine undergo complex loading situations, while performing routine daily activities[30]. The complex loading on the lumbar intervertebral disc (IVD) and its potential role in the lower back pain has been the basis of many experiments performed over the years for studying the lumbar spine mechanics. These studies were successful in determining the behavior of the motion segment under different loading conditions (simple and combined) and relative importance of individual elements of the motion segment. The experimental data available in the literature[58,180,181] generally reports the load-displacement behavior, intradiscal pressure measurements, radial strains in the disc and anisotropic properties of the annulus fibrosus (AF). There are also reports of pressure distributions in the disc and end plate deformation[46,72,182]. Considering the complex structure of the IVD and the diverse stresses to which it is subjected under physiological loading conditions, it is clear that experimental techniques alone are not sufficient to fully characterize the overall mechanical behavior of the motion segment. This was corroborated by the technical complexities which precluded the measurement of the stress state, deformation and disc bulge at different locations throughout the motion segment. This provided the motivation

for the development of numerical methods, such as finite element analysis, to expand the experimental data in order to characterize the IVD parameters, which may be difficult to measure experimentally.

Many researchers have simulated the intervertebral disc mechanics using the finite element method[72,116-118,128,183]. One study[108] performed the finite element analysis to assess the effect of nucleus replacement by a polymeric material on the compressive mechanics of the intervertebral disc. They observed the annular bulging in case of the intact and denucleated discs. The implant modulus was varied to observe the prevention of inward bulging of the inner annulus. Based on the experimental results and finite element analysis, they concluded that implant should have a Young's modulus of 3 MPa with total filling of the nuclear cavity.

Two main approaches are emerging for complete restoration of the IVD mechanical behavior: total disc replacement[14,171] and nucleus replacement[110,167]. At present, total disc replacement targets the later stages of disc degeneration where the AF is damaged and is beyond repair (Galante Grade IV)[55]. The nucleus replacement targets earlier stages of disc degeneration (Galante Grade I, II) where the annulus is still functional[55] but the nucleus pulposus (NP) is dehydrated / degenerated. The motivation behind exploration of these new solutions is mainly due to the limitation of current surgical treatments such as spinal fusion and discectomy[19,20]. These surgical treatments successfully relieve back pain but fail to restore the normal biomechanics of the spine. In many cases, patients suffer either from loss of motion (in case of spinal fusion) or an abnormal stress state produced within the disc (in case of discectomy)[14].

We propose the use of Poly (vinyl) alcohol (PVA) / Poly (Vinyl) Pyrrolidone (PVP) co-polymeric hydrogels for replacement of the nucleus pulposus. Prior work in our laboratory has focused on the development of a chemically stable hydrogel polymer system as a substitute for the degenerated nucleus pulposus (NP) of the IVD[173,178]. In our earlier experiments, we demonstrated that a PVA/PVP hydrogel nucleus implant can restore the compressive biomechanics of the denucleated lumbar functional spinal unit (FSU) to a significant level (88%) of the comparable experimental condition[179]. The hydrogel nucleus implant used, had a perfect line-to-line fit of the created nuclear defect with a modulus of 120 KPa (at 15% strain). Although, the concept of nucleus replacement by a polymeric hydrogel was demonstrated to be feasible, there are some concerns regarding the fact that restoration of the denucleated FSU was not complete. Specifically, we do not know what the ideal material properties (modulus) of the hydrogel nucleus implant should be to substitute for the degenerated nucleus pulposus.

The objective of the present study was three-fold. First, to simulate two different experimental conditions of intact and denucleated FSU using the finite element method and validate these models against corresponding experimental results for individual test specimens (n=6). Second, to determine the ideal hydrogel nucleus implant modulus having line-to-line fit, for individual test specimens, based on the predicted load-displacement behavior. Third, develop an average finite element model (AVFEM) based on the average dimensions and average material parameters of individual test specimens to predict a feasible range for hydrogel nucleus implant material moduli for nucleus replacement, using criteria of predicted load-displacement behavior, intradiscal stress, strains and radial displacement in the outer annulus.

Method

Material Properties. The properties of the cortical/cancellous bone of the vertebral body are well established and were taken from the literature[128]. This approach was not followed for the nucleus and annulus material properties, due to the variability of the opinions about the structure and material properties reported in the literature[10,72,108,183].

The nuclei of all six human cadaver lumbar specimens displayed some degree of age-appropriate degeneration, were very much dehydrated and looked more solid-like than fluid[179]. For this reason, the nucleus pulposus of all the specimens was modeled as an isotropic, elastic material with Young's modulus of 1 MPa and Poisson's ratio (0.4999) in contrast with the previously reported method of modeling the nucleus as an incompressible fluid[72].

Considering the intact condition of the annulus throughout the actual experiment and the lack of agreement about the AF material properties, a novel approach was proposed to model the annulus. The AF was modeled as an isotropic, hyperelastic material using a second order polynomial strain energy function. This facilitated the general definition of the annulus with mathematical coefficients, which can be back calculated to determine the AF material properties. The coefficients of the AF second order polynomial function were determined by adjusting and matching the finite element model (FEM) predicted Load-Displacement curve with that of intact experimental Load-Displacement curve, while keeping the material properties of NP and Vertebrae constant. Thus, every specimen that was modeled had unique AF parameters. The same AF parameters for each specimen were used in the corresponding denucleated and implanted FEMs for simulation and validation of the experimental data (Table 3).

The polymeric hydrogel implant was simulated in the partially denucleated FEMs. Hydrogel implant was modeled with a first order Mooney-Rivlin strain energy potential function. Considering the almost incompressible nature of the hydrogel, a very high Poisson's Ratio (0.4999) was assumed for modeling of the hydrogel nucleus implant. The Mooney-Rivlin coefficients for the polymeric hydrogel were then calculated for various hydrogel implant moduli. These Mooney-Rivlin coefficients were used for simulation of hydrogel implants in the implanted specimens. In this way, the effect of hydrogel implant modulus on the resulting stress state of the implanted condition could be analyzed.

Finite Element Model. Based on the actual dimensions of the test specimens, six individual FEMs were constructed. The specimens were free of any significant bone or disc abnormalities. The specific details of each specimen are given in Table 1. The material property definitions used in the model for cortical bone, cancellous bone and nucleus pulposus are given in Table 2. Simplified geometry was used for FEMs assuming the symmetry about the sagittal plane. Contribution of end plates was neglected in this analysis. Also, the height of the intervertebral disc was assumed to be uniform over the entire cross-sectional area. Mesh refinement studies were performed in order to have optimum results. The FEM used 2327 nodes and 1728 four-node axisymmetric elements, as shown in Figure 7.1.

Loading and Boundary Conditions. The loading simulated the test condition in which the bottom vertebra was constrained in the test fixture using a potting material. A fixed displacement of 15% strain (based on the IVD height) was applied to top vertebra and symmetric boundary conditions were used to perform the nonlinear analysis using

commercially available finite element software ABAQUS, version 6.3 (ABAQUS Inc., Pawtucket, RI).

Simulation of Experimental Conditions. In the actual experiment, three different conditions Intact, partially Denucleated (DN) and Implanted were tested in axial compression[179]. Our unique approach to denucleating the specimen avoided any damage to the annulus fibrosus (AF) and maintained it intact throughout the testing[176]. There was some residual NP left in the specimen after denucleation, about 20% by volume. These different conditions were simulated for each specimen and validated against the corresponding experimental results for compressive stiffness. As a crosscheck, the individual denucleated FEMs (using the corresponding AF parameters of intact specimen) were also compared against the experimental denucleated condition of individual specimen.

AVFEM Concept. Every test specimen was different in the sense that it had variations with respect to age, sex, (de) hydration level of nucleus and annulus structure. In order to have better idea of mechanical behavior of a "typical" lumbar disc, an average FEM (AVFEM) was built based on the average dimensions of the six specimens. The material properties used in this AVFEM were the average of the material parameters used for six individual FEMs. This AVFEM was analyzed with same loading and boundary conditions as those for individual FEMs. The AF parameters used for this AVFEM were taken as average of the corresponding six AF parameters determined for individual FEMs (Table 3).

As before, this AVFEM was converted into the denucleated AVFEM, to simulate the experimental denucleated condition. Then, the hydrogel implant was modeled in the

denucleated AVFEM to simulate the implanted condition. The required modulus of the hydrogel implant for complete restoration of intact AVFEM load level, having line-to-line fit, was determined based on the resultant load-displacement behavior.

Using this validated implanted AVFEM, a comparison of compressive load level, intradiscal stress distribution, radial displacement of peripheral nucleus and annulus layers, compressive stresses on NP and AF, interfacial stresses between the peripheral nucleus and inner annulus, and radial strains in the NP and AF was made (Table 5).

Effect of nucleus implant properties. Using the AVFEM, the Young's modulus of the nucleus implant was varied to assess the effect of implant modulus variation on the compressive mechanical behavior of the intervertebral disc. Using the parameters in Table 5, the hydrogel implant moduli, for which all of these parameters were within ± 3% of an intact AVFEM results, were identified as a feasible range for replacement of the degenerated nucleus pulposus in order to achieve the complete restoration of the intervertebral disc mechanics.

In summary, six individual FEMs were created for the intact condition and validated against the corresponding experimental results. The validation criterion was the exact matching of the FEM predicted Load – Displacement curve with the experimentally obtained nonlinear Load-Displacement curve. These six FEMs produced six AF parameter coefficients for individual specimens. All six FEMs were also validated against the corresponding experimental denucleated condition. The hydrogel nucleus implanted condition was then simulated by using the AF parameters determined earlier and ideal hydrogel implant modulus for each specimen was predicted. An AVFEM was constructed based on the average material and geometric parameters of six individual

FEMs and then, feasible hydrogel implant moduli range was predicted as a replacement of the degenerated nucleus pulposus.

Results

Figure 7.3 shows a comparison of finite element prediction vs. the experimental results, for both intact and denucleated conditions, for a representative specimen, in terms of load-displacement behavior. The individual FEMs prediction matched well with the experimental data for both conditions of intact and denucleated specimens, for all six specimens.

Figure 7.4 shows the AVFEM load-displacement prediction compared to the experimental data for six specimens, for intact condition. The predicted Load-Displacement curve falls within the range of the experimental data. Figure 7.5 shows the denucleated AVFEM prediction for load-displacement behavior compared to the experimental data for six specimens, for denucleated condition. Here also, the predicted Load-Displacement curve falls within the range of the denucleated experimental data. Figure 7.6 shows the Intact, DN and Implanted AVFEMs contour comparison for radial displacement. Figure 7.7 shows the Von Mises stress distribution for these three conditions. It is clearly seen that the intact and denucleated conditions are distinctly different while the implanted condition is more comparable to the intact condition rather than the denucleated condition.

Table 4 shows the details of the FEM prediction for individual ideal hydrogel nucleus implant moduli for these specimens. Table 5 shows the detailed comparison of some important parameters for three different conditions of intact, denucleated and implanted specimens for various implant moduli. All these values for implanted AVFEM

were within ± 3% of corresponding intact AVFEM prediction. Based on these criteria, implanted AVFEM predicted a feasible range of hydrogel nucleus implant moduli (120 KPa – 3 MPa) having line-to-line fit of the created nuclear defect, for replacement of the NP and thereby complete restoration of the spinal compressive biomechanics in terms of Load-Displacement behavior.

Discussion

In this work, a simplified axisymmetric finite element model of the lumbar intervertebral disc in compression was developed and validated against the experimental results of two different test conditions of intact and denucleated. The third test condition of implanted specimen was simulated by modeling the hydrogel nucleus implant in the created nuclear defect, in line with the experimental approach.

Extensive work has been performed in numerical modeling of the (lumbar) intervertebral disc mechanical behavior and simulation of various physiological conditions in order to better understand the role of the disc tissues under different loading conditions. First use of the finite element method for modeling of the spinal biomechanics was reported in the 1970s[116]. Since then, there has been a lot of progress in the modeling approach and understanding of intervertebral disc mechanics. Mostly, these models were validated against the experimental observations of Load-Displacement behavior, disc bulge, end-plate bulge and intradiscal pressure distribution[72]. Other parameters such as vertebral body/end plate stresses and annulus stress distribution have also been reported. The effect of annular incision was observed, showing the effect on the disc stability, radial bulge and disc height[130]. One study reported the effect of the intervertebral disc height variation on the overall mechanical behavior of the motion

segment, showing significant influence on the resulting axial displacement, disc bulge and tensile stresses in peripheral annulus fibers[129]. Some researchers also looked into the viscoelastic disc mechanics using the poroelastic definition of disc components and permeability coefficients[134,135]. Few numerical models have examined the nucleus implant mechanics of the intervertebral disc. Meakin et al.[108] modeled the disc as a cylinder, assigning elastic solid properties to the annulus. This definition of the annulus may have resulted in over-prediction of the required nucleus implant material properties. From the present study, we now understand that, it is the annulus which mainly determines the overall mechanical behavior of the lumbar disc mechanics.

However, to our knowledge no other studies have been reported on the human lumbar functional spinal units, to understand the nucleus implant biomechanics and the effect of nucleus implant material properties on the compressive spinal biomechanics.

This study also proposed a new concept of modeling the annulus using a second order polynomial strain energy function with material property as isotropic and hyperelastic. This approach allowed us to exactly mimic the experimental compressive behavior in terms of the Load-Displacement behavior, without dealing with the controversial details of the complex annulus structure/composition definition. This modeling approach is also supported by the fact that the physiological condition of each annulus is different. This precludes the use of universal composite structure definition for annulus as used earlier by peers, in view of our experimental denucleation approach (intact AF) and present study objectives at best for the compressive loading. However, additional loading conditions may suggest the need for full anisotropic approach for modeling of the annulus. This definition of the annulus as an isotropic and hyperelastic

material is in agreement with the work of Duncan et al.[184] where they proposed the porohyperelastic approach for annulus definition. This hyperelastic definition of the annulus mainly determined the non-linearity of the predicted Load-Displacement behavior of the FEM and allowed to exactly mimic the experimental nonlinear compressive behavior.

Figure 7.2 shows the deformed mesh for intact and denucleated FEM. In the intact disc, the nucleus radially displaced the annulus fibers, generating a positive disc bulge. In case of the denucleated disc, the annulus showed radial movements in both outward and inward directions, as seen from Figure 7.2. As a result, (for the same compressive strain) the load carrying capacity of the disc reduced significantly compared to the intact condition. The intradiscal stress acting on the interface of nucleus and annulus also reduced significantly (30% of the intact condition). The part of the annulus was observed to be in compression in the denucleated state, as compared to the intact condition. Thus, the denucleated condition stress state is dramatically different from the corresponding intact condition stress state.

Figure 7.3 shows the comparison (and thus validation) of FEM prediction of Load-Displacement behavior for both intact and denucleated conditions, against the corresponding experimental results, for a representative specimen. The FEM model well captured the compressive behavior of the specimen, for both intact and denucleated conditions, reproducing the non-linear load-displacement behavior as well as the magnitude of that behavior. This prediction and matching of Load-Displacement behavior was similar for rest of the six specimens. The precise matching of FEM results with the experimental results justifies our modeling approach.

Figure 7.4 shows the AVFEM Load-Displacement prediction of the intact specimen and Figure 7.5 shows the AVFEM Load-Displacement prediction of the denucleated specimen against the experimental data of six specimens, from which the AVFEM was constructed. The AVFEM prediction clearly falls within the experimental data and thus, represents an average behavior of the intact lumbar IVD in compression.

Figure 7.6 shows the contours of radial displacement for Intact, Denucleated and Implanted AVFEM. The inward radial deformation of the inner annulus is clearly visible in case of the denucleated specimen. A hydrogel nucleus implant with a suitable modulus can block this inward radial movement and can actually mimic the intact specimen condition in terms of load level, radial displacement and stress state. The implanted condition in Figure 7.6 has a nucleus implant with modulus of 150 kPa. The radial displacement produced by this nucleus implant is more comparable to the intact condition than to the denucleated one. Similarly, Figure 7.7 shows the comparison of Von Mises stress distribution for the conditions of Intact, Denucleated and Implanted, respectively. Again, the implanted condition is more comparable to the intact condition than to the denucleated one. The nucleus implant creates intradiscal stress on the inner annulus layers which is equivalent to the natural intradiscal pressure generated by the hydrated nucleus on the inner annulus, as predicted by the model. This results in positive radial deformation of the annulus, mimicking the result of natural load transfer mechanism observed in lumbar IVD. The radial strains at the disc center, after hydrogel nucleus implantation mimic the strains observed in case of intact disc and completely reverse the inward radial strains observed in case of the denucleated disc (Figure 7.8). The stiffness of the system also increases nonlinearly in case of the hydrogel implanted

specimen and is more comparable to the intact specimen stiffness, as showed in our earlier experimental studies[179].

Table 5 compares some important parameters for the Intact, Denucleated and Implanted AVEM prediction. For the implanted AVFEM, the modulus of the hydrogel nucleus implant was varied in order to determine the feasible range of the implant moduli. It also compares the radial displacement, compressive stresses, intradiscal pressure stress in the NP and the AF, for conditions of the Intact, Denucleated and hydrogel Implanted with different hydrogel moduli. Interestingly, the inward radial deformation of the inner annulus layers in case of the denucleated disc is totally reversed for the case of the hydrogel implanted disc. Similarly, the annulus is under compression in case of the denucleated disc, supporting the hypothesis that annulus is subjected to abnormal compressive stresses in case of degenerated / dehydrated disc. The implanted range reported here (120 kPa – 3 MPa) has ability to mimic the natural intact condition in terms of the load level, stress distribution and radial displacement in the annulus (Table 5). Moreover, the nucleus implant moduli in this range do not create excess interfacial stresses (on inner annulus) and do not exert abnormal stresses or strains on the vertebral bodies. Thus, it is safe to conclude that the (hydrogel) nucleus implant with modulus in the range of 120 kPa to 3 MPa and having a line-to-line fit will completely restore normal compressive biomechanics of the denucleated lumbar intervertebral disc to that of healthy intact intervertebral disc mechanical behavior.

Conclusion

Simple axisymmetric finite element models of six lumbar FSUs were created for the intact and denucleated conditions. The models were validated against corresponding

experimental results. The hydrogel nucleus implants with line-to-line fit were simulated in the denucleated models and ideal hydrogel nucleus implant modulus for each specimen was determined based on the restoration of corresponding experimental intact load level. It is possible to restore the normal compressive biomechanics of the lumbar IVD with a polymeric hydrogel implant with suitable modulus, having line-to-line fit. An average FEM was built based on the average material and geometric parameters of six specimens and was then used as a design tool to predict a feasible range of hydrogel nucleus implant moduli as replacement to the degenerated nucleus pulposus. The AVFEM predicts 120 kPa - 3 MPa as a moduli range suitable for replacement of the nucleus by a polymeric hydrogel implant.

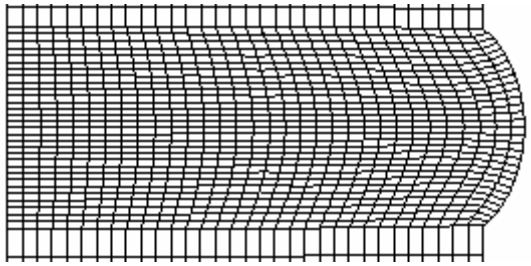

Figure 7.1. Finite element mesh of intact lumbar functional spinal unit in deformed state

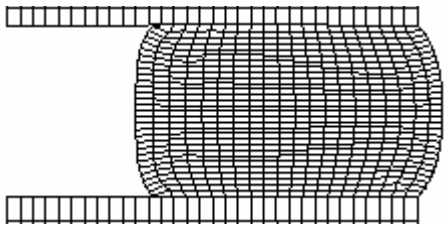

Figure 7.2. Finite element mesh of denucleated lumbar functional spinal unit in deformed state

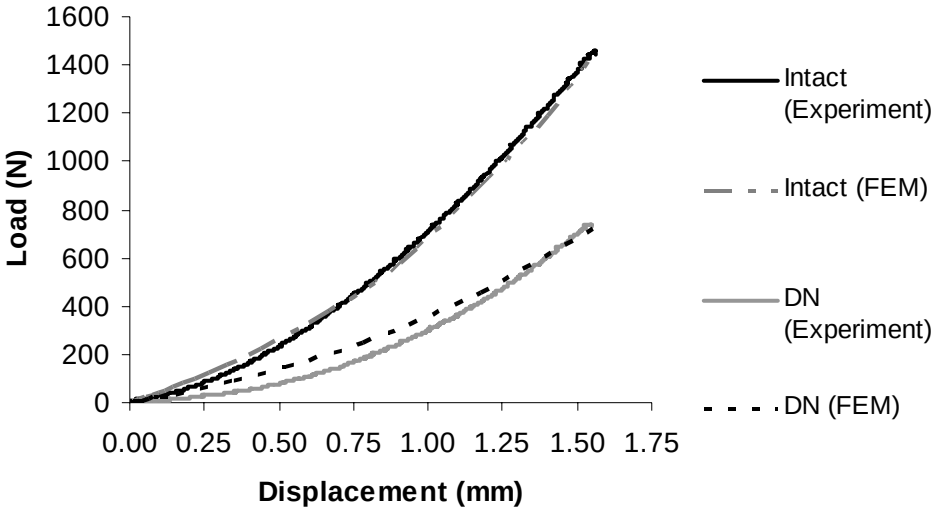

Figure 7.3. Load-Displacement behavior of a representative specimen, against corresponding experimental results for intact and denucleated condition

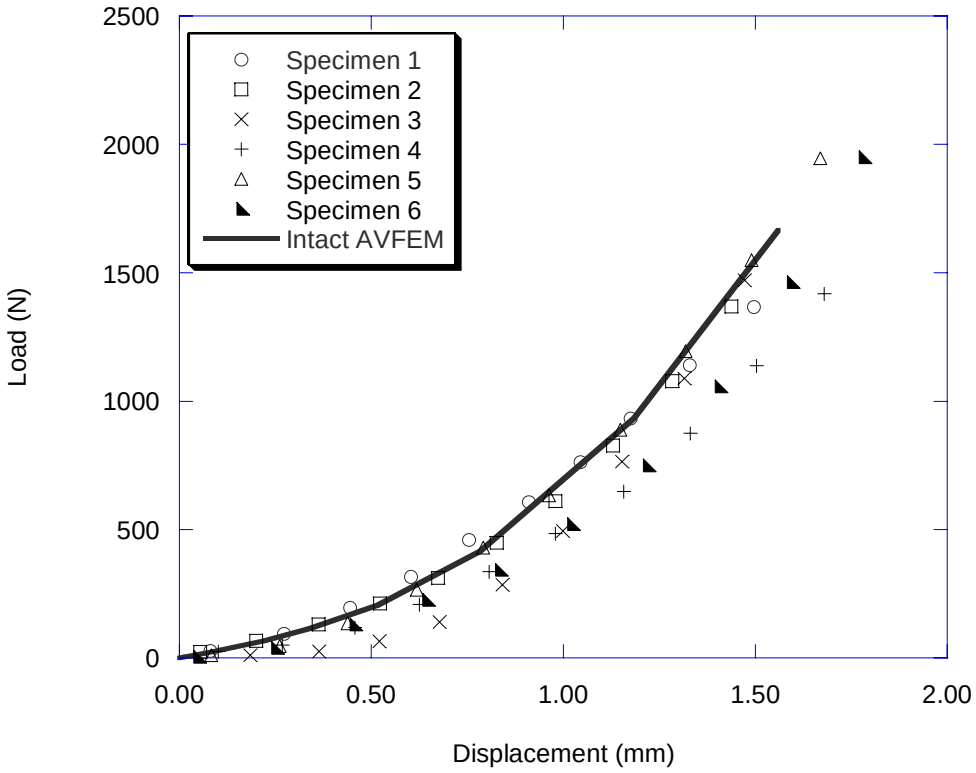

Figure 7.4. Intact AVFEM load-displacement prediction against the experimental data

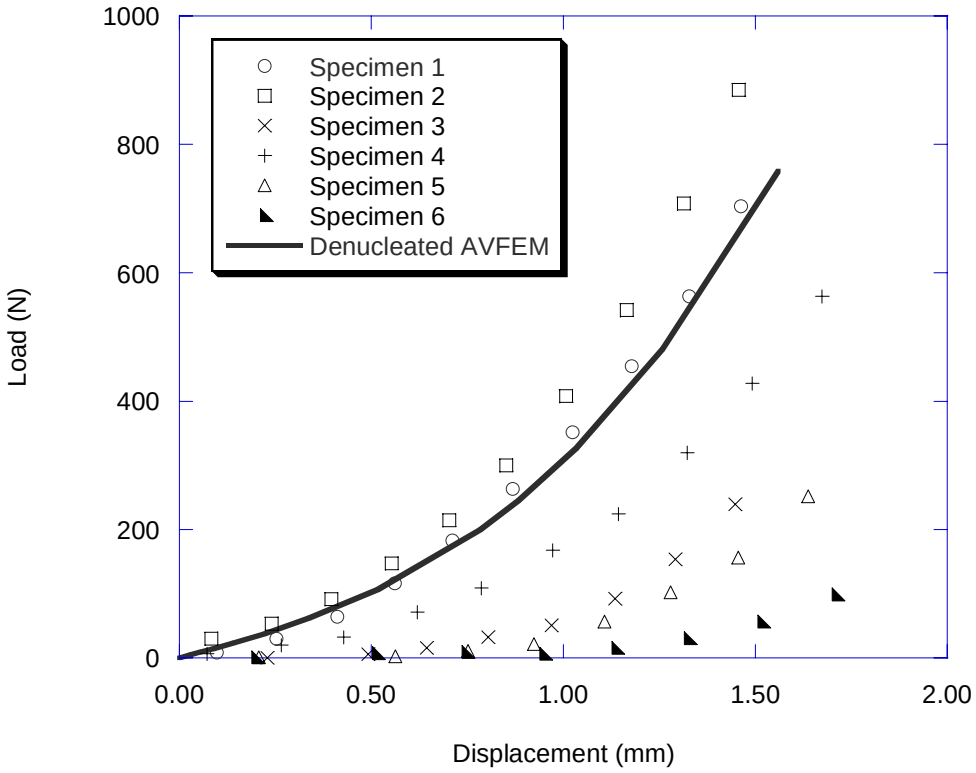

Figure 7.5. Denucleated AVFEM Load-Displacement prediction against the Denucleated experimental data

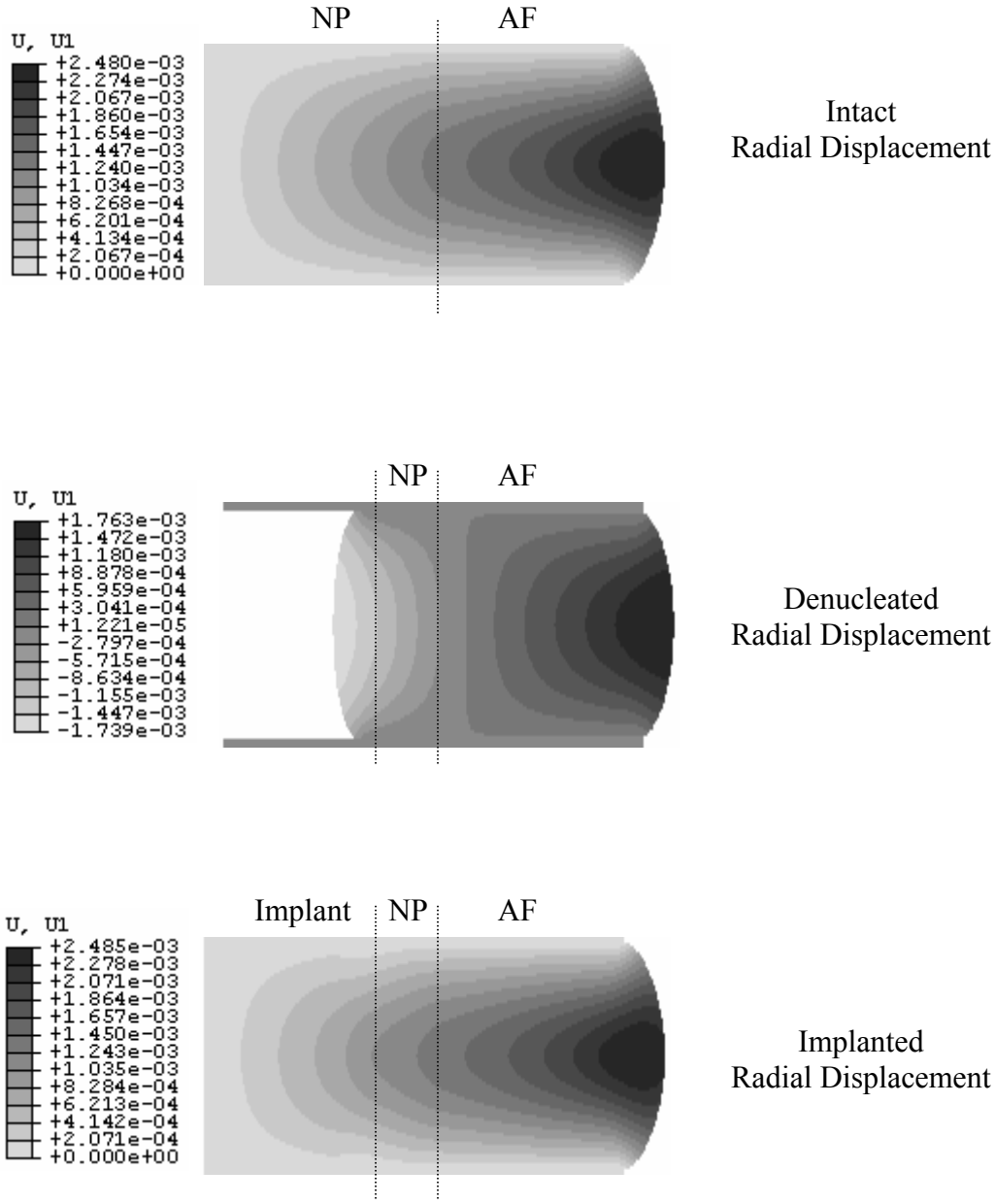

Figure 7.6. Radial displacement for Intact, Denucleated and Implanted condition

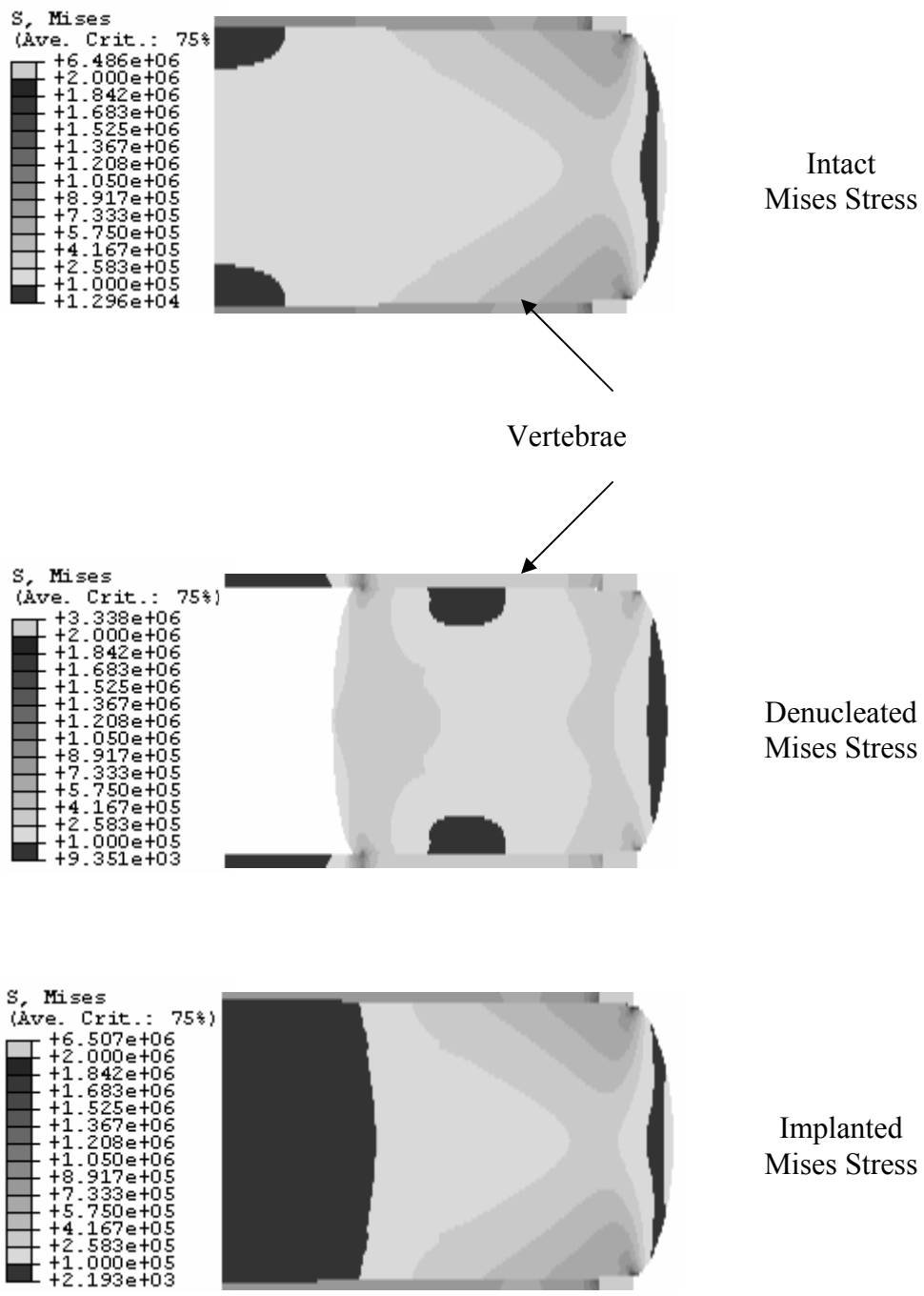

Figure 7.7. Von Mises stress distribution comparison for Intact, Denucleated and Implanted condition

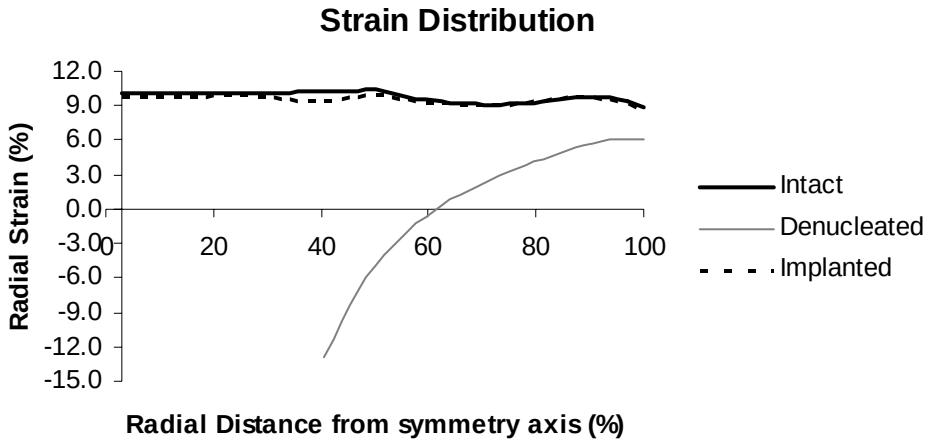

Figure 7.8. Radial Strain distribution for intact, denucleated and implanted disc

Table 7.1. Geometric details of six test specimens used

	Total Height	Disc Height	Upper Vertebra	Lower Vertebra	Major Diameter
Specimen 1	40.0	10.0	15.0	15.0	48.0
Specimen 2	38.0	9.5	10.5	17.5	38.0
Specimen 3	31.0	9.0	8.0	14.0	35.0
Specimen 4	33.0	11.0	7.0	15.0	42.0
Specimen 5	39.0	11.0	13.0	15.0	45.0
Specimen 6	37.5	12.0	11.0	14.5	47.0
AVFEM	**36.4**	**10.4**	**10.8**	**15.2**	**42.5**
All dimensions are in mm					

Table 7.2. Material properties used for the finite element model

	Young' Modulus (MPa)	Poisson's Ratio
Cortical Bone	12000	0.3
Cancellous Bone	100	0.2
Nucleus Pulposus	1	0.4999

Table 7.3. Annulus material parameters derived for six specimens and for AVFEM

	C_{10}	C_{01}	C_{20}	C_{11}	C_{02}	D_1	D_2
Specimen 1	3E04	8E04	3E04	3E04	5E04	1E-07	1E-07
Specimen 2	1E05	1E05	1E05	1E05	4E05	1E-07	1E-07
Specimen 3	4E04	4E04	4E05	4E05	4E05	1E-07	1E-07
Specimen 4	7E04	7E04	1E05	1E05	3E05	1E-07	1E-07
Specimen 5	8E04	8E04	2E05	2E05	3E05	1E-07	1E-07
Specimen 6	5E04	6E04	2E05	3E05	3E05	1E-07	1E-07
AVFEM	**6E04**	**7E04**	**2E05**	**2E05**	**3E05**	**1E-07**	**1E-07**
All values are in N/m^2							

Table 7.4. FEM prediction of ideal hydrogel nucleus implant modulus for six specimens compared to AVFEM prediction

FEM	**Intact Load Prediction (N)**	**Ideal Implant Modulus (kPa)**
Specimen 1	1442	150
Specimen 2	1397	120
Specimen 3	1559	270
Specimen 4	1407	150
Specimen 5	1953	200
Specimen 6	2058	210
AVERAGE	*1636*	*183*
AVFEM Prediction	**1666**	**210**

Table 7.5. Comparison of AVFEM prediction for Intact, Denucleated and Implanted conditions

AVFEM	**Intact**	**Denucleated**	**Implanted** (Moduli in kPa)			
			E=120	**E=1080**	**E=2040**	**E=3000**
Load (N)	1666	759	1620	1667	1695	1721
NP-S22 (Pa)	-1.46E06	-1.18E09	-1.42E06	-1.36E06	-1.45E06	-1.53E06
IDPS (Pa)	1.18E06	1.48E05	1.12E06	1.17E06	1.16E06	1.14E06
AF-S22 (Pa)	5.39E04	-8.37E04	5.36E04	5.38E04	5.24E04	5.11E04
U1-L (mm)	1.10	-0.52	1.11	1.10	1.08	1.06
U1-R (mm)	1.88	1.29	1.88	1.88	1.87	1.87
Stiffness (N/mm)	1068	486	1038	1068	1087	1103

NP-S22 ➔ Compressive stress acting on Nucleus Pulposus
IDPS ➔ Intradiscal pressure stress in the intervertebral disc
AF-S22 ➔ Compressive stress acting on Annulus Fibrosus
U1-L ➔ Radial displacement of inner Annulus Fibrosus layers
U1-R ➔ Radial displacement of outer Annulus Fibrosus layers

8. The Effect of Nucleus Implant Parameters on the Compressive Mechanics of the Lumbar Intervertebral Disc: A Finite Element Study

Introduction

Nucleus replacement by a polymeric material[167,178] or by tissue engineering approach[110] is currently being investigated to treat chronic lower back pain. The motivation behind this approach is mainly the limited success of the current surgical procedures such as discectomy and spinal fusion[19,20]. Although these procedures relieve back pain, they fail to restore the normal biomechanics of the lumbar spine. A need to find a better solution for treatment of lower back pain is propelled by the disadvantages associated with the discectomy and spinal fusion; discectomy may result in additional stress within the disc[20], while spinal fusion may generate additional stress in adjacent discs, after surgery[25]. In the case of fusion, the patient may lose mobility permanently[14].

The intervertebral disc is the largest avascular tissue in human body and mainly comprises of three different tissues[30]. The central core, the nucleus pulposus (NP), is surrounded by outer annulus fibrosus (AF) and the cartilaginous end plates (EP). The degeneration of the lumbar intervertebral disc (IVD) is mainly responsible for lower back pain in more than 75% of the cases reported[1]. With aging, the water content in the central NP reduces significantly, causing abnormal additional stresses in the outer AF. In case of the dehydrated disc, the NP no longer performs its normal function of load transfer to the annulus by creating an intradiscal pressure. The disc mechanics in the case of the degenerated disc are clearly altered as compared to the intact disc load transfer mechanics.

We propose the replacement of the degenerated NP using a polymeric hydrogel. Prior studies in our laboratory have focused on the development of a stable polymeric hydrogel to serve as a replacement to the degenerated nucleus pulposus[173,178]. In our previous experimental studies, the effect of hydrogel nucleus replacement on the compressive stiffness of the lumbar intervertebral disc was assessed. In that work, the feasibility of replacing the NP with the hydrogel implant was demonstrated. A novel trans-end plate approach for *in vitro* testing of the nucleus implant ability was developed, to avoid injury to the AF[176]. This was achieved by creating a bone plug from the superior vertebra using a standard core drill. The cylindrical hydrogel implant restored 88% of the compressive stiffness of the intact IVD when implanted in the created nuclear defect[179]. In another experimental study, we assessed the effect of nucleus implant (material and geometric) parameter variations on the alteration of compressive stiffness of the lumbar IVD and thus the compressive biomechanics of the IVD[185]. It was found that nucleus implant parameters do have significant effect on the disc compressive mechanics. The cylindrical implant geometrical variations (height and diameter) were found to be more effective in restoring the disc compressive mechanics compared to the implant material (modulus) variations, in the range examined. Interestingly, a corollary of this result was that implant diameter was more effective in restoring the compressive stiffness than the implant height. Thus, a small increase in implant diameter (6% press fit) achieved the stiffness level that was produced with 10% press fit of the implant height and 900% increase in the implant modulus[185]. However, little could be determined from the experimental results regarding the stress state at various locations and effect of

undersized/oversized implants (fit-fill effect of the nuclear cavity) on the overall mechanical behavior of the IVD.

The objective of this study was to confirm the hypothesis that the nucleus implant parameters would have significant effect on the mechanical behavior of the lumbar intervertebral disc and the resulting mechanics of the implanted disc would be mainly determined by fit of the implant in the created nuclear cavity.

Methods

A finite element model was constructed and validated to experimental data for the human lumbar intervertebral disc and have been previously discussed[186]. Here, we will briefly describe the modeling approach and detail the extensions of the original model made in this work.

Material Properties. The properties of the cortical/cancellous bone of the vertebral body are well established and were taken from the literature[128]. This approach was not followed for the nucleus and annulus material properties, due to the variability of the opinions about the structure and material properties reported in the literature[10,72,108,183]. Table 8.1 shows the material properties used in the model.

The nucleus of the test specimen displayed some degree of age-appropriate degeneration, was very much dehydrated[179] and looked more solid-like than the fluidic. For this reason, the nucleus pulposus was modeled as an isotropic, elastic material with Young's modulus of 1 MPa and very high Poisson's ratio (0.4999).

The annulus fibrosus was modeled as an isotropic, hyperelastic material using a second order polynomial strain energy function[186]. This facilitated the general definition

of the annulus with mathematical coefficients, which can be back calculated to determine the AF material properties.

The polymeric implant was simulated in the partially denucleated FEM. The polymeric nucleus implant was modeled with a first order Mooney-Rivlin strain energy potential function. The Mooney-Rivlin coefficients for the polymeric implant were then calculated for various nucleus implant moduli. These Mooney-Rivlin coefficients were used for simulation of nucleus implants in the implanted specimen. In this way, the effect of nucleus implant modulus on the compressive mechanics of the lumbar intervertebral disc was analyzed.

Finite Element Model. The finite element model used in this study is based on the L2-L3 specimen of a 49-year old male. The model was previously validated against the experimental results of the same specimen, details of which can be found elsewhere[186]. This model refers to the 'Specimen 2' in the earlier study. Simplified geometry was used for FEM assuming the symmetry about the sagittal plane. Contribution of end plates was neglected in this analysis. Also, the height of the intervertebral disc was assumed to be uniform over the entire cross-sectional area. Mesh refinement studies were performed in order to have optimum results. The FEM used 11,763 nodes and 7274 four-node axisymmetric elements.

Loading and Boundary Conditions. The loading simulated the test condition in which the bottom vertebra was constrained in the test fixture using a potting material. A fixed displacement of 15% strain (based on the IVD height) was applied to top vertebra and symmetric boundary conditions were used to perform the nonlinear analysis using

commercially available finite element software ABAQUS, version 6.3 (ABAQUS Inc., Pawtucket, RI).

Simulation of Experimental Conditions. In the cadaver experiment, three different conditions, Intact, partially Denucleated (DN) and Implanted were tested in axial compression[179]. These different conditions were simulated and validated against the corresponding experimental results for compressive stiffness[186].

Variation of Nucleus Implant Material (Modulus) Properties. The modulus of the nucleus implant was varied from 0.01 MPa to 100 MPa in the implanted condition (with constant Poisson ratio of 0.4999) to assess the effect on the compressive mechanics of the lumbar intervertebral disc. The nucleus implant was simulated with 'line-to-line fit' of the nuclear cavity.

Variation of Nucleus Implant Poisson Ratio. The effect of Poisson ratio of the nucleus implant on the mechanical behavior of the implanted disc was studied by varying the Poisson ratio of the nucleus implant, with the Young's modulus of 150 kPa and 'line-to-line' fit of the nuclear cavity.

Variation of Nucleus Implant Geometrical Parameters. The under-fill of the nuclear cavity was simulated by defining the nucleus implant with 3%, 5% and 10% under-fill, either with the height or with the diameter, keeping all other parameters constant. For example, for an implant with 5% underheight condition, the modulus (E=150 kPa), the Poisson ratio (υ=0.4999) and the diameter (D=16mm) were kept unchanged as in the case of 'line-to-line fit' and for an implant with 5% underdiameter condition, the modulus (E=150 kPa), the Poisson ratio (υ=0.4999) and the height (H=10mm) were kept

unchanged. Similarly, an over-fill of the nuclear cavity was simulated by defining the nucleus implant with 3%, 5% and 10% over-fill, either for the height or for the diameter.

A contact definition was used in the analyses where the nucleus implant was defined as a slave (surface) and the surrounding disc material was defined as a master (surface). This definition prohibited the penetration of the nucleus implant (slave nodes) into the disc material (master nodes), as described in the ABAQUS manual, version 6.3 (ABAQUS Inc., Pawtucket, RI). The under-fill cavity analysis was performed in single step. However, for simulation of over-fill condition, a two-step analysis was performed. During the first step of an analysis, the press fitted implant 'readjusts' itself within bounds of the nuclear cavity and puts some stress on the inner annular layers. In that 'readjusting' process, the implant slightly pushes the annulus radially outwards, putting some preload on the disc. In second step, normal compression occurs, starting with the preloaded condition.

Results

Figure 8.1 shows the effect of implant modulus on the predicted load-displacement behavior of the intervertebral disc. The finite element model predicted less significant change in the restored load level (1268 N – 2451 N), even when the implant modulus was varied over five orders of magnitude (0.01 MPa – 100 MPa). The effect of Poisson ratio variation of the nucleus implant on the predicted load-displacement behavior of the intervertebral disc was assessed (Figure 8.2). The significance of the implant Poisson ratio in the load transfer to the annulus and its overall role in the resulting compressive mechanics of the implanted disc is clearly visible. Especially, two distinct groups are observed in the resulting load-displacement behavior of the implanted

specimen; one with implant Poisson's ratio equal to 0.45 or greater and the other with implant Poisson's ratio less than 0.45.

Figure 8.3 shows the method used for modeling of the overfilled implant in a nuclear cavity. Simulation of the 10% overdiameter implant is shown here. This technique allowed us to mimic the experimental condition of the overfilled implant, for both height and diameter.

The effect of underfilling and overfilling of the nuclear cavity with the implant height variation is demonstrated (Figure 8.4). The finite element model predictions of the Load-Displacement behavior for the conditions of 3%, 5% and 10% underheight (UH) and overheight (OH) implant are compared against the intact experimental result (which is equivalent to the line-to-line fit implanted condition). Similarly, Figure 8.5 shows the effect of underfilling and overfilling of the nuclear cavity with the implant diameter variation.

Von Mises stress distribution for different implanted conditions is compared in Figure 8.6 (10% UH and 10% OH) and Figure 8.7 (10% UD and 10% OD) with the stress distribution for the line-to-line fit implant. Figure 8.8 and Figure 8.9 compare the radial displacement contours for different implanted conditions with the line-to-line fit contour. It was observed that with the underfilled implant (either height or diameter), the annulus showed less radial displacement compared to the line-to-line fit implant. As a result, the restoration load level was less for the underfilled condition.

Discussion

This work presented a simplified finite element model for understanding of the nucleus implant compressive mechanics of the lumbar intervertebral disc. The model

was validated earlier with the corresponding experimental results[186] and expanded here to accommodate the nucleus implant parameter variations. The effect on the stress distribution and radial strains within the intervertebral disc with respect to implant volume and implant material properties was assessed.

The first use of finite element method for simulating the intervertebral disc mechanics was in early 1970s[116]. Since then, there has been a lot of progress in the modeling approach and understanding of intervertebral disc mechanics. Mostly, these models were validated against the experimental observations of load-displacement behavior, disc bulge, end-plate bulge and intradiscal pressure distribution[72]. The effect of an annular incision was observed, showing the effect on the disc stability, radial bulge and disc height[130]. Some researchers also looked into the viscoelastic disc mechanics using the poroelastic definition of disc components and permeability coefficients[134,135]. Although, many models are available which explore the intervertebral disc mechanics, few numerical models have simulated the total disc replacement or nucleus replacement.

It was hypothesized by Bao and Yuan[93] that both nucleus implant modulus and nucleus implant cavity/conformity can affect the load distribution in the intervertebral disc. Meakin and colleagues[108] used sheep discs to asses the effect of nucleus replacement by synthetic implant. It was observed that the inner layers of the annulus bulged inwards in case of the denucleated disc. This inner bulging of the annulus was prevented by synthetic implants, when implanted in the denucleated disc. The experimental work with the sheep disc was further supported by a simplified finite element modeling of the intact human disc to investigate the effect of nucleus replacement. The model predicted that the effects of denucleation can be almost

completely reversed by a solid implant having line-to-line fit with a Young's Modulus of 3 MPa. However, the nucleus implant and the annulus were modeled as an elastic, isotropic material, which precluded the consideration of material nonlinearity in the model[108].

The model we have proposed here is a next step to the model proposed by Meakin et al.[108], in the sense that, it accommodates the nonlinearity (both geometric and material) for understanding of the nucleus replacement implant mechanics. The polymeric nucleus implant was modeled using a Mooney-Rivlin strain energy potential function and the annulus fibrosus is modeled as an isotropic, hyperelastic material with second order polynomial strain energy function. Moreover, this is the first model which indicates the relative importance of the nucleus implant material (modulus) and geometric (height and diameter) parameters for restoration of the denucleated intervertebral disc compressive mechanics. For the first time, the overfilling and underfilling of the nuclear cavity with the nucleus implant and its effect on the disc stress distribution (and on the overall disc mechanics) is assessed using a novel finite element technique for simulation of the overheight and overdiameter nucleus implants.

In general, the implant modulus seems to contribute little to the compressive disc mechanics, over the tested range (Figure 8.1). This is in agreement with the experimental results[185], where it was observed that an increase of 900% in the implant modulus (over three orders of magnitude) restored the load level, which was equivalent to or even less than the load level restored by either increasing the implant height by 10% or implant diameter by 6.25%. However, a very low implant modulus (approximately 1 kPa) would act similar to the denucleated condition and would not restore the compressive disc

mechanics. It leads us to the conclusion that some threshold exists for nucleus implant modulus, beyond which it contributes little as far as the restoration of the intervertebral disc mechanics is concerned. Figure 8.2 shows the effect of Poisson ratio variation of the nucleus implant on the predicted load-displacement behavior of the intervertebral disc. An inward bulging of the inner annulus was observed, when the nucleus implant Poisson ratio was less than or equal to 0.45. Because of this, the load-displacement curves with nucleus implant Poisson ratio, $\upsilon \leq 0.45$, were not different. Moreover, the predicted behavior with lower values of implant Poisson ratios ($\upsilon \leq 0.45$) was comparable to the predicted behavior of the denucleated disc. This indicates the importance of the incompressibility of the implanted material and suggests the use of implant materials with highest possible Poisson ratio.

Theoretically, if we press-fit an implant with higher geometrical dimensions than those of the created nuclear cavity in the denucleated disc, the implant will undergo shape change so as to fit within the bounds of the nuclear cavity and the annulus may deform to accommodate the large (height or diameter) implant. In the process of 'readjusting' itself within the nuclear cavity, the implant would exert some stress on the surrounding disc material, especially on the annulus. It also slightly pushes the annulus in the outward direction as seen. The bone would not be affected by this as it acts as a rigid body when compared to the polymeric nucleus implant and rest of the disc material. This technique allowed us to mimic the experimental condition of the overfilled implant, for both height and diameter. This technique proved valid only until 12.5% press fit, beyond which the present model failed to converge. This limitation of this technique is however, beyond the scope of the present analysis.

Figure 8.4 showed the effect of underfilling and overfilling of the nuclear cavity with the implant height variation. As expected, the OH implants, because of their increased volume, had better interaction with the intact annulus and thus restored the disc stiffness comparable to the intact than the line-to-line fit implanted condition. The vertebrae stress distribution in the case of the OH implants was not different than the vertebrae stress distribution in the case of the UH and the line-to-line fit implants. The relation between the resulting compressive stiffness and the ratio of implant volume/cavity volume has been demonstrated earlier[185]. The disc with UH implants initially showed less resistance to the deformation and thus, less restored the compressive mechanics. Thus, the implant with 10% overheight showed the maximum restoration of the load level and the implant with 10% underheight showed the least restoration of the load level.

Figure 8.5 showed the effect of underfilling and overfilling of the nuclear cavity with the implant diameter variation. The finite element model predictions of the load-displacement behavior for the conditions of 3%, 5% and 10% underdiameter (UD) and overdiameter (OD) implant are compared with the intact experimental result (which is equivalent to the line-to-line fit implanted condition). The predicted load-displacement behavior was similar to the one observed for the implant height variations. Interestingly, it was observed that the UD implants allow the inward bulging of the annulus initially. This resulted in least restoration of the load level of all the combinations tried here. This is not surprising considering the relationship among the nucleus implant volume, annulus interaction and the resulting stiffness[185]. Thus, in the ascending order, the effectiveness of the implant 'fit-fill' effect for load level restoration was –

10% UD → 10% UH → 5% UD → 3% UD → 5% UH → 3% UH → Line-to-Line fit → 3% OH → 5% OH → 3% OD → 10% OH → 5% OD → 10% OD.

It is clear that the underfilled cavity (especially underdiameter implant) is not desirable as it allows for the inward bulging of the annulus in the initial stages of the deformation.

Von Mises stress takes into consideration the principal stresses in three directions and can be used as a single representative stress value at a point. The resulting stress distribution (Figure 8.6 and 8.7) with implant geometrical variations is clearly different than the line-to-line fit condition as shown, with a higher stress in the annulus for conditions of overfilled implant as compared to the line-to-line fit and undersized implant. Also, the region of high stress is larger in the press fit implanted conditions. Moreover, the annulus stress state (with lesser magnitudes) in the underfilled implants (both 10% UH and 10% UD) explains the incomplete restoration of the load level compared to the line-to-line/intact condition.

The radial displacement contours for different implanted conditions with the line-to-line fit contour are compared (Figure 8.8 and 8.9). An overfilled implant (either height or diameter) put some 'pre-stress' on the annulus layers in the first step, before undergoing actual deformation in the second step. This resulted in the slight radial first step displacement in case of the 10% OH implant and significant radial first step displacement in case of the 10% OD implant, as shown. Although, both overfilled implants (10% OH and 10% OD) achieve the better load restoration, 10% OD implant is more effective probably because it displaces the annulus more while 'readjusting' itself within the bounds of the nuclear cavity.

The current model however, does not take into account the other loading conditions such as anterior/posterior bending, extension and torsion for analysis of the nucleus implanted intervertebral disc mechanics. In that case, the anisotropy of the annulus fibrosus may become more dominant and may affect the material definition of the annulus (as a hyperelastic, isotropic) used in this study.

It was concluded that the nucleus implant with suitable material properties and dimensions exerts the stress on the inner annulus layers, equivalent to the natural intradiscal pressure in the case of healthy disc. This implantation of the nucleus implant mimics the natural load transfer phenomenon of the healthy disc, by pushing the annulus radially outwards. Nucleus implant design may be bettered by consideration of the implant material/geometric parameters and relative implant volume to the cavity volume.

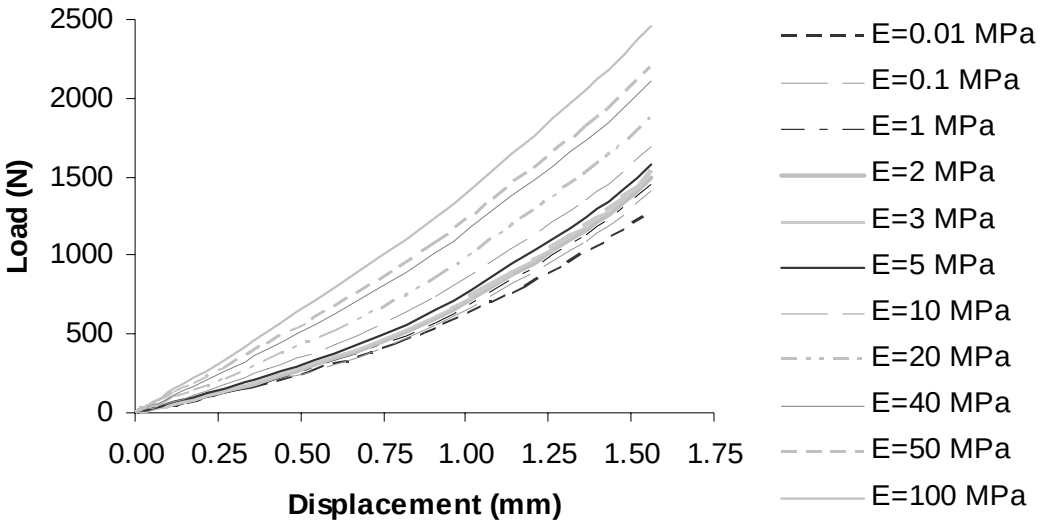

Figure 8.1. Effect of nucleus implant modulus (υ=0.4999) variation on the compressive mechanical behavior of the human lumbar intervertebral disc

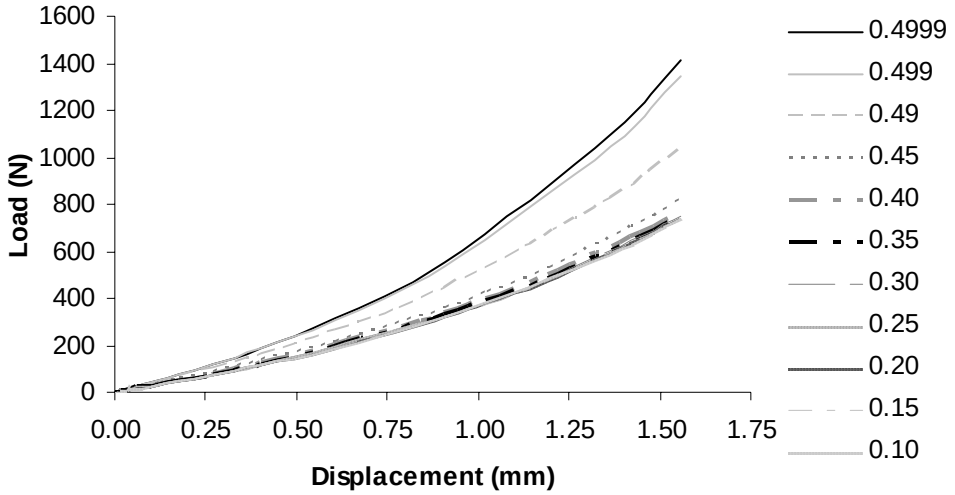

Figure 8.2. Effect of nucleus implant Poisson ratio variation on the compressive mechanical behavior of the human lumbar intervertebral disc

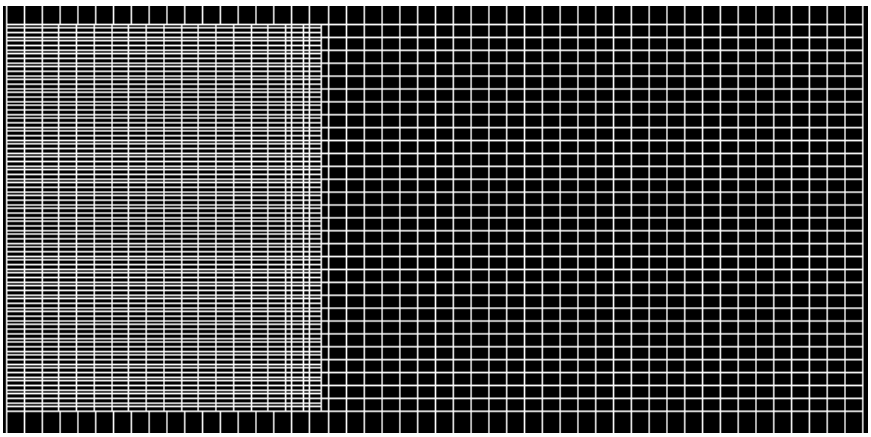

Undeformed State

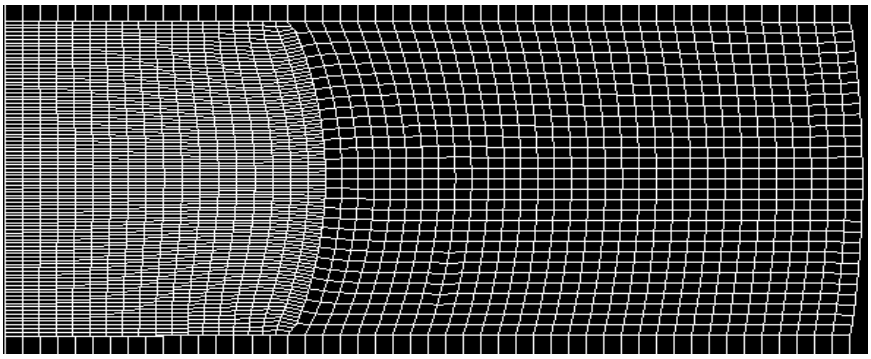

After completion of first step

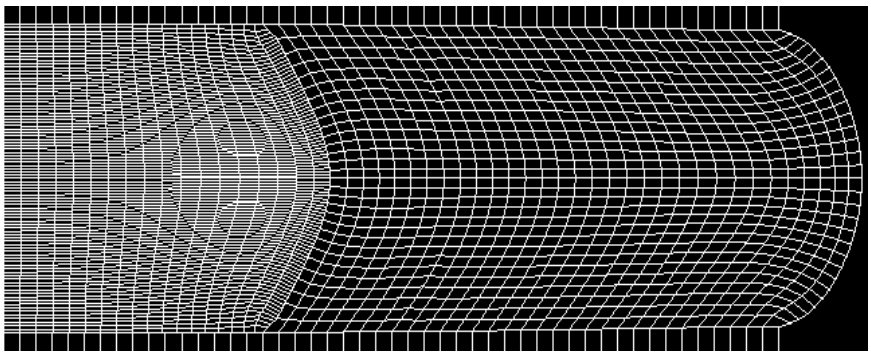

After completion of second step

Figure 8.3. Concept of two-step analysis for an overfilled nucleus implant within the specified nuclear cavity

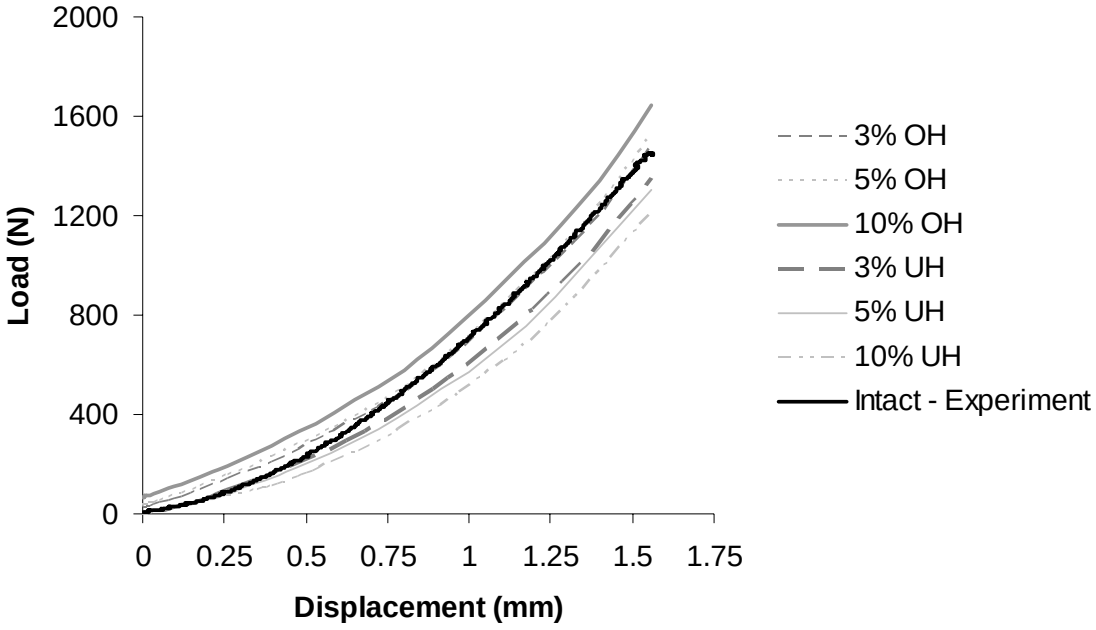

Figure 8.4. Effect of nucleus implant height variation (Underfill and Overfill of the nuclear cavity)

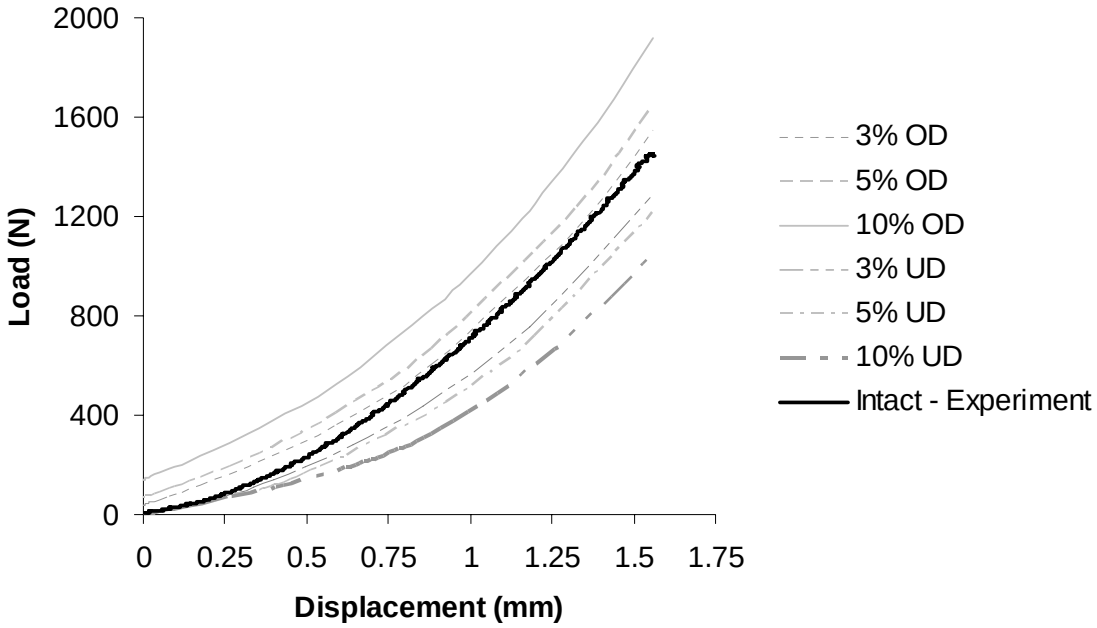

Figure 8.5. Effect of nucleus implant diameter variation (Underfill and Overfill of the nuclear cavity)

10% Under-Height Implant

Line - to – Line fit Implant

10% Over-Height Implant

Figure 8.6. Von Mises stress distribution for resulting from the nucleus implant height variation

10% Under-Diameter Implant

Line - to – Line Fit Implant

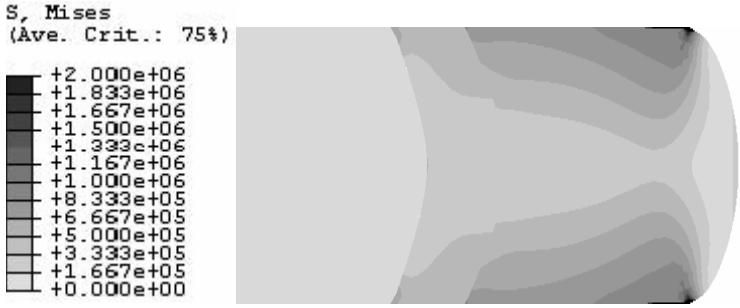

10% Over-Diameter Implant

Figure 8.7. Von Mises stress distribution for resulting from the nucleus implant diameter variation

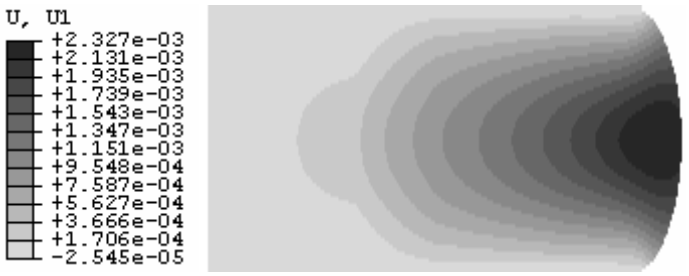

10% Under-Height Implant

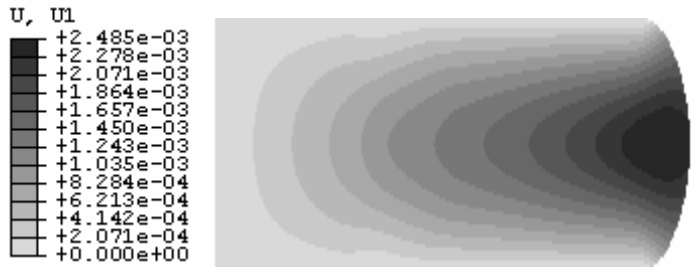

Line – to – Line Fit Implant

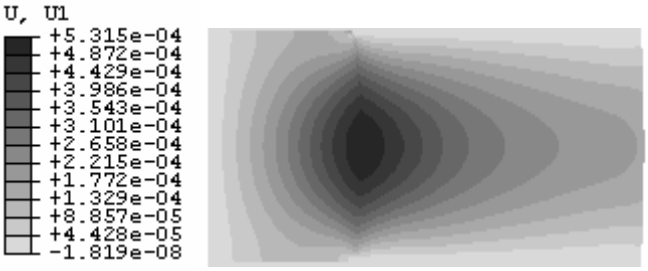

10% Over-Height Implant (after completion of first step)

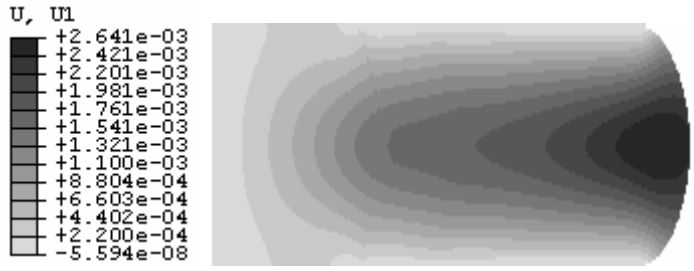

10% Over-Height Implant

Figure 8.8. Radial Displacement resulting from the nucleus implant height variation

10% Under-Diameter Implant

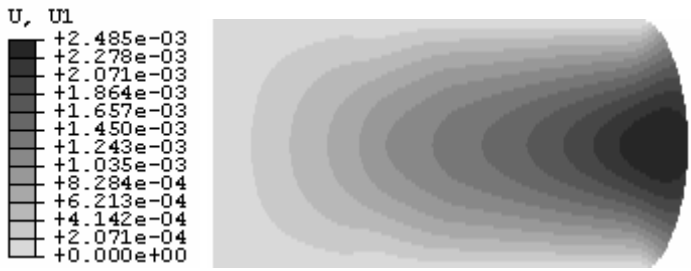

Line – to – Line Fit Implant

10% Over-Diameter Implant (after completion of first step)

10% Over-Diameter Implant

Figure 8.9. Radial Displacement resulting from the nucleus implant diameter variation

Table 8.1. Material Properties used for the Parametric Finite Element Model

	Young's Modulus (MPa)	Poisson's Ratio
Cortical Bone	12000	0.3
Cancellous Bone	100	0.2
Nucleus Pulposus	1	0.4999
Annulus Fibrosus (N/m^2)	C_{10}=3E04, C_{01}=8E04, C_{20}=3E04, C_{11}=3E04, C_{02}=5E04, D_1=1E-07, D_2=1E-07	

9. Conclusions

9.1 Summary

This work proposed the use of PVA/PVP hydrogel as a potential substitute for the degenerated nucleus pulposus of the human lumbar intervertebral disc. The concept of the nucleus replacement by a polymeric PVA/PV hydrogel was demonstrated to be feasible using an *in vitro* human cadaveric mechanical testing of the lumbar intervertebral disc and understanding of the nucleus implant mechanics of the lumbar intervertebral disc was further expanded using the finite element models of the lumbar intervertebral disc.

The nucleus pulposus of the lumbar intervertebral disc is known to play major role in the natural load transfer mechanism of the intervertebral disc. The contribution of the nucleus towards the compressive behavior of the intervertebral disc was studied. The annulus fibrosus is mainly responsible for the resulting disc stiffness. In order to keep the annulus intact (and thus, to assess the pure contribution of the nucleus in the disc mechanics), a novel denucleation method was used. The denucleation was achieved through the vertebra/end plate route instead of generally followed approach of the annulus incision. Although, this created significant damage to the bone, it kept the soft tissue (annulus fibrosus) intact, which was most important from the experimental objective point of view. Drilling into the vertebra reduced the compressive stiffness of the disc (19% reduction) as compared to the intact condition. A more dramatic reduction in the compressive stiffness of the disc was observed (59% reduction) after removal of the significant amount (3-4 g) of the bulk nucleus pulposus material. Three mechanisms were proposed for the observed loss of the compressive stiffness after drilling of the

vertebra; nucleus volume loss, end plate structural change and nucleus depressurization. It was concluded that the nucleus depressurization is the most likely candidate for the observed decrease of the stiffness after vertebra drilling. A more dramatic reduction in the stiffness of the disc after denucleation, lead to speculation that nucleus itself contributes to resist the deformation and also contributes significantly towards the compressive mechanics of the disc. Three potential mechanisms were proposed for nucleus contribution towards the stiffness of the lumbar intervertebral disc; hydrostatic pressurization of the end plate and annulus, direct loading of the end plate and loading of the annulus as a result of Poisson's effect of the hydrated nucleus. It appeared that the nucleus can exhibit an effective hydrostatic pressurization and Poisson effect to load the annulus and the end plate, which in turn is dependent on the bulk modulus and (the bulk modulus dependency on) water content. It is therefore hypothesized that the nucleus loads the end plate and the annulus through such a mechanism.

The implantation of the hydrogel nucleus implant with line-to-line fit of the created nuclear cavity restored the compressive stiffness to 88% of the intact condition. A non-linear increase in the intervertebral disc stiffness was observed when implanted with the hydrogel nucleus implant. It was hypothesized that this non-linear increase in the stiffness resulted from the interaction of the hydrogel nucleus implant and the intact annulus. The Poisson's effect ($\upsilon \approx 0.49$) of the polymeric hydrogel resulted in a significant radial displacement in compression. The general premise that the intervertebral disc biomechanics and load transfer mechanism results from synergistic effect between the implanted hydrogel and the surrounding intact annulus is shown through this experimentation.

Nucleus implant parameters were observed to have a significant effect on the compressive mechanics of the lumbar intervertebral disc. It was observed that the nucleus implant geometrical parameter (height and diameter) variations are more effective than that of implant modulus variations for the stiffness restoration of the intervertebral disc and the implant volume plays major role in the restoration of the disc biomechanics. It was also demonstrated that underfilled implants does not restore the normal mechanics of the intervertebral disc.

Further understanding of the nucleus implant mechanics of the intervertebral disc was achieved through the use of finite element modeling. It was proved that the intact and denucleated stress states are significantly different. The annulus showed inward radial deformation and was subjected to abnormal stresses in the denucleated condition. The insertion of the polymeric implant with suitable material properties in the denucleated state completely reversed the radial inward bulging of the annulus observed and the implanted condition was identical to the intact condition in terms of the restored load level, annulus stress distribution, radial displacement and strains.

The feasible nucleus implant modulus range was also predicted using the validated finite element model. The effect of overfilling (press fit) and underfilling (under fit) of the nuclear cavity by the nucleus implant was predicted using the validated finite element model. The model also confirmed the experimental observations about the nucleus implant geometry/volume being more effective than the implant material properties in alteration of the resulting disc stiffness.

9.2 Novel contributions

This study for the first time, dealt systematically with the understanding of the nucleus implant mechanics of the human lumbar intervertebral disc, in pure compression. The novel contributions of this study to the literature can be summarized as follows:

- Development of an *in vitro* method for the nucleus implants insertion into the lumbar intervertebral disc without injury to the annulus.
- Understanding and explanation of the role of the nucleus pulposus towards the compressive biomechanics of the lumbar intervertebral disc and overall load transfer mechanism.
- Restoration of the compressive biomechanics of the lumbar intervertebral disc using the polymeric hydrogel nucleus implant.
- Contribution of the nucleus implants material and geometric parameters towards the compressive biomechanics of the lumbar intervertebral disc.
- Proposed the novel approach of modeling the annulus fibrosus as an isotropic, hyperelastic material.
- Predictions of the feasible range of the desired material properties of the nucleus implant using validated finite element model.
- Predictions of the nucleus implant modulus effect on the stress distribution within the lumbar intervertebral disc and on the overall compressive behavior.
- Development of an average finite element model with average derived material parameters as a general representation of the average lumbar intervertebral disc behavior.

- Modeling of the 'fit and fill' effect of the nucleus implant within a created nuclear cavity. Prediction of the stress distribution and the resulting compressive mechanics of the lumbar intervertebral disc with respect to implant geometry variation.

The clinical relevance of these findings is significant. It was shown that the nucleus implant modulus may have a threshold beyond which it does not contribute much to the resulting mechanics of the implanted disc. In comparison, the relative ratio of the implant volume to the nuclear cavity volume played major role in the resulting stiffness of the implanted disc. The alteration in the geometry of the implant (height or diameter) significantly altered the resulting compressive disc mechanics. It was also shown that the underfill of the nuclear cavity is not desirable, as the interaction between the implant and the annulus would be less significant. The underfilled implanted disc in most of the cases, behaved similar to the denucleated disc. All these findings may significantly influence the nucleus implant prosthesis design.

9.3 Limitations

Although this study revealed many details of the nucleus implant mechanics of the lumbar intervertebral disc in pure compression, a few important limitations associated with this study are worth mentioning.

First of all, the implantation method followed in this study (approach through vertebra/end plate route) is useful for *in vitro* studies only and that too is intended for the studies which would assess the effectiveness and the feasibility of the nucleus replacement with a synthetic material. The method proposed and developed here is not intended for *in vivo* implantation and obviously would need a significant modification.

This significant modification could either be in the implantation approach or in the nucleus implant material properties. The *in vivo* implantation approach may follow the lateral incision through the vertebrae/end plate (as compared to the normal incision proposed here) or may follow the standard approach of postero-lateral annulus incision.

Human (lumbar) spine is subjected to complex loading modes during the routine daily activities, such as compression (most important loading mode), flexion-extension, axial torsion and lateral bending. This study, however dealt only with the compressive behavior of the nucleus implanted intervertebral disc. In reality, spine is subjected to all kinds of load simultaneously. The results discussed and the findings explained here, are limited in the sense that they do not deal with the exact *in vivo* complex loading condition. The general behavior of the nucleus implanted intervertebral disc however, is expected to be similar in other loading modes also.

The static compression study of the nucleus implanted lumbar intervertebral disc is not sufficient to characterize fully the mechanics of the nucleus implant as a potential substitute for the degenerate nucleus pulposus. This study, did not attempt for fatigue studies (at least 10 million cycles) of the nucleus implanted intervertebral disc, completion of which would help to better prove the feasibility of the nucleus replacement by a polymeric hydrogel and better design of the nucleus implant.

The annulus definition proposed here (as an isotropic, hyperelastic), although good for compression studies, could be a point of concern when one is considering the mechanical behavior of the lumbar intervertebral disc under other complex loading modes. Especially, the current annulus definition with second order polynomial strain energy function may need a significant modification for the loading modes of axial

torsion and lateral bending, where the annulus anisotropy might come into picture. This may prompt the use of composite model of the annulus or fully anisotropic material definition of the annulus for more realistic representation. However, the present lack of knowledge and agreement about the annulus structure/properties may require detailed characterization studies before one can utilize more complex material definition for the annulus to better understand its role and overall contribution in the lumbar intervertebral disc mechanics.

Consideration of other complex loading modes with the modified definition of the annulus and with the new boundary conditions may alter the predictions of the present finite element model about the desired properties of the nucleus implant. Especially, the predicted feasible range of the implant modulus may see some significant changes. Also, it is likely that the predictions of the present finite element model for the overfilled and underfilled implanted conditions may not exactly hold true for other complex loading modes as the stress distribution within the intervertebral disc for these conditions would be significantly different.

10. Moving Ahead…

10.1 Future Work

This study meant to be the first step towards feasibility of the concept of nucleus pulposus replacement by a polymeric PVA/PVP hydrogel nucleus implant. This study should act as a foundation for number of things to be accomplished in the process of reaching to our final goal of cure of lower back pain.

Some of the things that could enhance the findings of this study and current understanding of the polymeric hydrogel nucleus implant mechanics of the lumbar intervertebral disc are summarized below.

a. *Poisson's ratio determination of the hydrogel implant*: The analysis of the experimental findings and numerical modeling of the nucleus implanted lumbar disc was based on the assumption that this hydrogel nucleus implant has very high Poisson's ratio ($\upsilon = 0.49$) and is almost incompressible.

   This assumption is based on the literature reports about the Poisson's ratio of similar gels[187] and is valid considering the rubber-like polymeric nature of the hydrogel implant proposed here. However, the determination of the Poisson's ratio of this implant would greatly bolster the proposed hypothesis proposed in this study about the nonlinear increase in the stiffness of the hydrogel implanted specimen and clinical efficacy of this implant.

b. *Shape of the nucleus implant*: Considering that only cylindrical implants were used in this study, it would be helpful to observe the resulting mechanical

behavior of the implanted disc, after implantation with various shapes such as ball, spiral, tubular, cubic and conical.

c. *Mechanical testing in complex loading modes:* Biomechanical testing of the lumbar intervertebral disc implanted with a PVA/PVP hydrogel implant (in the water bath maintained at 37ºc), in the complex loading conditions of lateral bending, axial torsion and flexion-extension would surely reveal some more details about the behavior of this nucleus implant.

d. *Fatigue testing:* Fatigue testing of the lumbar intervertebral disc implanted with PVA/PVP hydrogel needs to be carried out to see the long-term stability of the whole system from the mechanical and chemical point of view.

e. *Finite element model expansion:* The finite element model can be expanded and modified to assess the effect of complex loading conditions on the stress distribution of the intervertebral disc. A 3-D model with close representation of the actual geometry of the spinal motion segment(s) would help to better understand the stress distribution within the disc at anterior, lateral and postero-lateral location. It would be helpful to characterize the annulus tissue to determine the anisotropic elastic constants and utilize them in the finite element model for more detailed analysis.

The finite element model can also be expanded for consideration of the fluid flow within the disc employing biphasic tissue definition, as a poroelastic / porohyperelastic finite element model. This would help to better the design of the current and future nucleus implants, especially in terms of the permeability of the

implant material and capability to act as an effective 'diffusion pump' to mimic the natural nucleus pulposus structure and mechanical behavior.

10.2 Recommendations

The final goal of this project is to develop a hydrogel nucleus implant as a potential substitute to the degenerated nucleus pulposus of the intervertebral disc and thereby fully restore the spinal biomechanics. Certain measures which may prove effective to reach this ultimate goal and strengthen its claim as a best alternative to the degenerated nucleus pulposus are mentioned as follows:

a. Annulus sealing mechanism: Most likely the *in vivo* implantation of this nucleus implant would be done through annular incision. If the annulus injury is sealed with help of some material, the nucleus implant may not 'pop out' of the disc through the incisional route. The sealing material may also provide extra strength to the annulus and in the process would contribute towards the stiffness restoration of the system.

b. Implant positioner: It is highly likely that once the implant is in the body and subjected to constant loading, it may undergo the size reduction/shrinkage and may change its location within a disc. This can be prevented either by -

- Reinforcing the hydrogel implant with particulates of hydroxide apatite (HA) or glass fibers arranged in a systematic manner.
- Wrapping an implant with a material (mesh) which would prohibit it from collapsing.
- Constraining and directing the implant with help of the springs, thus maintaining the desired central location of an implant within the disc.

- Biologically gluing the nucleus implant top and bottom (assuming it is a cylindrical shaped implant) to the proximal and distal end-plates.

Bibliography

1. MedPro Month. 1998;V. VIII: Number 1.

2. Andersson GBJ. Epidemiologic Aspects of Low-Back Pain in Industry. Spine 1981;6(1):53-60.

3. Hedman TP, Kostuik JP, Fernie JR, Hellier WG. Design of an Intervertebral Disc Prosthesis. Spine 1991;16(6):S256-60.

4. Cats-Baril WL, Frymoyer JW. Identifying Patients at Risk of Becoming Disabled Because of Low-Back Pain - the Vermont Rehabilitation Engineering Center Predictive Model. Spine 1991;16(6):605-07.

5. Sehgal N, Fortin JD. Internal Disc Disruption and Low Back Pain. Pain Physician 2000;3(2):143-57.

6. Heliovaara M, Makela M, Knekt P, Impivaara O, Aromaa A. Determinants of Sciatica and Low-Back Pain. Spine 1991;16(6):608-14.

7. Manchikanti L. Epidemiology of Low Back Pain. Pain Physician 2000;3(2):167-92.

8. Bao QB, Yuan HA. Artificial Disc Technology. Neurosurgical Focus 2000;9(4):1-9.

9. Bibby SRS, Jones DA, Lee RB, Yu J, Urban JPG. The Pathophysiology of the Intervertebral Disc. Joint Bone Spine 2001;68:537-42.

10. Iatridis JC, Weidenbaum M, Setton LA, Mow VC. Is the Nucleus Pulposus a Solid or a Fluid? Mechanical Behaviors of the Nucleus Pulposus of the Human Intervertebral Disc. Spine 1996;21:1174-84.

11. Ayad S, Weiss JB. Biochemistry of the Intervertebral Disc. In Jayson MIV (ed.). The Lumbar Spine and Back Pain. 3rd ed. New York: Churchill-Livingstone, 1987:100-37.

12. Buckwalter JA. Aging and Degeneration of the Human Intervertebral Disc. Spine 1995;20:1307-14.

13. Humzah MD, Soames RW. Human Intervertebral Disc: Structure and Function. Anat Rec 1988;220:337-56.

14. Bao QB, McCullen GM, Higham PA, Dubleton JH, Yuan HA. The Artificial Disc: Theory, Design and Materials. Biomaterials 1996;17:1157-66.

15. Akeson WH, Woo SYL, Taylor TKF, Ghosh P, Bushell GR. Biomechanics and Biochemistry of the Intervertebral Disc. Clin Orthop Rel Res 1977;129:133-39.

16. Urban JPG, McMullin JF. Swelling Pressure of the Lumbar Intervertebral Discs: Influence of Age, Spinal Level, Composition and Degeneration. Spine 1988;13:179-87.

17. McNally DS, Adams MA. Internal Intervertebral Disc Mechanics as Revealed by Stress Profilometry. Spine 1992;17:66-73.

18. Osti OL, Vernon RB, Moore R, Fraser RD. Annular Tears and Disc Degeneration in the Lumbar Spine. J Bone Joint Surg (Br) 1992;74B:678-82.

19. Kambin P, Savitz MH. Arthroscopic Microdiscectomy: An Alternative to Open Disc Surgery. The Mount Sinai Journal of Medicine 2000;67(4):283-7.

20. Weber H. Lumbar Disc Herniation: A Controlled Prospective Study with Ten Years of Observation. Spine 1993;8:131-40.

21. Goel VK, Goyal S, Clark C, Nishiyama K, Nye T. Kinematics of the Whole Lumbar Spine - Effect of Discectomy. Spine 1985;10:543-54.

22. Shea M, Takeuchi TY, Wittenberg RH, White AA. A Comparison of the Effects of Automated Percutaneous Discectomy and Conventional Discectomy on Intradiscal Pressure, Disc Geometry and Stiffness. Journal of Spinal Disorders 1994;7:317-25.

23. Tibrewal SB, Pearcy MJ, Portek I, Spivey J. A Prospective Study of Lumbar Spinal Movements before and after Discectomy. Spine 1985;10:455-9.

24. Lee CK, Parsons JR, Langrana NA, Zimmerman MC. Relative Efficacy of the Artificial Disc Versus Spinal Fusion. In J W Frymoyer ed. Clinical Efficacy and Outcome in the Diagnosis and Treatment of Low Back Pain. New York: Raven Press, 1992:237-44.

25. Leong JC, Chun SY, Grange WJ, Fang D. Long Term Results of Lumbar Intervertebral Disc Prolapse. Spine 1983:793-9.

26. Lee CK, Langrana NA. Lumbosacral Spinal Fusion: A Biomechanical Study. Spine 1984;9:574-81.

27. Oka M, Noguchi T, Kumar P, Ikeuchi K, Yamamuro T, Hyon SH, Ikada Y. Development of an Artificial Articular Cartilage. Clinical Materials 1990;6(4):361-81.

28. Ratner BD, Hoffman AS, Schoen FJ, Lemons JE. Biomaterials Science - an Introduction to Materials in Medicine ed. San Diego: Academic Press, 1996.

29. Risbud MV, Bhat SV. Properties of Polyvinyl Pyrrolidone/Beta-Chitosan Hydrogel Membranes and Their Biocompatibility Evaluation by Haemorheological Method. Journal of Materials Science: Materials in Medicine 2001;12:75-79.

30. White AA, Panjabi MM. Clinical Biomechanics of the Spine. II ed. Philadelphia: J.B. Lippincott Company, 1990.

31. Bushell GR, Ghsoh P, Taylor TFK, Akeson WH. Proteoglycan Chemistry of the Intervertebral Disc. Clin Orthop Rel Res 1977;129:115-22.

32. Eyre D, Benya P, Buckwalter J. Intervertebral Disk: Basic Science Perspectives. In Frymoyer JW, Gordon SL ed. New Perspectives on low back pain. Park Ridge, IL: American academy of orthopaedic surgeons, 1989:147-207.

33. Iatridis JC, Setton LA, Weidenbaum M, Mow VC. The Viscoelastic Behavior of the Non-Degenerate Human Lumbar Nucleus Pulposus in Shear. Journal of Biomechanics 1997;30(10):1005-13.

34. Bogduk N, Twomey LT. Clinical Anatomy of the Lumbar Spine. Second ed. Melbourne: Churchill Livingstone, 1991.

35. Best BA, Guilak F, Setton LA, Zhu WB, Saed-Nejad F, Ratcliffe A, Weidenbaum M, Mow VC. Compressive Mechanical Properties of the Human Annulus Fibrosus and Their Relationship to Biochemical Composition. Spine 1994;19(2):212-21.

36. Ghosh P. The Biology of the Intervertebral Disc, Vol. I and II ed. Roca Baton: CRC Press, 1988.

37. Mooney V. A Perspective on the Future of the Low Back Research. In RD G ed. Spine: State of the Art Reviews. Philadelphia: Hanley and Belfus, 1989:173-83.

38. Ray CD. The Artificial Disc: Introduction, History and Socioeconomics ed. New York: Raven Press, 1992.

39. Keller TS, Hansson TH, Holm SH, Pope MM, Spengler DM. In Vivo Creep Behavior of the Normal and Degenerated Porcine Intervertebral Disc: A Preliminary Report. J Spinal Disord 1989;4:267-78.

40. Taylor JR, Twomey LT. The Development of the Human Intervertebral Disc. In Ghosh P ed. The Biology of the Intervertebral Disc. Boca Raton: CRC Press, 1988.

41. Maroudas A, Stockwell RA, Nachemson A, Urban J. Factors Involved in the Nutrition of the Human Lumbar Intervertebral Disc: Cellularity and Diffusion of Glucose in Vitro. J Anat 1975;120.

42. Moore RJ. The Vertebral End Plate: What Do We Know? European Spine Journal 2000;9:92-96.

43. Broberg KB. On the Mechanical Behavior of the Intervertebral Disc. Spine 1983;8:851-56.

44. Langrana NA, Edwards WT, Sharma M. Biomechanical Analyses of Loads on the Lumbar Spine. In Wiesel SW, Weinstein J, Herkowitz H, Dvorak J, Bell G ed. The Lumbar Spine. Philadelphia: W.B. Saunders Company, 1996:163-71.

45. Brinckamnn P, Frobin W, Hierholzer E, Horst M. Deformation of the Vertebral End-Plate under Axial Loading of the Spine. Spine 1983;8:851.

46. Rolander SD, Blair WE. Deformation and Fracture of the Lumbar Vertebral End Plate. Orthop Clin North Am 1975;6:75-81.

47. Reuber M, Schultz AB, Denis F, Spencer D. Bulging of Lumbar Intervertebral Disc. J Biomech Eng 1982;104:187-92.

48. Brown T, Hanson R, Yorra A. Some Mechanical Tests on the Lumbo-Sacral Spine with Particular Reference to the Intervertebral Discs. J Bone Joint Surg 1957;39A:1135.

49. Brinckamnn P, Horst M. The Influence of Vertebral Body Fracture, Intradiscal Injection and Partial Discectomy on the Radial Bulge and Height of Human Lumbar Discs. Spine 1985;10:138-45.

50. Farfan HF. Mechanical Disorders of the Low Back ed. Philadelphia: Lea and Febiger, 1973.

51. Hirsch C. The Reaction of Intervertebral Discs to Compression. J Bone Joint Surg 1955;37A:1188.

52. Hirsch A, Nachemson AL. New Observation on the Mechanical Behavior of the Lumbar Discs. Acta Orthop Scand 1954;23:254-83.

53. Virgin W. Experimental Investigations into Physical Properties of Intervertebral Disc. J Bone Joint Surg 1951;33B:607.

54. Markolf KL, Morris JM. The Structural Components of the Intervertebral Disc: A Study of Their Contributions to the Ability of the Disc to Withstand Compressive Forces. J Bone Joint Surg 1974;56A:675-87.

55. Galante JO. Tensile Properties of the Human Annulus Fibrosus. Acta Orthop Scand 1967;Suppl. 100:4-91.

56. Fujita Y, Duncan NA, Lotz JC. Radial Tensile Properties of the Lumbar Annulus Fibrosus Are Site and Degeneration Dependent. Journal of Orthopaedic Research 1997;15(6):814-19.

57. Roaf R. A Study of the Mechanics of Spinal Injuries. J Bone Joint Surg 1960;42B:810.

58. Farfan HF, Cossette JW, Robertson GH, Wells RV, Kraus H. The Effect of Torsion on the Lumbar Intervertebral Joints: The Role of Torsion in the Production of Disc Degeneration. J Bone Joint Surg 1970;52A:468-97.

59. Markolf KL. Stiffness and Damping Characteristic of the Thoracic-Lumbar Spine. Bioengineering approaches to the problems of the Spine, NIH, 1970.

60. Kazarian LE. Creep Characteristics of the Human Spinal Column. Orthop Clin North Am 1975;6:3.

61. Panjabi MM, Krag MH, White AA, Southwick WO. Effects of Preload on Load Displacement Curves of the Lumbar Spine. Orthop Clin North Am 1977;88:181.

62. Vernon-Roberts B. Age-Related and Degenerative Pathology of Intervertebral Discs and Apophyseal Joints. In Jayson MIV ed. The Lumbar Spine and Back Pain. New York: Churchill Livingstone, 1992:17-41.

63. Vernon-Roberts B. Disc Pathology and Disease States. In Ghosh P ed. The Biology of the Intervertebral Disc. Boca Raton: CRC Press, 1988:73-120.

64. Kirkaldy-Willis WH, Wedge JT, Young-Hing K, Reilly J. Pathology and Pathogenesis of Lumbar Spondylosis and Stenosis. Spine 1978;3:319-28.

65. Boden SD, Wiesel SW, Laws ER, Rothman RH. The Aging Spine - Essentials of Pathophysiology, Diagnosis and Treatment ed. Philadelphia: W.B Saunders Company, 1991.

66. Frymoyer JW, Moskowitz RW. Spinal Degeneration - Pathogenesis and Medical Management. In JW Frymoyer ed. The Adult Spine: Principles and Practice. New York: Raven Press, 1991.

67. Coventry MB, Ghormley RK, Kernohan JW. The Intervertebral Disc: Its Microscopic Anatomy and Pathology. Part III. Pathologic Changes in the Intervertebral Disc. J Bone Joint Surg 1945;27A:460-74.

68. Friberg S, Hirsch C. Anatomical and Clinical Studies on Lumbar Disc Degeneration. Acta Orthop Scand 1949;19:222-42.

69. Harris RI, Macnab I. Structural Changes in the Lumbar Intervertebral Discs. Their Relationship to Low Back Pain and Sciatica. J Bone Joint Surg 1954;36B:304-22.

70. Hoof VD. A: Histological Age Changes in the Annulus Fibrosus of the Human Intervertebral Disk. Gerontology 1964;9:136-49.

71. Lipson SJ. Biochemistry and Cell Biology of the Intervertebral Disc: Aging versus Degeneration. In Wiesel S, Weinstein J, Herkowitz H, Dvorak J, Bell G eds. The Lumbar Spine. Philadelphia: W.B. Saunders Company, 1996:310-16.

72. Shirazi A, Shrivastava SC, Ahmed SM. Stress Analysis of the Lumbar Disc-Body Unit in Compression. Spine 1984;9(2):120-34.

73. Miller JAA, Schmatz C, Schultz AB. Lumbar Disc Degeneration: Correlation with Age, Sex and Spine Level in 600 Autopsy Specimens. Spine 1988;13:173-8.

74. Lehman TR, Spratt KF, Tozzi JE, Weinstein JN, EL-Khoury GY. Long-Tem Follow-up of Lower Lumbar Fusion Patients. Spine 1987;12:97-104.

75. Hellier WG, Hedman TP, Kostuik JP. Wear Studies for the Development of an Intervertebral Disc Prosthesis. Spine 1992;16:S256-S60.

76. Knowles FL. Apparatus for Treatment of the Spinal Column: US Patent 2,677,369, 1954.

77. Schmiedberg SK, Chang CG, Frondoza CG, Valdevit ADC, Kostuik JP. Isolation and Characetrization of Metallic Wear Debris from a Dynamic Intervertebral Disc Prosthesis. Journal of Biomedical Materials Research 1994;28:1277-88.

78. Patil A. Artificial Intervertebral Disc. US Patent , 4309777, 1982.

79. Lee CK, Langrana NA, Parsons JR, Zimmerman MC. Prosthetic Intervertebral Disc. In Frymoyer JW ed. The Adult Spine: Principles and Practice. New York: Raven Press, Ltd.,, 1991:2007-14.

80. Salib RM, Pettine KA. Intervertebral Disk Arthroplasty. US Patent, 5258031, 1993.

81. Stubstad JA, Urbaniak JR, Kahn P. Prosthesis for Spinal Repair. US Patent, 3867728, 1975.

82. Downey EL. Replacement Disc. US Patent, 5035716, 1991.

83. Lee CK, Langrana NA, Alexander H, Clemow AJ, Chen EH, Parsons JR. Functional and Biocompatible Intervertebral Disc Spacer. US Patent, 4911718, 1990.

84. Parsons JR, Lee CK, Langrana NA, Clemow AJ, Chen EH. Functional and Biocompatible Intervertebral Disc Spacer Containing Elastomeric Material of Varying Hardness. US Patent, 5171281, 1992.

85. Langrana NA, Lee CK, Yang SW. Finite Element Modeling of the Synthetic Intervertebral Disc. Spine 1991;16(6):S245-S52.

86. Kostuik JP. Intervertebral Disc Replacement. Clin Orthop Rel Res 1997;337:27-41.

87. Cinotti G, David T, Postacchini F. Results of Disc Prosthesis after a Minimum Follow-up Period of 2 Years. Spine 1996;21:995-1000.

88. Steffee AD. Artificial Disc. US Patent, 5071437, 1991.

89. Fuhrmann G, Kaden B, Schmitz HJ, Fritz T, Kranz C. Intervertebral Disc Endoprosthesis. US Patent, 5002576, 1991.

90. Pisharodi M. Artificial Spinal Prosthesis. US Patent, 5123926, 1992.

91. Main JA, Wells ME, Keller TS. Vertebral Prosthesis. US Patent, 4932975, 1990.

92. Marnay T. Prosthesis for Intervertebral Discs and Instruments for Implanting It. US Patent, 5314477, 1994.

93. Bao QB, Yuan HA. New Technologies in Spine: Nucleus Replacement. Spine 2002;27:1245-47.

94. Nachemson AL. Some Mechanical Properties of the Lumbar Intervertebral Disc. Bull Hosp Joint Dis (NY) 1962;23:130-32.

95. Fernstrom U. Arthroplasty with Intercorporal Endoprostheis in Herniated Disc and Painful Disc. Acta Chir Scand 1966;355:154-59.

96. Eysel P, Rompe JD, Schoemayr R, Zoellner J. Biomechanical Behavior of a Prosthetic Lumbar Nucleus. Acta Neurochir (Wien) 1999;141:1083-87.

97. Bain AC, Sherman T, Norton BK, Hutton WC. A Comparison of the Viscoelastic Behavior of the Lumbar Intervertebral Disc before and after Implantation of a Prosthetic Disc Nucleus. Advances in Bioengineering ASME 2000;48:203-4.

98. Ledet E, Dirisio D, Tymeson M, Andersen L, Kallakury B, Sheehan C, Sachs B. The Raymedica PDN Prosthetic Disc Nucleus Device in the Baboon Lumbar Spine. The Spine Journal 2002;2:47s-128s.

99. Yuksel U, Walsh S, Curd D, Black K. Fatigue Durability of a Novel Disc Nucleus Repair System: In Vitro Studies in a Calf Spine Model. The Spine Journal 2002;2:47S-128S.

100. Dooris A, Hudgins G, Goel VK, Bao QB. Biomechanics of a Multisegmental Lumbar Spine with a Prosthetic Nucleus. The Spine Journal 2002;2:3s-44s.

101. Hou TS, Tu KY, Xu YK, Li ZB, Cai AH, Wang HC. Lumbar Intervertebral Disc Prosthesis. Chinese Medical Journal 1991;104(5):381-86.

102. Froning EC. Intervertebral Disc Prosthesis and Instruments for Locating Same. US Patent, 3875595, 1975.

103. Bao QB, Higham PA. Hydrogel Intervertebral Disc Nucleus. US Patent, 5976186, 1999.

104. Mallapragada SK, Peppas NA. Dissolution Mechanism of Semicrystalline Poly(Vinyl Alcohol) in Water. Journal of Polymer Science: Part B: Polymer physics 1996;34:1339-46.

105. Mallapragada SK, Peppas NA, Columbo P. Crystal Dissolution Controlled Release Systems. Ii. Metronidazole Release from Semicrystalline Poly(Vinyl Alcohol) Systems. Journal of Biomedical Materials Research 1997;36:125-30.

106. Bao QB, Yuan HA. Implantable Tissue Repair Device. US Patent, 6334630, 2001.

107. Reid JE, Meakin JR, Robins SP, Skakle JMS, Hukins DWL. Sheep Lumbar Intervertebral Discs as Models for Human Discs. Clinical Biomechanics 2002;17:312-14.

108. Meakin JR, Reid JE, Hukins DWL. Replacing the Nucleus Pulposus of the Intervertebral Disc. Clinical Biomechanics 2001;16:560-65.

109. Stone KR. Prosthetic Intervertebral Disc. US Patent, 5108438, 1992.

110. Gan JC, Ducheyne P, Vresilovic E, Shapiro IM. Bioactive Glass Serves as a Substrate for Maintenance of Phenotype of Nucleus Pulposus Cells of the

Intervertebral Disc. Journal of Biomedical Materials Research 2000;51(4):596-604.

111. Gan JC, Ducheyne P, Vresilovic E, Shapiro IM. Compositions and Methods for Intervertebral Disc Reformation. US Patent, 5964807, 1999.

112. Fassie B, Ginestle JF. Disc Prosthesis Made of Silicone - Experimental Study and First Clinical Cases. Nouvelle Presse Medical 1978;21:207.

113. Frei H, Oxland T, Rathonyi G, Orr T, Nolte L. The Effect of Nucleus Prosthesis Device on a Lumbar Spine Mechanics. Orthopaedic Research Society (47th Annual Meeting). San Francisco, CA, 2001.

114. Meakin JR, Hukins DWL. Effect of Removing the Nucleus Pulposus on the Deformation of the Annulus Fibrosus During the Compression of the Intervertebral Disc. Journal of Biomechanics 2000;33:575-80.

115. Meakin JR, Redpath TW, Hukins DWL. The Effect of Partial Removal of the Nucleus Pulposus from the Intervertebral Disc on the Response of the Human Annulus Fibrosus to Compression. Clinical Biomechanics 2001;16:121-28.

116. Belytschko TB, Kulak RF, Schultz AB, Galante JO. Finite Element Stress Analysis of an Intervertebral Disc. J Biomech 1974;7:277-85.

117. Kulak RF, Belytschko TB, Schultz AB, Galante JO. Nonlinear Behavior of the Human Intervertebral Disc under Axial Load. Journal of Biomechanics 1976;9:377-86.

118. Lin HS, Liu YK, Adams KH. Mechanical Response of the Lumbar Intervertebral Joint under Physiological (Complex) Loading. J Bone Joint Surg 1978;60A:41-55.

119. Spilker RL. A Simplified Finite Element Model of the Intervertebral Disc. In Simon BR ed. Finite Elements in Biomechanics. Tuscon: University of Arizona, 1980:729-47.

120. Iatridis JC, Setton LA, Weidenbaum M, Mow VC. Alterations in the Mechanical Behavior of the Human Lumbar Nucleus Pulposus with Degeneration and Aging. Journal of Orthopaedic Research 1997;15:318-22.

121. Shirazi A, Ahmed AM, Shrivastava SC. Mechanical Response of a Lumbar Motion Segment in Axial Torque Alone and Combined with Compression. Spine 1986;11(9):914-27.

122. Shirazi A, Ahmed AM, Shrivastava SC. A Finite Element Study of a Lumbar Motion Segment Subjected to Pure Sagittal Plane Moments. Journal of Biomechanics 1986;19(4):331-50.

123. Shirazi A. Finite Element Simulation of Changes in the Fluid Content of Human Lumbar Discs: Mechanical and Clinical Implications. Spine 1992;17(2):206-12.

124. Crisco JJ, Panjabi MM. The Intersegmental and Multisegmental Muscles of the Lumbar Spine: A Biomechanical Model Comparing Lateral Stabilizing Potential. Spine 1991;16(7):793-99.

125. Goel VK, Kong W, Han JS, Weinstein JN, Gilbertson LG. A Combined Finite Element and Optimization Investigation of Lumbar Spine Mechanics with and without Muscles. Spine 1993;18(11):1531-41.

126. Mizrahi J, Silva MJ, Keaveny TM, Edwards WT, Hayes WC. Finite Element Stress Analysis of the Normal and Osteoporotic Lumbar Intervertebral Body. Spine 1993;18(14):2088-96.

127. Natarajan RN, Ke JH, Andersson GBJ. A Model to Study the Disc Degeneration Process. Spine 1994;19(3):259-65.

128. Goel VK, Monroe BT, Gilbertson LG, Brinckmann P. Interlaminar Shear Stresses and Laminae Separation in a Disc: Finite Element Analysis of the L3-L4 Motion Segment Subjected to Axial Compressive Loads. Spine 1995;20(6):689-98.

129. Lu YM, Hutton WC, Gharpuray V. Can Variations in Intervertebral Disc Height Affect the Mechanical Function of the Disc? Spine 1996;21(19):2208-17.

130. Natarajan RN, Andersson GBJ. Modeling the Annular Incision in a Herniated Lumbar Intervertebral Disk to Study Its Effect on Disk Stability. Computers and Structures 1997;64(5/6):1291-97.

131. Pitzen T, Geisler F, Matthis D, Muller-Storz H, Barbier D, Steudel W, Feldges A. A Finite Element Model for Predicting the Biomechanical Behavior of the Human Lumbar Spine. Control Engineering Practice 2002;10:83-90.

132. Wang JL, Parnianpour M, Shirazi A, Engin AE, Li S, Patwardhan A. Development and Validation of a Viscoelastic Finite Element Model of an L2/L3 Motion Segment. Theoretical and Applied Fracture Mechanics 1997;28:81-93.

133. Simon BR, Carlton MW, Wu JSS, Evans JH, Kazarian LE. Structural Models for Human Spinal Motion Segments Based on a Poroelastic View of the Intervertebral Disc. Journal of Biomechanical Engineering 1985;107:327-35.

134. Laible JP, Pflaster DS, Krag MH, Simon BR, Pope MH, Haugh LD. A Poroelastic Swelling Finite Element Model with Application to the Intervertebral Disc. Spine 1993;18(5):659-70.

135. Argoubi M, Shirazi A. Poroelastic Creep Response Analysis of a Lumbar Motion Segment in Compression. Journal of Biomechanics 1996;29(10):1331-39.

136. Martinez JB, Oloyede V, Broom ND. Biomechanics of Load-Bearing of the Intervertebral Disc: An Experimental and Finite Element Model. Med. Eng.Phys. 1997;19(2):145-56.

137. Cheung J, Zhang M, Chow D. Biomechanical Responses of the Intervertebral Joints to Static and Vibrational Loading: A Finite Element Study. Clinical Biomechanics 2003;18:790-99.

138. Yao J, Ducheyne P, Shapiro IM, Turteltaub SR. A Three-Dimensional Nonlinear Finite Element Analysis of the Mechanical Behavior of Tissue Engineered Intervertebral Discs under Complex Loads. Society for Biomaterials(28th Annual Meeting). Tampa, FL, 2002:80.

139. Peppas NA. Infrared Spectroscopy of Semicrystalline Poly(Vinyl Alcohol) Networks. Makromol. Chem 1977;178:595-601.

140. Peppas NA, Merrill EW. Poly(Vinyl Alcohol) Hydrogels: Reinforcement of Radiation -Crosslinked Networks by Crystallization. Journal of Polymer Science: Polymer Chemistry Edition 1976;14:441-57.

141. Peppas NA, Merrill EW. Development of Semicrystalline PVA Networks for Biomedical Applications. Journal of Biomedical Materials Research 1977;11:423-34.

142. Hickey AS, Peppas NA. Mesh Size and Diffusive Characteristics of Semicrystalline Poly (Vinyl) Alcohol Membranes Prepared by Freezing/Thawing Techniques. Journal of Membrane Science 1995;107:229-37.

143. Mondino AV, Gonzalez ME, Romero GR, Smolko EE. Physical Properties of Gamma Irradiated Poly(Vinyl Alcohol) Hydrogel Preparations. Radiation Physics and Chemistry 1999;55:723-26.

144. Tsuk AG, Trinkaus-Randall V, Leibowitz HM. Advances in Polyvinyl Alcohol Keratoprostheses: Protection against Ultraviolet Light and Fabrication by a Molding Process. Journal of Biomedical Materials Research 1997;34:299-304.

145. Young TH, Chaung WY, Yao NK, Chen LW. Use of a Diffusion Model for Assessing the Performance of Poly (Vinyl Alcohol) Bioartificial Pancreas. Journal of Biomedical Materials Research 1998;40:385-91.

146. Stammen JA, William DN, Guldberg RE. Mechanical Properties of a Novel PVA/PVP Hydrogel in Shear and Unconfined Compression. Biomaterials 2001;22:799-806.
147. Allock HR, Lampe FW. Contemporary Polymer Chemistry ed. Englewood Cliffs: Prentice-Hall Inc., 1990.

148. Kao FJ, Manivannan G, Sawan SP. UV Curable Bioadhesives: Copolymers of N-Vinyl Pyrrolidone. Journal of Biomedical Materials Research 1997;38(3):191-96.

149. Cassu SN , Felisberti MI. Poly(Vinyl Alcohol) and Poly (Vinyl Pyrrolidone) Blends: Miscibility, Microheterogeneity and Free Volume Change. Polymers 1997;38(15):3907-11.

150. Antoniou JA, Steffen T, Nelson F, Winterbottom N, Hollander AP, Poole AR, Aebi M and Alini M. The Human Lumbar Intervertebral Disc: Evidence for Changes in the Biosynthesis And Denaturation of the Extracellular Matrix with Growth, Maturation, Ageing, and Degeneration. J Clin Invest 1996;98(4):996-1003.

151. Nachemson AL. Lumbar Intradiscal Pressure. Acta Orthop Scand 1960;Suppl. 43.

152. Nachemson AL, Elfstrom G. Intravital Dynamic Pressure Measurements in Lumbar Discs: A Study of Common Movements, Maneuvers and Exercises. Scand J Rehabil Med 1970;Suppl 1:1-40.

153. Panjabi MM, Brown M, Lindahl S, Irstam L, Hermens M. Intrinsic Disc Pressure as a Measure of Integrity of the Lumbar Spine. Spine 1988;13:913-7.

154. Thompson JP, Pearce RH, Schechter MT, et al. Preliminary Evaluation of a Scheme for Grading the Gross Morphology of the Human Intervertebral Disc. Spine 1990;15:411-15.

155. Andersson GH, Schultz AB. Effects of Fluid Injection on Mechanical Properties of Intervertebral Discs. Journal of Biomechanics 1979;12:453-58.

156. Goel VK, Nishiyama K, Weinstein JN, Liu YK. Mechanical Properties of Lumbar Spinal Motion Segments as Affected by Partial Disc Removal. Spine 1986;11:1008-12.

157. Seroussi R, Krag M, Muller D, Pope MH. Internal Deformations of Intact and Denucleated Human Lumbar Discs Subjected to Compression, Flexion and Extension Loads. Journal of Orthopaedic Research 1989;7:122-31.

158. Panjabi MM, Krag MH, Chung TQ. Effects of Disc Injury on Mechanical Behavior of the Human Spine. Spine 1984;9:107-13.

159. Brinckmann P, Grootenboer H. Change of Disc Height, Radial Bulge and Intradiscal Pressure from Discectomy: An in Vitro Investigation on Human Lumbar Discs. Spine 1991;16:641-46.

160. Brinckmann P. Injury of the Annulus Fibrosus and Disc Protrusions - an in Vitro Investigation on Human Lumbar Discs. Spine 1986;11:149-53.

161. Ethier DB, Cain JE, Lauerman WC, Glover M, Yaszemski MJ. The Influence of Annulotomy Selection on Disc Competence - a Radiographic, Biochemical and Histologic Analysis. Spine 1994:2071-76.

162. Akkerveeken V, O'Brian JP, Park WM. Experimentally Induce Hypermobility in the Lumbar Spine: A Pathologic and Radiologic Study of the Posterior Ligaments and Annulus Fibrosus. Spine 1979;4:236.

163. Ahlgren BD, Vasavada A, Browser RS, Lydon C, Herkowitz HN, Panjabi MM. Annular Incision Technique on the Strength and Multidirectional Flexibility of the Healing Intervertebral Disc. Spine 1994;19:948-54.

164. Kim YE, Goel VK. Biomechanics of Chemonucleolysis. Computational methods in Bioengineering, ASME BED 1988;9:461-71.

165. Frei H, Oxland TR, Rathoyni GC, Nolte LP. The Effect of Nucleotomy on Lumbar Spine Mechanics in Compression and Shear Loading. Spine 2001;26(19):2080-89.

166. Adams MA, Freeman BJC, Morrison HP, Nelson IW, Dolan P. Mechanical Initiation of Intervertebral Disc Degeneration. Spine 2000;25(13):1625-36.

167. Chan M, Chowchuen P, Workman T, Eilenberg S, Schweitzer M, Resnick D. Silicone Synovitis: MR Imaging in Five Patients. Skeletal Radiol 1998;27(1):13-17.

168. Karduna A, Williams GR, Williams JL, Iannotti JP. Glenohumeral Joint Translations before and after Shoulder Arthroplasty: A Study in Cadavera. J Bone Joint Surg 1997;79-A(8):1166-74.

169. Ordway NR, Han ZH, Bao QB. Experimental Measurement of Pressure Distribution and Disc Height on the Human Lumbar Intervertebral Disc after Discectomy. Orthopaedic Research Society. New Orleans, LA, 1994:136.

170. Bao QB, Yuan HA. Prosthetic Disc Replacement: The Future? Clin Orthop Rel Res 2002;394:139-45.

171. Baumgartner W. Intervertebral Disk Prosthesis. US, 5320644, 1994.

172. Gomes K, Thomas J, Lowman A, Marcolongo M. Shape Memory Behavior of a PVA/PVP Hydrogel for Nucleus Pulposus Replacement. J Biomat Sci, Polymer Ed. 2002;submitted.

173. Liu X, Marcolongo M, Lowman A. Short Term in Vitro Response of Associating Hydrogels. Polymers 2001;submitted.

174. Hara Y, Matsuura T, Taketani F. Biocompatibility of Polyvinylalcohol Gel as a Vitreous Substitute. Nippon Ganka Gakkai Zasshi 1998;102(4):247-55.

175. Bagga CS, Wiliams P, Higham PA Bao QB. Development of Fatigue Test Model for a Spinal Nucleus Prosthesis with Preliminary Results for a Hydrogel Spinal Prosthetic Nucleus. Bioengineering Conference BED, 1997:441-42.

176. Joshi A, Marcolongo M, Karduna A, Vresilovic E. Contribution of the Nucleus Pulposus Towards the Compressive Stiffness of the Human Lumbar Functional Spinal Unit. The Spine Journal 2003;submitted.

177. Gomes K, Thomas J, Lowman A, Marcolongo M. The Effect of Dehydration History on Associating Hydrogels for Nucleus Pulposus Replacement. Society for Biomaterials (28th Annual Meeting). Tampa, FL, 2002.

178. Thomas J, Lowman A, Marcolongo M. Novel Associated Hydrogels for Nucleus Pulposus Replacement. Journal of Biomedical Materials Research 2003;submitted.

179. Joshi A, Marcolongo M, Vresilovic E, Lowman A, Karduna A. The Effect of a Hydrogel Nucleus Replacement on the Compressive Stiffness of the Human Lumbar Functional Spinal Unit. Journal of Orthopaedic Research 2003;submitted.

180. Berkson MH, Nachemson AL, Schultz AB. Mechanical Properties of Human Lumbar Spine Motion Segments. Ii Response in Compression and Shear, Influence of Gross Morphology. J Biomech Eng 1979;101:53-57.

181. Schultz AB, Warwick DN, Berkson MH, Nachemson AL. Mechanical Properties of Human Lumbar Spine Motion Segments. I Responses in Flexion, Extension, Lateral Bending and Torsion. J Biomech Eng 1979;101:46-52.

182. Ranu HS, Denton RA, King AI. Pressure Distribution under an Intervertebral Disc - an Experimental Study. J Biomech 1979;12:807-12.

183. Nagy GT, Gentle CR. Significance of the Annulus Properties to Finite Element Modeling of Intervertebral Discs. Journal of Musculoskeletal Research 2001;5(3):159-71.

184. Duncan N, Lotz JC. Experimental Validation of a Porohyperelastic Finite Element Model of the Annulus Fibrosus. In Middleton M, Jones ML, Pande GN ed. Computer methods in biomechanics and biomedical engineering - 2: Gordon and Breach Science Publishers, 1997:527-34.

185. Joshi A, Mehta S, Vresilovic E, Karduna A, Marcolongo M. Nucleus Implant Parameters Significantly Change the Compressive Stiffness of the Human Lumbar Intervertebral Disc. Journal of Biomechanical Engineering 2003;submitted.

186. Joshi A, Karduna A, Vresilovic E, Marcolongo M. The Effect of Nucleus Replacement on the Stress Distribution of the Lumbar Intervertebral Disc: A Finite Element Study. Clinical Biomechanics 2003;submitted.

187. Takigawa T, Morino Y, Urayama K, Masuda T. Poisson's Ratio of Polyacrylamide (PAAm) Gels. Polymer Gels and Networks 1996;4:1-5.

Vita

Abhijeet Joshi was born in Pune, India on December 10, 1975. He was the recipient of numerous awards in academics and sports activities in the high school. He was also a recipient of prestigious National Merit Scholarship awarded by the Government of India, in 1991. He received a Bachelor of Engineering Degree in Mechanical Engineering (with Distinction) from Shivaji University, India in July 1997.

After graduation, he worked in the automobile and steel industry, in the capacity of techno-commercial engineer from September 1997 to August 2000.

He joined Drexel University, Department of Materials Science and Engineering in September 2000 to pursue a PhD degree. During his tenure at Drexel, he worked on the understanding of the human lumbar intervertebral disc biomechanics and contributed in the development of a novel polymeric hydrogel nucleus implant as a potential substitute for the degenerated nucleus pulposus of the lumbar intervertebral disc.

His work in the area of intervertebral disc biomechanics and spinal nucleus implant mechanics has yielded twelve journal publications and conference papers.